# SOLAR COSMIC RAY PHENOMENA

K. G. McCRACKEN and U. R. RAO
*Physical Research Laboratory, Ahmedabad, India*

(Received 15 June, 1970)

**Abstract.** This review attempts to present an integrated view of the several types of solar cosmic ray phenomena. The relevant large and small scale properties of the interplanetary medium are first surveyed, and their use in the development of a quantitative understanding of the cosmic ray propagation processes summarised. Solar cosmic ray events, in general, are classified into two phenomenological categories: (a) prompt events, and (b) delayed events. The properties of both classes of events are summarised. The properties considered are the frequency of occurrence, dependence on parent flare position, the time profile, energy spectra, anisotropies, particle species, velocity dispersions, etc. A single model is presented to explain the various species of delayed event. Thus the halo and core events, energetic storm particle events, EDP events and proton recurrent regions are suggested to be essentially of common origin. The association of flare particle events with electromagnetic phenomena, including optical, X-ray and microwave emissions is summarised. The conditions in a sunspot group, and solar flare that are considered to be conducive to cosmic ray acceleration processes are discussed. Considerable discussion is devoted to physical processes occurring near the Sun. Near Sun particle storage, and diffusion, and secondary injection processes that are triggered by a far distant solar flare are reviewed. In order to explain the considerable differences between aspects of the prompt and delayed events, we propose selective diffusion processes that only occur at early times in a solar flare. The type IV radio emissions at metric wavelengths are suggested to yield direct evidence for the storage processes that are necessary to explain the properties of the delayed events, and also as yielding direct evidence of secondary injection processes. We conclude by briefly summarising the ionospheric effects of the solar cosmic radiation.

## 1. The Fundamentals of Solar Cosmic Ray Phenomena

Solar cosmic ray phenomena exhibit wide variations in behaviour from event to event. This can be due to (a) inherent variability in the production process; (b) storage processes in the vicinity of the Sun, the extent of which can vary widely from event to event; (c) variability due to differences in the large scale magnetic field configuration between the points of production and observation, and (d) local modulation effects due to the observer sampling small scale features in the distribution of the solar cosmic rays in the solar system. Consequently, no two events are exactly alike.

Certain broad features of solar cosmic ray phenomena are, however, very well established. We will, therefore, first enunciate these facts, without making detailed comments, to constitute a working model against which to describe and discuss various detailed observations. The working model is:

(a) Cosmic ray ions of $1 \leqslant Z \leqslant 26$; with kinetic energies, $E \gtrsim 10^6$ eV/nucleon, and electrons of $E \gtrsim 40$ keV, can be generated in the vicinity of solar flares, in approximate synchronism with the flash phase of the flare and the occurrence of maximum X-ray and microwave radio emissions from the flare.

(b) Two distinctly different phenomenological classes of solar cosmic ray events can be identified: (1) the prompt event, occurring within hours of the parent flare, and

*Space Science Reviews* **11** (1970) 155–233. 

(2) the delayed event, occurring $\gtrsim 24$ h after the parent flare, or even without any obvious association with a solar flare.

(c) The interplanetary magnetic field plays a dominant role in the cosmic ray propagation processes, since for all particle energies observed to date ($< 30 \times 10^9$ eV), the particle gyroradius is $\lesssim 0$ (0.1 AU) near the orbit of Earth.

Three features of the magnetic field are of importance.

(c1) The large scale average configuration of the lines of force of the field are in the form of Archimedes spirals (Figure 1), with spiral angle $\theta = \arctan(\Omega R/V_P)$, where $\Omega$ is the Sun's angular rotation velocity, $V_P$ is the plasma velocity, and $R$ is the radial distance from the Sun.

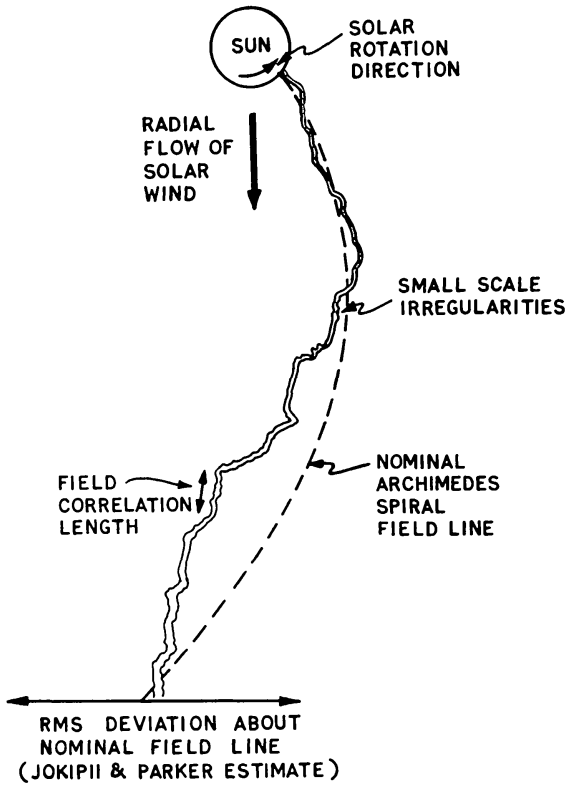


Fig. 1. The configuration of the interplanetary magnetic field inside the orbit of Earth. The dashed line gives the ideal configuration predicted by a uniform, radial expansion of the solar wind, and the solid line the meandering field lines produced as the result of temporal and spatial inhomogeneities in this flow. After Michel (1967).

(c2) The field contains small scale irregularities. These will scatter charged particles from simple guiding centre orbits, the scattering for a particle of rigidity $R$ being maximum when its cyclotron radius $r_c = 0(L)$, where $L$ is the scale size of the irregularities of interest. The scattering of particles of rigidity $R$ GV is therefore primarily due to power in the vicinity of the 'resonant' frequency $f_r(R) = 10^{-4} R^{-1}$ Hz. Some of the power spectra of the interplanetary field observed to date are summarized in Figure 2.

(c3) The magnetic field is embedded in the solar wind, which is streaming radially

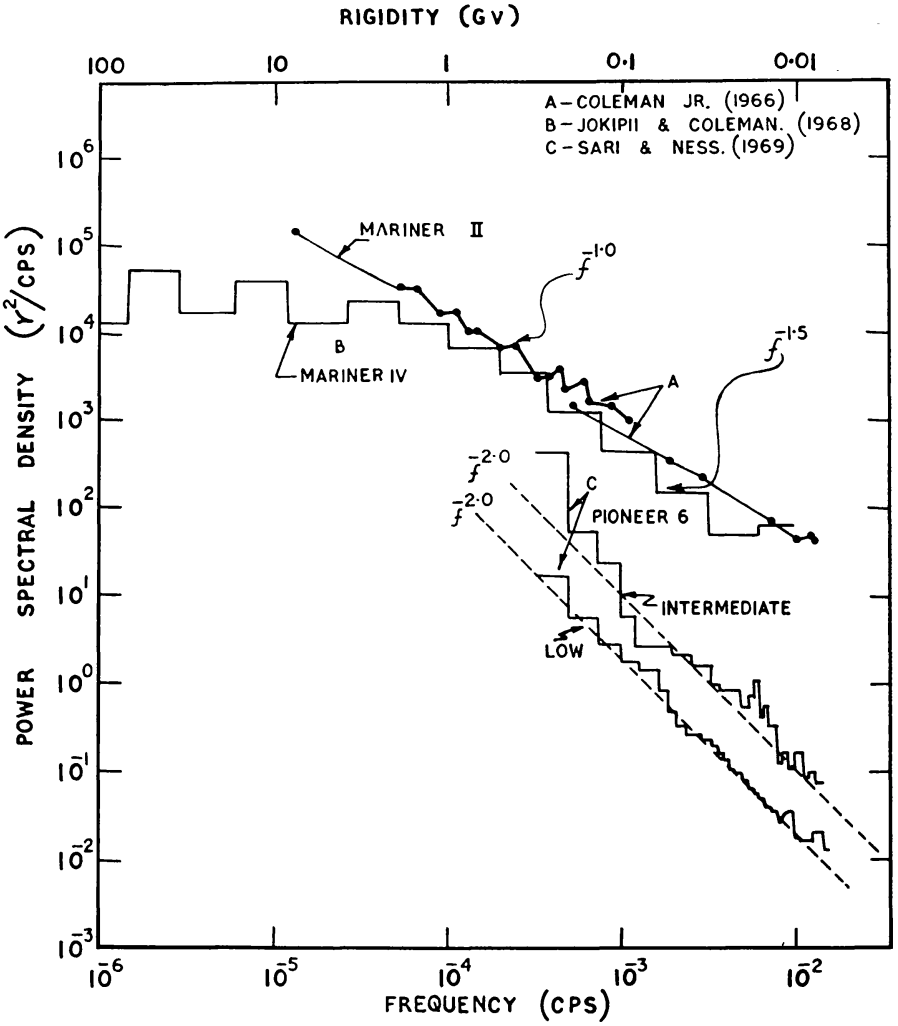


Fig. 2. Power spectra of the co-latitudinal component of the interplanetary magnetic field near the orbit of Earth. The epochs are: Mariner II, 1962; Mariner IV, late 1964; Pioneer 6, early 1966. The two graphs for Pioneer 6 correspond to periods of low, and intermediate disturbance of the magnetic field.

away from the Sun. Consequently, the cosmic ray gas is convected outwards at the solar wind velocity.

## 2. Relevant Properties of the Interplanetary Magnetic Field

A considerable body of experimental data now exists pertaining to the interplanetary magnetic field near the orbit of Earth. These data permit a quantitative (and ideally, absolute) evaluation of the particle propagation processes near Earth, on which extrapolation to other portions of the solar system may be based. That is, we can hopefully regard them as relatively well known boundary conditions, on which our study of the propagation process, in general, will be based. We consequently review them, briefly, prior to any discussion of the cosmic ray data.

The average, large scale structure of the interplanetary field has been shown (Ness

*et al.*, 1964) to be in good agreement with the theoretical prediction that the field lines would be in the shape of an Archimedes spiral (Parker, 1958). In addition, a sector structure of the field has been demonstrated (Wilcox and Ness, 1965; Coleman *et al.*, 1966) and the field had been shown to be related to photospheric magnetic fields (Ness and Wilcox, 1966).

On the small scale, the field shows marked, and very frequent deviation from the Archimedes spiral field direction (Figure 1). Power spectra of the various field components have been calculated by several authors and representative spectra are given in Figures 2 and 3 (Jokipii and Coleman, 1968; Siscoe *et al.*, 1968: Holzer *et al.*, 1966; Sari and Ness, 1969), corresponding to the several observations in the interval 1962–66.

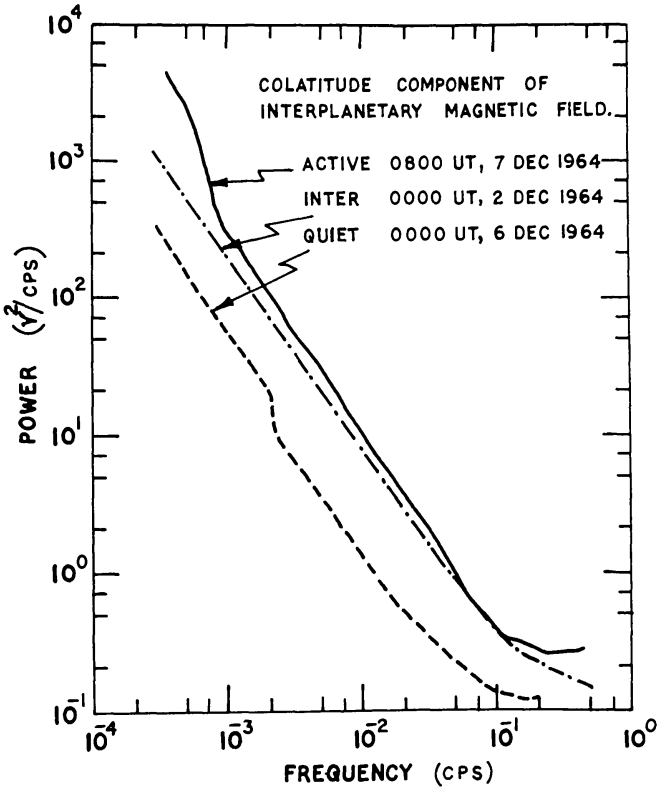


Fig. 3. Power spectra of the co-latitudinal component of the interplanetary magnetic field observed by the Mariner IV magnetometer. Spectra are given corresponding to periods of low, intermediate, and great disturbance of the magnetic field. After Siscoe *et al.* (1968).

Since particles of rigidity $R$ GV are principally scattered by the irregularities that introduce power into these spectra at the frequency $f = 10^{-4} R^{-1}$ Hz, these spectra indicate scattering throughout the rigidity range 10 GV $\gtrsim R \gtrsim 10^{-2}$ GV (9 GeV $\gtrsim E_p \gtrsim$ $\gtrsim 5 \times 10^{-2}$ MeV; $E_e \lesssim 10$ MeV).

Jokipii (1966, 1967), Roeloff, (1966) and Dolginov and Toptygin (1966) have developed the formalism to use the observed power spectra to calculate the details of the particle propagation process near Earth. Previously, the theoretical studies of the propagation process had invoked the concept of 'scattering centers' (e.g. Krimigis, 1965; Parker, 1965; Axford, 1965b; Burlaga, 1967), whose properties were derived on

an 'ad hoc' basis from the cosmic ray phenomena under study. While these earlier studies have given very valuable insights into the physical processes of importance, and are in some cases asymptotic limits of the more recent formulations, they are clearly superseded in principle at least by these more recent studies. Of greatest importance in this regard is the fact that the quantities characterising the propagation process are now derived from the magnetic field, which is the physical property that is causally related to the propagation process.

It should be stressed, however, that many difficulties still remain even if the magnetic data are explicitly employed. Firstly, the observed magnetic data pertain to the fluctuations that result when different tubes of magnetic force are convected past the observer by the solar wind, while it is the fluctuations along individual tubes of force that determine the cosmic ray effects. Secondly, even if due allowance can be made for the foregoing effect, current data will still only provide a typical boundary condition, and a knowledge of its range of variation. That is, study of the cosmic ray propagation process in depth still requires explicit extrapolation of the propagation characteristics to other parts of the solar system (i.e. extrapolation in $r$, $\theta$, $\varphi$), while the actual, near Earth, propagation characteristics (i.e. the boundary condition) can be inferred to vary over a very wide range (factor of 10) from day to day (Siscoe *et al.*, 1968). For the present time, in fact, the main consequence of the explicit use of the magnetic data is a more absolute knowledge of the manner in which the propagation process depends upon particle rigidity and a clearer understanding of the relative roles of diffusion-like motion parallel and perpendicular to the interplanetary magnetic field. Nevertheless, as our understanding of the physical nature of the magnetic irregularities improves, our ability to extrapolate in ($r$, $\theta$, $\varphi$) will undoubtedly improve. We believe that this improvement will come from studies of the plasma and fields in interplanetary space (and not from cosmic ray studies) and from the development of an ability to identify the physical nature of irregularities observed in the magnetic data (e.g. Burlaga, 1968). We also note that another important goal is the estimation of the boundary condition at Earth on any given day, and that this will be greatly aided if the correlation of the total spectral power in the magnetic field variations with an easily observable geophysical quantity is established. In our view, the explicit use of the 'scattering centre' in theoretical studies has served its purpose, and will in future be replaced by the obvious fact of continuous, small angle scattering in the ever present interplanetary magnetic irregularities.

It has long been recognized that the particle motion in the interplanetary magnetic field can be considered as an anisotropic diffusion process, with $K_{\parallel} > K_{\perp}$, where $K_{\parallel}$ and $K_{\perp}$ are the diffusion coefficients parallel and perpendicular to the mean large scale magnetic field direction (Axford, 1965b; Parker, 1965; Burlaga, 1967). From the power spectra in Figure 2, and on the basis of a number of reasonable assumptions, Jokipii (1966, 1967, 1968) and Jokipii and Parker (1968) derive a number of relationships which will aid us in the discussion of the observed cosmic ray data.

Writing the spectral power density of the fluctuations in the magnetic field component parallel to the mean large scale field as $P_{ss}(f)$ and approximating it by a power

law in $f$, i.e. $P_{ss}(f) \sim f^{-\alpha}$, then

$$K_{\parallel} = \begin{cases} K\beta R^{2-\alpha} & \text{for} \quad R_u > R > R_l \\ \frac{1}{3}cL\beta & \text{for} \quad R < R_l, \end{cases} \tag{2.1}$$

where $R_u$ and $R_l$ are the rigidities at which (1) the cyclotron radius begins to approach the mean free path $\lambda = 3\, K_{\parallel}/\beta c$ and (2) the mean free path begins to approximate the correlation length, $L$, of the interplanetary field.

The 'perpendicular' diffusion coefficient $K_{\perp}$ due to the spectral power at the 'resonant' frequency is $0\,(r_c^2/\lambda^2)\, K_{\parallel} \ll K_{\parallel}$, where $r_c$ is the cyclotron radius, and $\lambda = 3\, K_{\parallel}/\beta c$. After allowing for the estimates of Jokipii and Parker (1968) for the 'meandering' of the interplanetary field lines (see below), Jokipii and Coleman (1968) obtain $K_{\perp}^m = 0\,(10^{21}\ \text{cm}^2\ \text{sec}^{-1})$, which approximates $K_{\parallel}$, where the superscript $m$ is introduced to indicate the meandering origin of this 'diffusion'.

For the rigidity range of immediate interest, $10^7 < R < 10^9$ V, the various power spectra in Figure 2 exhibit significantly different values of the spectral exponent, $\alpha$. This therefore implies differing rigidity dependencies for $K_{\parallel}$, and also varying values of $R_l$. Table I summarises the situation. In particular we note

TABLE I

Summarizing the rigidity dependences predicted by the several power spectra ($10^{-5} < f < 10^{-2}$ Hz) observed during 1962–66. In calculating $R_l$, a correlation length ($L$) of $2 \times 10^{11}$ cm has been assumed (Jokipii and Coleman, 1968).

| Epoch of observations | 1962 | Nov./Dec. 1964 | Dec. 1965/Jan. 1966 |
|---|---|---|---|
| $S/C$ | Mariner 2 (Coleman, 1966) | Mariner 4 (Jokipii and Coleman, 1968) | Pioneer 6 (Sari and Ness, 1969) |
| $\alpha$ | 1 | 1.5 | 2 |
| $R_l$ | 0.4 GV | 0.16 GV | 0 |
| $E_p$ (Proton) | 80 MeV | 12 MeV | 0 |
| $E_e$ (Electron) | 400 MeV | 160 MeV | 0 |
| $K_{\parallel}(R,\beta)$ for $R_u > R > R_l$ | $K_0\beta R$ | $K_0\beta R^{1/2}$ | $K_0\beta$ |
| $\lambda(R,\beta)$ for $R_u > R > R_l$ | $\lambda_0 R$ | $\lambda_0 R^{1/2}$ | const. |

where $K_0$ and $\lambda_0$ are constants

(a) that the observed spectra imply mean free paths that vary as $R^1$, $R^{1/2}$, and $R^0$.

(b) that the lower limit, below which Jokipii (1968) intuitively estimates the mean free path to be constant, and equal to the magnetic correlation length, ranges $0 < E_p < < 80$ MeV, according to the spectral exponent of the power spectrum.

(c) that if $K_{\perp}^m = 0\,(10^{21}\ \text{cm}^2\ \text{sec}^{-1})$ as implied by the meandering magnetic field, then $K_{\perp}^m \approx 0\,(K_{\parallel})$ for $R < R_l$ in the case of $\alpha = 1$ and 1.5, and for all $R < R_u$ for the case $\alpha = 2$. For these cases, then, the diffusion approximates isotropic diffusion in a macroscopic sense (i.e. insofar as spatial distribution in the solar system is concerned). For 'microscopic' phenomena, in which the meandering diffusion coefficient $K_{\perp}^m$ plays no

part, then $K_\perp$ is negligible compared to $K_\parallel$ at all rigidities $R < R_u$. Thus the anisotropy of the cosmic radiation for $R < R_u$ is insensitive to $K_\perp^m$, and since $K_\perp^m \ll K_\parallel$, the anisotropy will still be greatly independent of meandering effects.

Jokipii and Coleman (1968) have presented power spectra derived from two periods of 32 days each, during which the Mariner IV spacecraft was at average distances of 1.00 and 1.43 AU from the Sun. From these spectra they infer that $K_\parallel$ is only weakly dependent on $r$ over this range. By contrast, Siscoe *et al.* (1968) show that the power spectra at $r$=const. vary strongly from day to day (Figure 3), the power density varying by as much as a factor of 10 without major changes in the spectral shape or slope. Similar changes are reported by Sari and Ness (1969). The power density observed in 1962 by Mariner II was at least a factor of 2 more than that observed by Mariner IV in 1965 while there appears to be a surprisingly large difference (>factor of 10) between the later data, and those obtained by Pioneer 6 some 12 months later. Since the diffusion coefficients are, in first order, linearly related to the spectral power densities (Jokipii, 1966; Roeloff, 1966), these results imply that $K_\parallel$ and $K_\perp^m$ vary by upward of a factor of 10 from day to day, and by upward of a factor of 100 over longer periods of time. Arbitrarily taking the 'quiet' day power levels in Figure 3 as representative of quiet sunspot minimum conditions, we obtain $K_\parallel \approx 6 \times 10^{20}$ cm$^2$ sec$^{-1}$, implying $\lambda = 6 \times 10^{10} \beta^{-1}$ cm. These values are almost an order of magnitude different from the values derived from the 32 days average Mariner IV spectra (Jokipii and Coleman, 1968), indicating the very variable nature of even the near Earth boundary condition on the propagation parameters.

The origin and physical nature of the small scale irregularities in the interplanetary magnetic field is clearly of interest in respect to both the near Earth calculation and the extrapolation of $K_\parallel$ and $K_\perp$ to points in the solar system other than near the orbit of Earth. Michel (1967) and Jokipii and Parker (1968) have discussed the roles that the spatial dependence of coronal temperature across the solar granulation and super-granulation, and their finite lifetimes, will have on the interplanetary field. They conclude that these aspects of the granulation and super-granulation will be major contributors to the irregularities in the interplanetary field. Thus the observed correlation lengths in the near Earth field appear to be understandable as projections of the solar granulation/super-granulation correlation lengths via the solar wind (Jokipii and Parker, 1968). Furthermore, Jokipii and Parker (1968) deduce that the stochastic nature of the deviations of a line of force from its Archimedes spiral direction implies an 0 (0.1 AU) random walk of the field lines from their ideal Archimedes spiral shape (see Figure 1). As mentioned previously, this implies that transverse diffusion of charged particles will be dominated by this 'meandering field' effect, the transverse diffusion of the particles being virtually entirely due to strict guiding centre motion along meandering field lines.

All the preceding discussion has been predicated on the assumption that the magnetic power spectra, as observed, accurately indicate the power that would be observed by an observer moving along a magnetic field line. Recent studies of the correlated field and plasma measurements (Burlaga, 1968) suggest, however, that a

large number of the sharp discontinuities seen in the magnetic data, and which contribute power with a $f^{-2}$ frequency dependence to the power spectrum particularly at $f \gtrsim 10^{-4}$ Hz, are of the nature of tangential field discontinuities: that is, characteristic of the difference between adjacent tubes of force, and not characteristic of the properties of the fields within the tubes. That is, these discontinuities and the spectral power they introduce have no effect on low energy ($R < R_u$) cosmic rays. They therefore introduce a spurious component into the diffusion coefficients derived from the power spectra. Sari and Ness (1969), using a mathematical modelling technique, conclude that half, if not more of the power in 1965/66 was of this nature. From the cosmic ray point of view, the effect of correction for such a situation is four fold.

(a) The effective diffusion coefficients will increase by roughly a factor of 2 or more at rigidities $R < R_u$.

(b) The effective correlation length for the cosmic rays will be considerably increased, and hence the lower limit $R_l$ will decrease in value.

(c) In those cases where the observed spectra obey a law other than $f^{-2}$, the subtraction of the $f^{-2}$ spectrum due to the tangential discontinuities would result in distortion of the effective power spectra, with consequent changes in the rigidity dependence of $K_{\|}$ and the mean free path.

(d) Sari and Ness have only considered the more prominent discontinuities in the measured field in setting up their mathematical model. In so doing, they account for at least half of the spectral power. It remains an open question as to how much of the remaining power is introduced by tangential discontinuities below the Sari and Ness threshold. Since any such power will cause an over estimate of $K_{\|}$ to be made, an estimation of the size spectrum of such tangential discontinuities is urgently needed.

## 3. Prompt Solar Flare Events

The prompt flare event characteristically occurs shortly after the observation of a flare at optical, microwave and X-ray wavelengths. Writing the transit time for a particle of energy $E$ along the nominal 1.2 AU Archimedes spiral field line from the Sun as $\tau$, the characteristic properties of the prompt event are:

(1) The time of flight of the first particles to be detected at the orbit of Earth, for a given energy, is comparable to $\tau$.

(2) The intensity rises relatively rapidly ($\lesssim 10\tau$) to a maximum and then decays away smoothly, with time.

(3) The onset time of the event is consistent with the initial particle acceleration being at the time of the hard X-ray burst.

(4) There is well defined velocity dispersion, the particles of highest velocity arriving first. The dispersion is consistent with travel distances of 5–10 AU.

(5) The radiation may be strongly anisotropic at early times in the event, the anisotropy being field aligned. At later times, the anisotropy becomes much less pronounced, and is directed radially away from the Sun ($1 \lesssim T \lesssim 4$ days). At very late times ($T \gtrsim 4$ days), the anisotropy is from a direction $\simeq 45\,^{\circ}$E of the Sun.

(6) The prompt event is normally the only species of particle enhancement observed at ion energies of $\gtrsim 10^8$ eV.

(7) Virtually all the observable properties of the prompt solar event are greatly affected by the position of the parent flare on the solar disc.

These and other properties of the prompt event will be discussed in detail.

### 3.1. Event visibility versus parent flare position

Figure 4a presents representative data regarding the distribution in longitude of the parent flares that have resulted in the observation of ion and electron flare effects. In

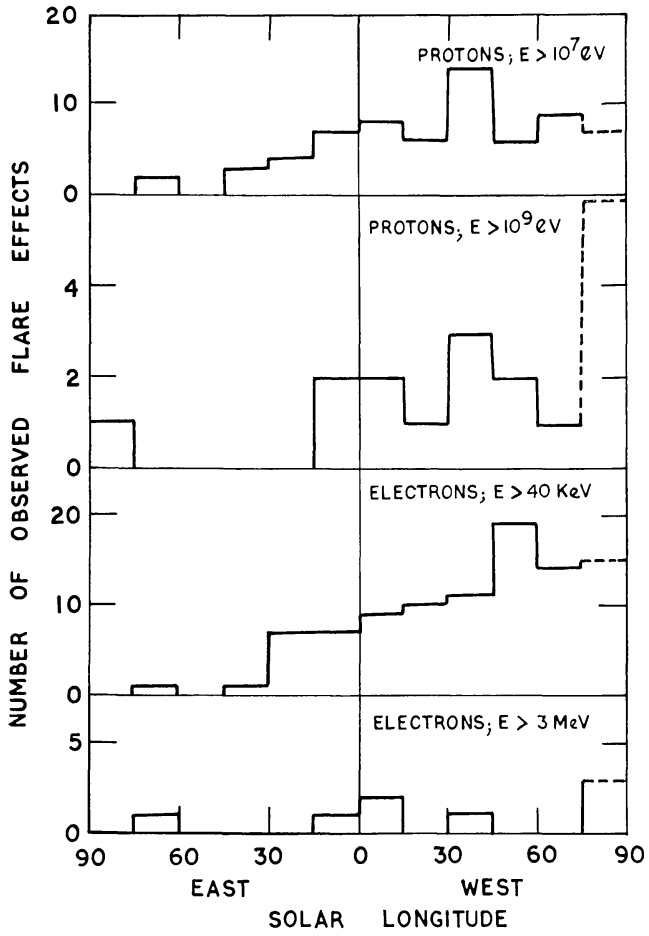


Fig. 4a. The longitude distribution of parent flares that have produced relativistic, and sub-relativistic proton and electron events. Since the determination of longitude is difficult for flares near the limb, and since the upper portion of large flares occurring past the limb will be visible from Earth, and recorded as limb flares, the numbers are unreliable near 90° W. The data are derived from McCracken *et al.* (1967), Lin and Anderson (1967), Lin (1970a) and Cline and McDonald (1968).

each case, the distribution exhibits a pronounced bias to the western solar hemisphere. This was one of the pieces of evidence that provided the first confirmation of the validity of Parker's theory of the interplanetary magnetic field (McCracken, 1962c).

Considering the low energy ion and electron data, both histograms suggest a full width at half maximum (FWHM) of about 120°, and such a FWHM is consistent

with the effects observed at relativistic energies. This indicates that the propagation effects bias the observations in such a way that we only see about 33% of the actual population of events similar to those detected.

As noted above, the histograms for $10^7$ eV protons, and $5 \times 10^4$ eV electrons are not greatly dissimilar. By constrast, the rigidities (and cyclotron radii) for these particles differ by a factor of $\simeq 400$, and consequently, considerable differences in the histograms are to be expected in terms of any process that is dependent upon particle rigidity*.

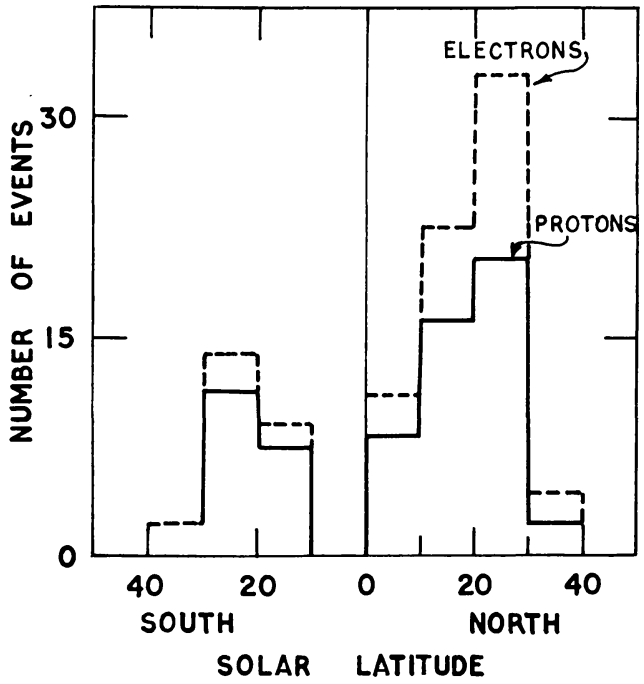


Fig. 4b. The latitude distribution of parent flares that have produced sub-relativistic proton and electron flare effects. The data are derived from Lin and Anderson (1967) and Lin (1970a).

Resonant, or guiding centre transverse diffusion is moderately rigidity dependent ($\sim R$, or stronger), whether it be in interplanetary space, or very close to the Sun. 'Meandering' field line diffusion, (Jokipii and Parker, 1968; McCracken *et al.*, 1967; Fan *et al.*, 1968) and catastrophic distribution processes (e.g. 'Flare' waves in the chromosphere; Athay and Moreton, 1961; Anderson, 1969) are, on the other hand, only weakly rigidity dependent, and would lead directly to the type of independence noted in these statistical data.

From the foregoing, it is clear that the maximum value of the cosmic ray flux must depend on the longitude of the parent flare. This question is examined in Figure 5, using data from two different cosmic ray detectors. In the Lin and Anderson proton data, the maximum intensities in both hemispheres appears to be quite similar, while

* This is not, a priori, completely obvious. The time scale of an event is clearly affected by the transverse diffusion coefficient ($K_\perp$) that applies to the model in question. The dependence of intensity upon $K_\perp$ will come through the escape of the cosmic rays to infinity prior to partaking in appreciable transverse diffusion. An intensity modulation will be produced when the characteristic times for direct escape, and diffusion to the field line of interest become comparable.

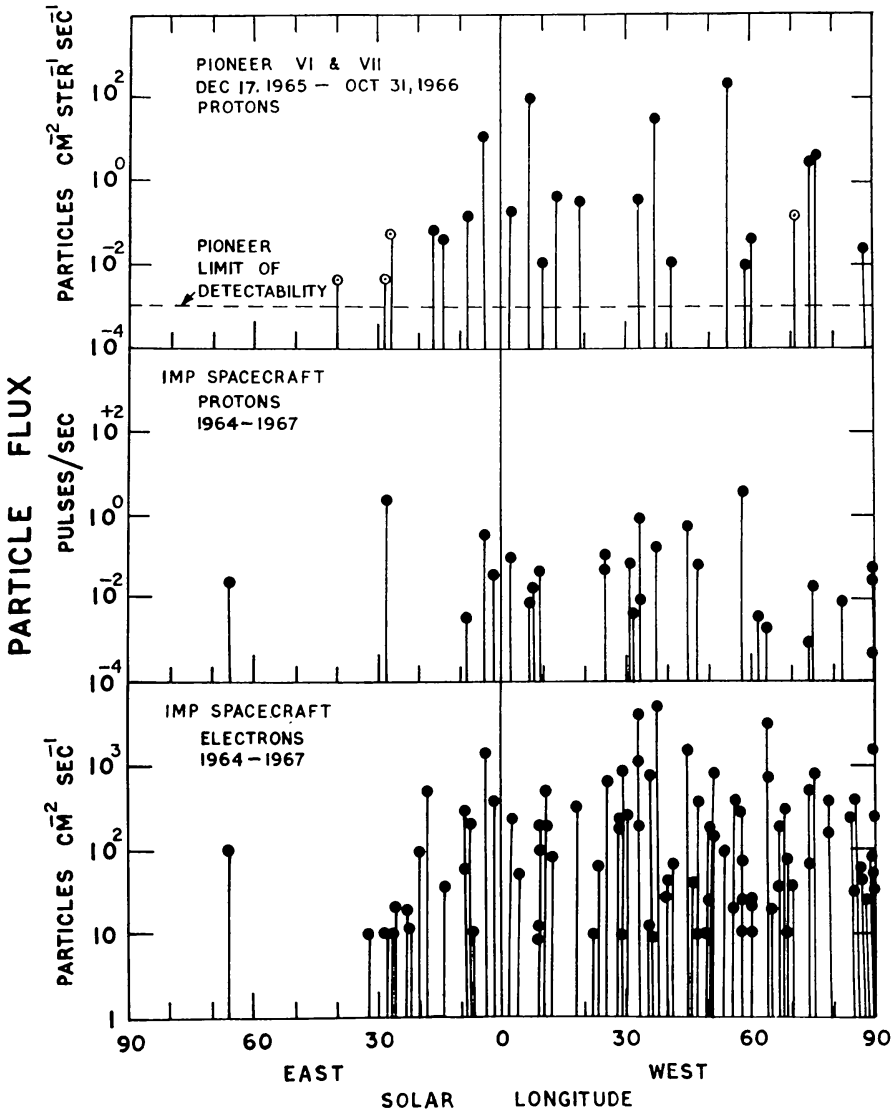


Fig. 5. Demonstrating the dependence of prompt event peak intensity upon solar longitude. All data correspond to sub-relativistic particle energies (Protons $\gtrsim$ 10 MeV; Electrons $\gtrsim$ 40 keV). The data are derived from McCracken *et al.* (1967); Lin and Anderson (1967) and Lin (1970a).

there is an almost complete absence of small events from the eastern hemisphere. We presume that this behaviour is due to the occurrence of two very large cosmic ray flare effects on the eastern disk. By way of contrast, the data of McCracken *et al.* (1967), suggest that the peak intensity falls off by about two orders of magnitude for each 60° of solar longitude (at $\simeq 10^7$ eV). This dependence is crudely in agreement with observations of the same flare effect made by two spacecrafts (McCracken *et al.*, 1967).

Anderson and Lin (1966) and Lin and Anderson (1967) have introduced two classes of prompt low energy electron event, the *C* (complex) and *S* (simple) according to whether or not the parent flare occurs in a solar region that is responsible for the generation of significant Type I radio noise continuum (Kundu, 1965). As shown in Figure 6, the *S* events so defined (i.e. not accompanying Type I) are almost invariably at solar longitudes to the west of 30° W, while the *C* events define a distribution that is

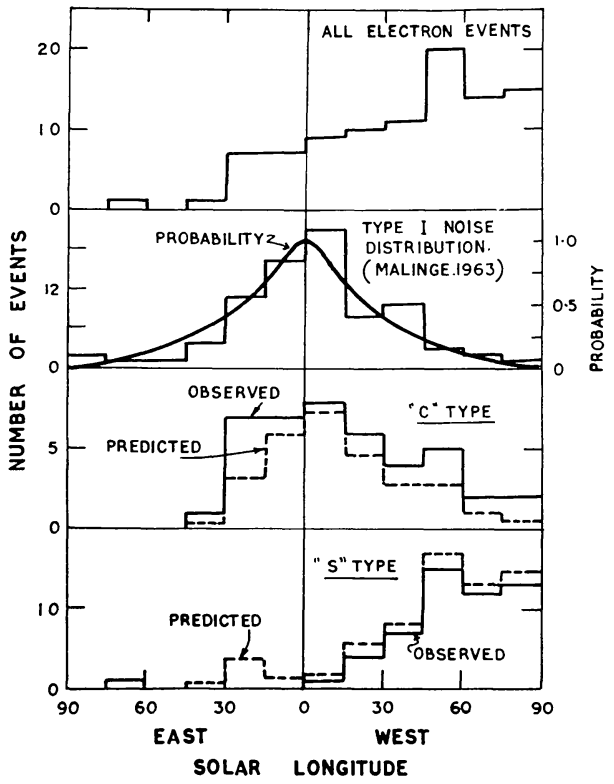


Fig. 6. The observed distributions of electron events, and type I noise continuum as functions of solar longitude. The observed and predicted distributions of $S$ and $C$ type electron events are compared in the two lower graphs.

approximately symmetrical about CMP (Central Meridian Passage). On the basis of these two distributions, Lin and Anderson deduce that the dimensions of the 'cones of propagation' depend critically on whether the parent region exhibits Type 1 continuum emission.

It is our opinion that the differences between the $S$ and $C$ species of events are more apparent than real. Thus it is known that the directivity of Type I radio noise is a very strong function of the longitude of the noise region relative to CMP (e.g. the attenuation for a noise region at 60° relative to the meridian is between 6 and 10 db relative to that when at CMP (page 467, Kundu, 1965)). Consequently, there is a strong bias towards seeing Type I noise regions near CMP, as illustrated by the data of Malinge (1963) in Figure 6. These data can be used to estimate the probability that a given noise region which would be detected at CMP will be seen at any given longitude. Such a probability function is indicated in Figure 6. Clearly, while a region itself may be very noisy, an associated flare event may be classified as an $S$ event if the region is sufficiently far removed from CMP so that the Type I continuum is reduced to the threshold level. This class of $S$ event would then automatically cluster on the western portion of the solar disc, without implying anything about the electron propagation process.

To demonstrate this qualitatively, we have calculated $C(\varphi) = P(\varphi)\, N(\varphi)$ and $S(\varphi) = 1 - P(\varphi)\, N(\varphi)$, the longitude distribution of fictitious $C$ and $S$ events due to

the pre-selection bias introduced by the radio directivity effect alone. In these formulae $N(\varphi)$ is the longitude distribution of all electron events reported by Lin and Anderson (1967) and Lin (1970a) and $P(\varphi)$ is the probability function (Figure 6). These distributions are displayed in Figure 6, and it is clear that they are very similar to the $S$ and $C$ distributions derived from the tabulated data of Lin and Anderson (1967) and Lin (1970a). That is, the marked difference between the $S$ and $C$ distributions which was interpreted as indicating that 55% of all electron events was due to a restricted injection into a $\simeq 16°$ propagation cone can be seen to have been introduced by a systematic bias in the selection criteria, which was unrelated to the cosmic ray propagation process.

The most important result of Lin and Anderson (1967) that electrons are injected into a wide propagation cone of generating angle 45° is of course unaltered by the above considerations. Lin (private communication) also reports other unpublished studies that have established that some of their electron events which were due to parent flares near CMP were not accompanied by detectable Type I continuum noise, these studies being insensitive to the directivity difficulties noted above. On the assumption that the Type I noise event population in 1964–67 was broadly similar to that studied by Malinge (1963), however, it is clear that the incidence of electron generating flares in noise free regions is much less frequent than the 55% of all electron events deduced by Lin and Anderson.

When the distribution of parent flares in heliographic latitude is examined, there is a very marked bias towards the northern solar hemisphere, both in frequency of occurrence, and in mean intensity (see Figure 4b). Thus for low energy proton events in 1964–67, 70% were due to parent flares in the northern hemisphere. For low energy electron events over the same period, 76% originated in the northern hemisphere. However, during this period, and during the previous solar cycle, the frequency of occurrence of solar flares was strongly biased towards the northern hemisphere. For example, 77% of all importance $\geqslant 2$ flares during the period 1964–67 occurred in the northern hemisphere. In our opinion, the evidence is consistent with the hypothesis that there has been a bias for solar flare occurrence and hence particle production processes to occur preferentially in the northern hemisphere, during the past decade, with there being no propagation bias towards either hemisphere.

### 3.2. Intensity distribution of flare events

The frequency of occurrence of flare events is strongly dependent upon the detection threshold of the recording device. To establish this in a quantitative manner, Figure 7 displays the event frequency as a function of $T_d$, the detection threshold normalized to 10 MeV.

$$T_d = T_{E_d} \int_{10}^{\infty} S(E)\, j(E)\, \mathrm{d}E \Big/ \int_{E_d}^{\infty} S(E)\, j(E)\, \mathrm{d}E\,, \tag{3.1}$$

where $T_{E_d}$ is the actual threshold flux for an average flare spectrum of $j(E)$, $E_d$ is the instrumental cut-off energy of the detector, and $S(E)$ is the yield function of the

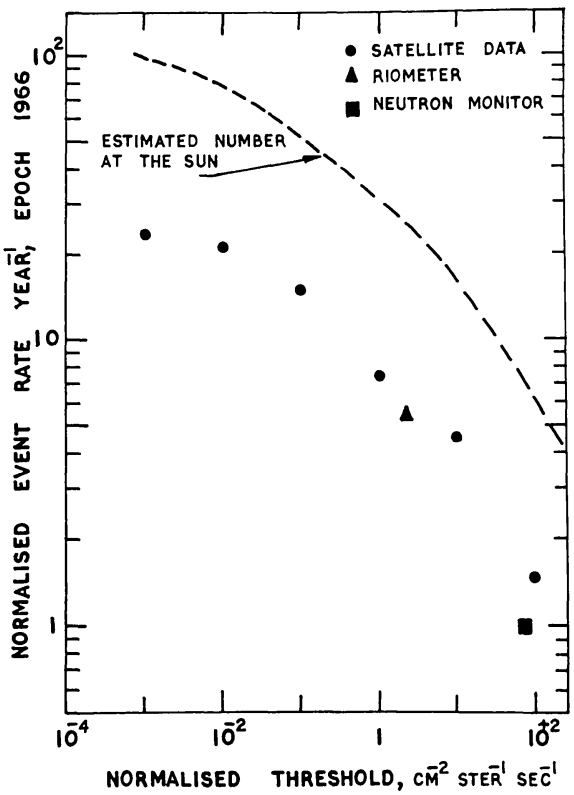


Fig. 7. The estimated annual rate of observance of flare effects greater than a given threshold, plotted as a function of detector threshold, normalised to 10 MeV. The satellite data are from McCracken *et al.* (1967). The dashed line indicates the estimate of the annual rate of occurrence for the whole Sun. These data apply to epoch 1966.

detector. To preserve some degree of homogeneity, the data have been restricted to those with parent flares between 0° and 90°W. The event frequency can be seen to be still rising at the detection threshold of the most sensitive instrument. That is, there is no suggestion in these data that the emission of energetic particles will define a unique class of solar flare.

Allowance for the 0–90° data selection criteria employed above (which approximately matches the selection enforced by propagation effects) yields the estimates of the whole sun event rate for epoch 1966. These estimates indicate that even for 1966 (near solar minimum), the flare effect occurs at a rate of order $10^2$ $yr^{-1}$ at the current sensitivity levels. It is clear from this result that ion and electron events are common features of the solar flare effect.

Figure 7 demonstrates one aspect of a radical change that has occurred in solar cosmic ray studies since 1965. Prior to this date the majority of the substantive facts pertaining to the flare effect had been obtained using neutron monitors. For these, the event rate is low, and since the mean energy of response is high, the data are automatically averaged over small scale interplanetary irregularities (Scale size 0(0.1 AU)). Furthermore, the low counting rates of the instruments mean that relatively few of the observed events provide really definitive data. Consequently, it was practicable to study each of the well observed events individually (there being only about 6

such events), and develop an ad hoc model to accommodate the few substantive facts that could be derived from them. In such models, the human mind was used as the 'filter' to separate the common features from the random aspects of the events. By virtue of the high mean energy of the detector, the models developed in this manner were inevitably pertinent to the average, large scale interplanetary magnetic field.

Nowadays, the situation is greatly different. The annual event rate is great; a large number of the events are well observed; a wide variety of time variability is noted; and since the mean energy of detection is low, small scale facets of the interplanetary regime strongly influence the observations. It has become humanly impractical to study all of the events individually in detail, and 'filter' out the facts of importance in the mind. We believe it has also become futile to study every single event in great depth, thereby building up detailed 'ad hoc' models for each event alone, since the variability from event to event is large (i.e. there is a small signal to noise ratio, where the noise is now the random effects due to the small scale features of the interplanetary field). With the recognition of the existence of stochastical meandering effects; a real possibility of multiple point injection at the Sun; and the very presence of 'noise' in the magnetic field, it becomes clear that future studies of the propagation properties of the solar flare effect must recognise that it, too, is inherently stochastic in nature. That is, the aim is now to derive the properties of the statistical population from which the observed flare effects are drawn. This has now become practicable, since the sample at our disposal (that is, all the flare effects observed to date) is quite large. An example of this trend is the recent introduction of cosmic ray flare effect indices of importance, analogous to the optical importanc of solar flares (Smart and Shea, 1970).

### 3.3. Solar cycle dependence of event frequency

Data demonstrating the temporal dependence of event frequency are presented in Figure 8. Clearly, there is qualitative agreement between the time variations of frequency of low energy ion and electron events, and the usual solar indices.

The fact that the relativistic ion events appeared to avoid years of high sunspot number during solar cycle, 17, 18, and 19 is well known (Carmichael, 1962; Obayashi, 1964). Three small relativistic effects were observed near the maximum of sunspot cycle 20, and might suggest that the avoidance is of periods of high solar activity, as distinct from the period near sunspot maximum, however, even this conclusion must be suspect since the events were so small that they might not have been detected during previous solar cycles.

The proposition that there is an avoidance effect rests most firmly on the cosmic ray and radio observations made during sunspot cycle 19. Boorman *et al.* (1961) and Takakura and Ono (1962) considered the microwave radio bursts observed during this period, and noted that the most intense bursts ($>10^{-18}$ W m$^{-2}$ Hz$^{-1}$ at $\sim$8 cm and 3 cm) behaved in a similar manner to the relativistic ion events: that is, they did not occur during the years of greatest solar activity (1967, 1968). These microwave data, therefore, reinforce the view that high solar activity is not conducive to the most

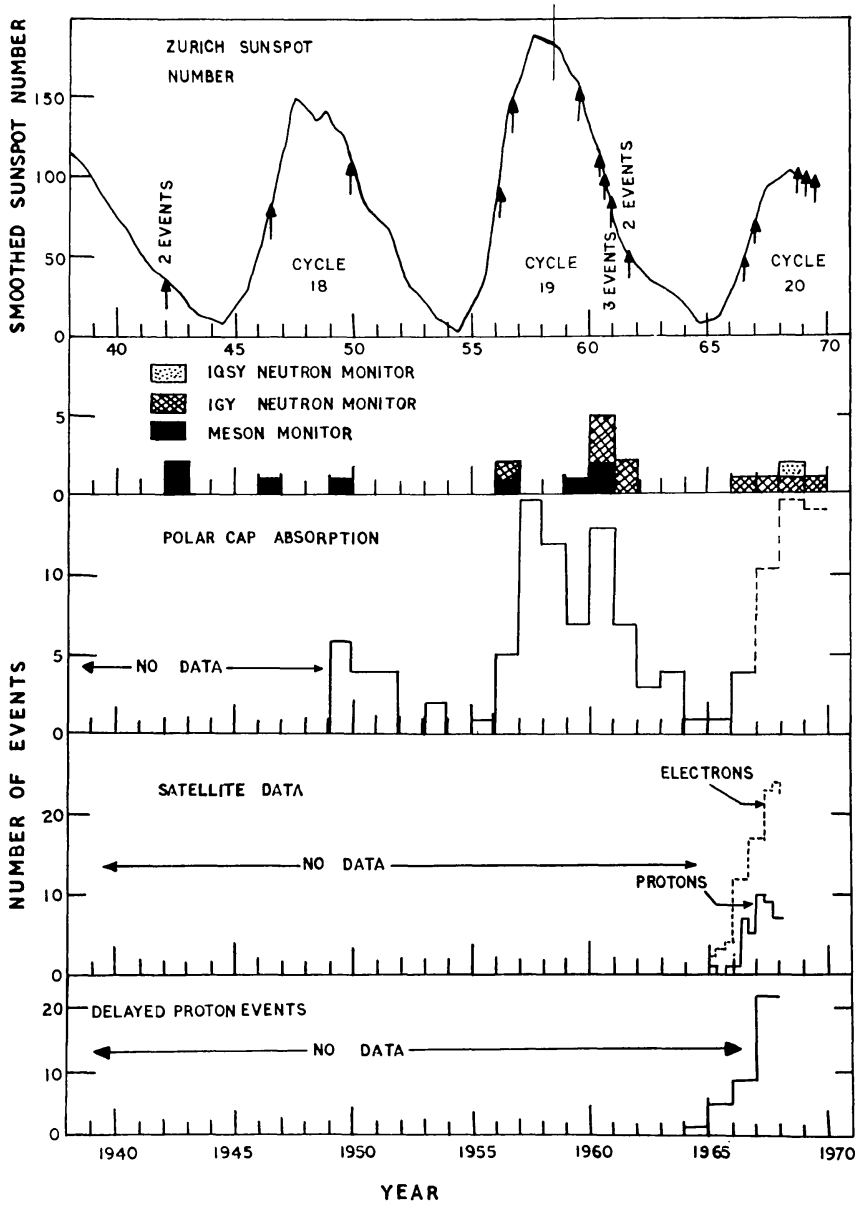


Fig. 8. The frequency of prompt and delayed flare effects as a function of time. The detection thresholds of Meson monitors, IGY and IQSY Neutron monitors differ in the ratio 30:3:1, and the relevant graph indicates the least sensitive detector that observed any given flare event. Thus while relativistic events have been numerically common in sunspot cycle 20, the events themselves have been much smaller than in previous cycles. A fair comparison with cycle 18 would indicate 4 events in that cycle, and no events in cycle 20. Polar cap absorption data are primarily sensitive in the $5 < E < 30$ MeV cosmic energy range. The satellite data are for $E \gtrsim 40$ keV for electrons and $E \gtrsim 0.5$ MeV for ions. The arrows on the top-most graph indicate the times at which the relativistic prompt events have occurred, relative to the sunspot cycle.

effective acceleration of high energy ions and electrons. Švestka (1970) has suggested that under conditions of maximum solar activity the development of the extreme conditions needed for significant $10^9$ V acceleration is prevented by premature initiation of a solar flare by outside influence; e.g. that the flare occurs prematurely as a 'sympathetic flare'.

### 3.4. The time profile of the prompt solar flare effect (1) Early Times

The time profiles of a number of prompt solar flare events at representative energies are displayed in Figure 9. The majority of prompt events exhibit a basically simple time profile, consisting of a rapid rise to maximum intensity, followed immediately by a roughly exponential or power law decay phase. Exceptions to this 'classical' behaviour are observed, however, as are shown in Figure 9. Such behaviour in the case of the ion component is the result of the chance coincidence of a prompt event, and the passage past the observer of a major inhomogeneity in the interplanetary magnetic field. Such modulation is characterised by negligible energy dispersion (that is, the fluctuations are coincident in time at different energies), and correlation with other geophysical phenomena (e.g. Steljes *et al.*, 1961; Bryant *et al.*, 1965a). The enhancements near 20 h, 12 November, 1960 and on 30 September, 1961 in Figure 9 are examples of this phenomenon.

The observation of velocity dispersion is the most characteristic feature of prompt flare events. The electron population is usually observed first, and consequently

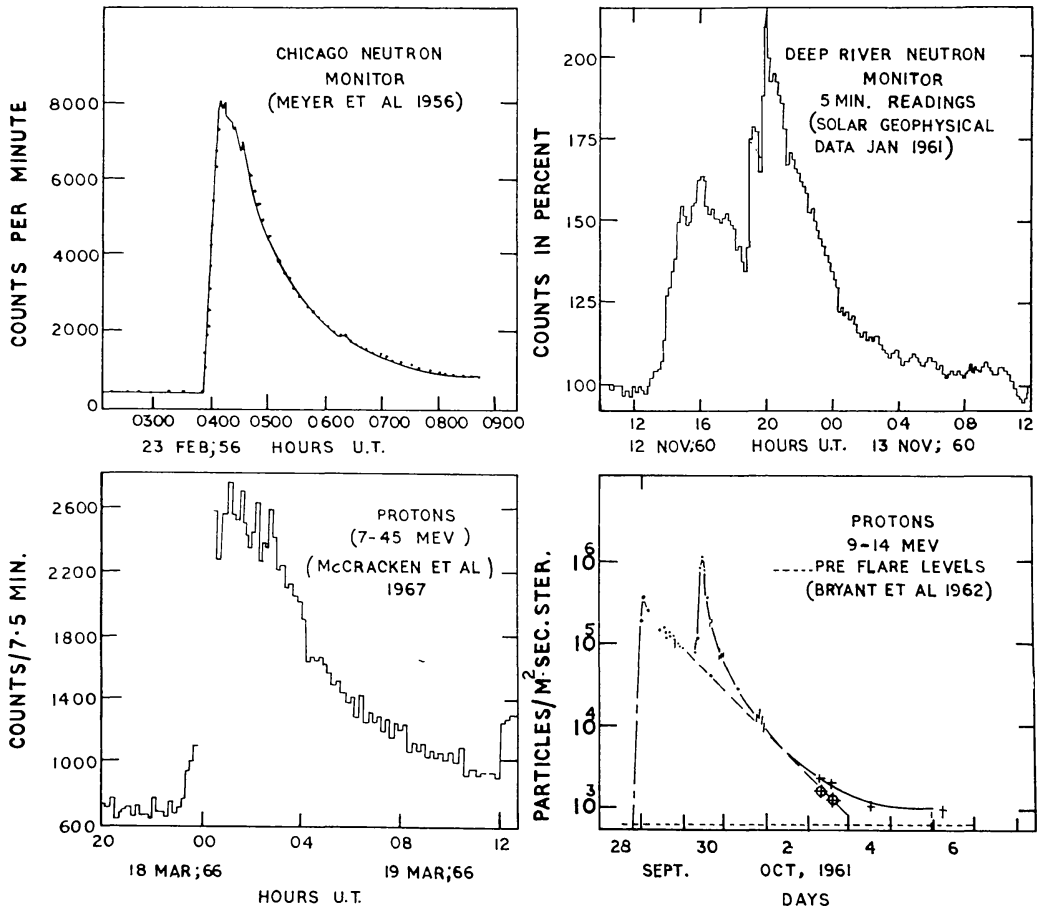


Fig. 9. Time profiles of some typical prompt events. The event of 12 November, 1960 (relativistic energies) is an example of the effect of a major interplanetary inhomogeneity upon a prompt event (Steljes *et al.*, 1961). The event of 28 September, 1961 illustrates a delayed event (an 'energetic storm particle event') superposed upon a prompt event.

electron data are to be preferred in the identification of the parent flare (Anderson and Lin, 1966). The ion components are then observed, in order of descending velocity. The rise times to maximum intensity usually vary approximately as the reciprocal of the velocity.

By plotting the data for a given energy interval against a scale of (particle velocity × true time since the occurrence of the hard X-ray burst) Bryant *et al.* (1962, 1965a) demonstrated that identical curves were obtained for the various particle energies present in the flare effect of September 28, 1961 ($0.18 < \beta < 0.4$). That is, the profiles were identical if plotted against the distance travelled by the particles since their release at the Sun. This indicated that the propagation process was the same at all energies, and that the complexity of the orbits followed by the solar cosmic rays was independent of energy. In terms of a diffusion model, this implied a parallel diffusion coefficient that was independent of rigidity, i.e. $K_{\|} \sim \beta R^{\circ}$, from the vicinity of the Sun to the orbit of Earth.

Other examples of this behaviour have been found, e.g. October 23, 1962 (Bryant *et al.*, 1962, 1965a) and July 7, 1966 (Cline and McDonald, 1968). The latter event (see Figure 10) is particularly noteworthy in that the relativistic electron profile is in good agreement with that of the low energy ions, after the application of velocity compensation. That is, the same propagation conditions are experienced by electrons of $\beta > 0.99$, and ions of $0.18 < \beta < 0.4$, corresponding to a rigidity range of $4 < R < 400$

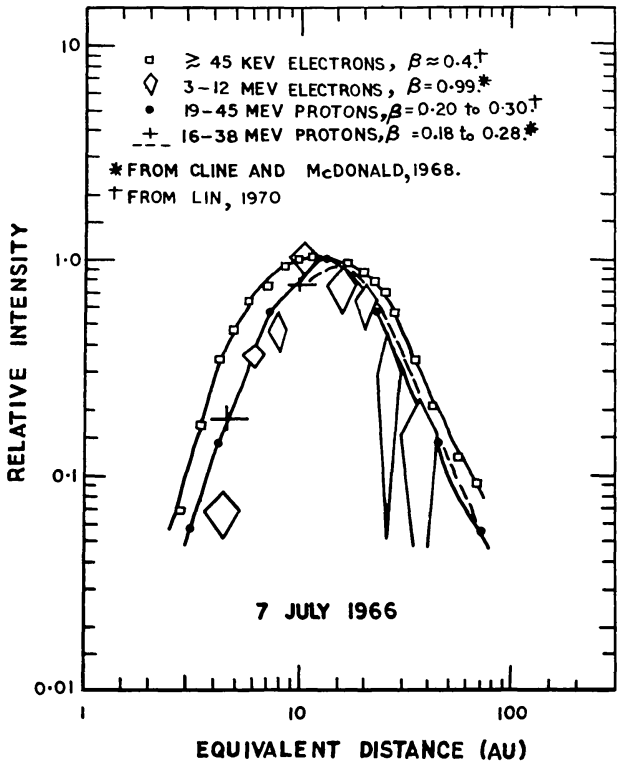


Fig. 10. Illustrating the similarity of time profile obtained for particles of different energy, and species, when the intensities are plotted against (particle velocity × time since particle release from the Sun). See also Bryant *et al.* (1965a). Note that the low energy electron profile shows significant differences to those for the other data. After Lin (1970a).

MV. Note that the electrons are extending this study to *lower* rigidities (and hence smaller gyroradii) than in the case of the ions. To extend this study to these rigidities using ion measurements would necessitate study of 0.01 MeV ions, i.e. ions at near solar wind velocity. The phenomena at these energies would no longer be propagation phenomena; they would be dominated by local convective effects. Hence the electron data are the only means whereby we can examine the Sun-Earth diffusion process at these rigidities and scale sizes.

Lin (1970a) has extended the work of Cline and McDonald (1968) outlined above to lower electron energies ($E \geqslant 50$ keV; $\beta \geqslant 0.42$). He demonstrates that velocity compensation does not cause the low energy electron profile to agree with the profiles pertaining to the other particulate radiations. As Figure 10 demonstrates, the low energy electrons appear consistently ahead of the velocity compensated profile of the other particles. Lin interprets this as evidence that the low energy electrons are being released from a different region on the Sun than are the ions and relativistic electrons, as will be discussed later.

While the foregoing events, in the large, exhibit simple velocity dependent propagation (i.e. $K_{\parallel} \sim \beta R^0$), such is not true for all events. Bryant *et al.* (1962, 1965a) and Cline and McDonald (1968) have discussed the events of 10 September, 1961; 10 November, 1961; and 14 September, 1966 in this regard, and demonstrate a marked departure from simple velocity dependence. They point out, however, that these three events exhibit ragged intensity profiles quite dissimilar from the smoothly varying 'classical' profile. Furthermore, the ragged features are synchronous at different energies. It is therefore certain (Bryant *et al.*, 1965a) that these time fluctuations are of a local nature, being due to spatial inhomogeneities in the cosmic ray density distribution being swept past the observer by the solar wind. It is clearly futile to expect events exhibiting the effects of marked spatial inhomogeneities to respond to the velocity compensation technique even if $K_{\parallel}$ along any tube of force is given by $K_{\parallel} \sim \beta R^0$ (i.e. rigidity independent).

As will be discussed later, studies of the relative abundance of protons and helium nuclei permit examination of the velocity and rigidity dependence of the propagation process. Thus the data at late times in the events of November 15, 1960 and September 2, 1966 (Biswas and Fichtel, 1965) are indicative of an explicit rigidity dependence (i.e. $K_{\parallel} = \beta R^n$ where $n \neq 0$) while the data of November 12, 1960 are consistent with $n = 0$. Paradoxically, the latter 'well behaved' event is the most striking example of the local modulation phenomena that we have in the whole history of cosmic ray research (e.g. Steljes *et al.*, 1961).

Table II summarises the epochs of the various events for which estimates of the $\beta$ and $R$ dependence of $K_{\parallel}$ are available. It will be noted that the velocity compensation technique has been applied primarily to early times in the event, while to date, the proton/helium technique has been applied at late times. It is therefore to be expected that the latter technique will be more sensitive to propagation conditions farther removed from the Sun than will the former. The data obtained to date are therefore not strictly comparable.

TABLE II

Comparison of the epochs during which the properties of the diffusion coefficient have been investigated, using velocity compensation, and charge spectrum techniques.

| Techniques | Event | Epoch employed |
|---|---|---|
| Time profile at different energies | September 28, 1961 | $< 30$ h |
| | October 23, 1962 | $< 10$ h |
| | July 7, 1966 | $< 10$ h |
| Relative abundance of protons and He nuclei | November 12, 1960 | $34^h$ |
| | November 15, 1960 | $51.9^h$, $73.5^h$ |
| | September 2, 1966 | $18^h$, $37^h$ |

Van Allen and Krimigis (1965) have reported similarity of the time profiles of 40 keV electrons and 75 MeV protons in prompt events observed in 1965. While the velocities of 40 keV electrons and 75 MeV protons are similar, their rigidities are widely dissimilar, and hence this event is further evidence in favour of propagation that is independent of rigidity (i.e. $K_{\parallel} \sim \beta R^0$). This led Nathan and Van Allen (1968) to suggest that the magnetic power spectrum varied as $f^{-2}$ for $2.7 \times 10^{-4} < f < 0.5$ Hz (since $P_{SS}(f) \sim f^{-2}$ predicts $K_{\parallel} \sim \beta R^0$). An alternate explanation, due to Jokipii (1968), is that at the rigidities in question the predicted mean free path $(3 K_{\parallel}/\beta c) > L$, the correlation length of the interplanetary magnetic field, and that consequently the diffusion coefficients $K_{\parallel}$ derived from $P_{SS}(f)$ are invalid. He has proposed that in this situation, the mean free path approximates the correlation length, $L$, for all rigidities, i.e. $K_{\parallel} = \frac{1}{3} c\beta L$. This assumption automatically guarantees propagation effects that are independent of rigidity. On the basis of correlation lengths, $L$, similar to those inferred by Jokipii and Coleman (1968) this hypothesis could be valid. However, if the effective value of $L$ is greater as the results of Sari and Ness (1969) might suggest the hypothesis of Nathan and Van Allen would be necessary to explain the observations.

In analysing the flare event of 23 February, 1956 (Figure 9), Meyer *et al.* (1956) demonstrated a good agreement with a time profile based on the solution of a 3 dimensional diffusion equation, in which the diffusion coefficient was a scalar. Their analysis predicted that

$$\ln\left(t^{1.5} \times I(t)\right) = \text{const.} \quad \frac{r^2}{4\bar{D}} \frac{1}{t}, \tag{3.2}$$

where $I(t)$ is the intensity as a function of $t$, the time after the release of the radiation, where $r$ is the distance from the Sun, and $\bar{D} = \frac{1}{3} \beta c \lambda$ is the diffusion coefficient ($\lambda$ is the mean free path). It has subsequently been shown that $I(t)$ frequently shows the predicted linearity between $\ln(t^{1.5} I(t))$ and $t^{-1}$, the slope of the line of best fit yielding values of $\bar{D} = 0$ $(2 \times 10^{21}$ cm$^2$ sec$^{-1})$. A number of the observed values are tabulated in Table III.

It is now abundantly clear that the diffusion coefficient in the interplanetary medium

TABLE III

Diffusion coefficients observed during various events

| S. No. | Event | Energy range | Approximate mean energy | $\bar{D}$ ($\times 10^{21}$) cm$^2$/sec. | Reference |
|---|---|---|---|---|---|
| 1 | Feb. 23, 1956 | 2–4 BeV | 2.5 BeV | 11.0 | Meyer *et al.* (1956) |
| 2 | May 4, 1960 | 2–5 BeV | 2.0 BeV | 5.5 | Charakhchyan *et al.* (1961) |
| 3 | Sept. 3, 1960 | | 500 MeV | 1.6 | Winckler and Bhavsar (1963) |
| 4 | July 18, 1961 | > 40 MeV | 50 MeV | 3.5 | Krimigis (1965) |
| 5 | July 18, 1961 | > 80 MeV | 100 MeV | 2.2 | Hoffman and Winckler (1963) |
| 6 | July 20, 1961 | > 80 MeV | 100 MeV | 3.4 | |
| 7 | Sept. 28, 1961 | > 23 MeV | 30 MeV | 4.8 | Krimigis (1965) |
| 8 | Sept. 28, 1961 | > 40 MeV | 50 MeV | 5.2 | |
| 9 | Sept. 28, 1961 | 55–118 MeV | 87 MeV | 5.2 | |
| 10 | Sept. 28, 1961 | 118–150 MeV | 125 MeV | 6.2 | |
| 11 | Sept. 28, 1961 | 150–200 MeV | 175 MeV | 6.4 | |
| 12 | Sept. 28, 1961 | 200–255 MeV | 220 MeV | 7.3 | |
| 13 | Sept. 28, 1961 | 255–335 MeV | 275 MeV | 7.9 | |
| 14 | Sept. 28, 1961 | 335–500 MeV | 400 MeV | 8.9 | |
| 15 | Sept. 28, 1961 | 200–300 MeV | 250 MeV | 3.8 | Bryant *et al.* (1965) |
| 16 | Sept. 28, 1961 | > 600 MeV | 950 MeV | 5.4 | |
| 17 | April 15, 1963 | > 23 MeV | 30 MeV | 6.5 | Krimigis (1965) |
| 18 | May 25, 1965 | Electrons 40–150 keV | 70 keV | 13.0 | Van Allen and Krimigis (1965) |
| 19 | March 20, 1966 | 7.5–45 MeV | 13 MeV | 3.6 | McCracken *et al.* (1967) |
| 20 | July 7, 1966 | Electrons > 3 MeV | 4 MeV | 3.9 | Cline and McDonald (1968) |
| 21 | Sept. 20, 1966 | 7.5–45 MeV | 13 MeV | 1.4 | McCracken *et al.* (1967) |
| 22 | Sept. 27, 1966 | 7.5–45 MeV | 13 MeV | 1.6 | McCracken *et al.* (1967) |
| 23 | Jan. 28, 1967 | > 1 BeV | 2 BeV | 5.0 | Lockwood (1968) |

is not a scalar, but a tensor. However, Burlaga (1967), Jokipii (1968) and Fisk and Axford (1969) conclude that the above, or a similar equation *, will still hold, provided that the anisotropy of the cosmic radiation is not great (Fisk and Axford set a limit of $\leqslant 30\%$), and provided that $\bar{D}$ is taken as the parallel diffusion coefficient, $K_{\|}$. Table III therefore provides a set of estimates of $K_{\|}$ averaged over the region between the Sun, and a point a few mean free paths outside the orbit of Earth.

The 8 independent values of $K_{\|}$ in Table III for 10 MeV $\leqslant E \leqslant$ 100 MeV range between 1.4 and $6.5 \times 10^{21}$ cm$^2$ sec$^{-1}$. This suggests that they are drawn from a

* Burlaga derives

$$\ln (t^{2.5} \times I(t)) = \text{const.}\,(\Delta\varphi) - \frac{f(D_\varphi, D_r, \varphi, r)}{t}, \tag{3.3}$$

where the slope and intercept of the straight line fit are dependent on the heliocentric angle between the parent flare, and the foot of the line of force through the observer. Since ln $t$ is usually small compared to ln $(t^{1.5} \times I(t))$, there is little practical difference between the two equations.

statistical population of mean $\simeq 3.5 \times 10^{21}$ cm$^2$ sec$^{-1}$ and standard error $\simeq 2.5 \times 10^{21}$ cm$^2$ sec$^{-1}$. We judge this to be a remarkably small standard error in view of the factor of 10 day to day variation observed for the various spot measurements of the power spectral density (Figure 3), and the 0(100) variation noted between measurements separated by a year (Figure 2). If anything, the reverse might be expected, i.e. the variation in observed $K_{\|}$ varying by $>0(100)$ in that the average $K_{\|}$ derived from the flare effect should incorporate a large and variable component due to near-Sun effects. Since the power spectral data have been averaged over 0(1 day), i.e. over a region of scale size $\simeq 0.3$ AU of the interplanetary medium, the Sun-Earth propagation path could encounter $\simeq 3$ independent regions, so the variability in $K$ could be reduced by a factor of $\sqrt{3}$. This is not sufficient to reconcile the measurements.

The paradox might be resolved if a large, and variable fraction of the observed magnetic power has no effect on the cosmic rays. As discussed in Chapter 1, this is the situation suggested by the studies of Burlaga (1969) and the mathematical modelling calculations of Sari and Ness (1969).

It will be noted that the $K_{\|}$ derived from electron data are broadly similar to those for ions, despite the $0(10^3)$ difference in the particle rigidity. This is further evidence for the independence of $K_{\|}$ on $R$. The fact that the value derived from the 150 keV electron data is one of the highest recorded values of $K_{\|}$ may be partially due to the fact that this event is the closest event in this table to a sunspot minimum event (see below).

It is clear from Equation (3.2) that linearity would be destroyed by taking a different origin of time. This therefore provides a technique whereby the instant of injection can be found by a trial and error search for the origin of time providing greatest linearity. Lockwood (1968), and Cline and McDonald (1968) have used this technique* and have achieved results that were consistent with other knowledge. The precision of the estimate of the instant of particle release is $\approx 10^{-1}$ times the rise time of the event.

The time scales of relativistic ion events show variability over a range of 36:1 (McCracken and Palmeira, 1960) which is correlated with the longitude of the parent flare (McCracken, 1962; Burlaga, 1967). This effect is clearly the result of an anisotropic particle propagation. Burlaga (1967) has considered the problem defined by $K_{\|}$ independent of $r$; $K_{\perp} = \text{const. } r^2$; a totally absorbing barrier at 2.3 AU. On these assumptions, he shows that the rise time to maximum intensity $\tau_r$ varies as $\theta_0^2$, where $\theta_0$ is the heliocentric angle between the parent flare, and the foot of the magnetic field line through the observer. The observed dependence of $\tau_r$ on $\theta_0^2$ at relativistic energies is presented in Figure 11a. The flare of July 17, 1959 was observed under extremely atypical interplanetary conditions (Carmichael, 1962) which certainly violated the assumptions of Burlaga's theory. Excluding this data point, a reasonable agreement obtains. Burlaga further shows that his model gives ad hoc agreement to the time profiles of relativistic effects, but that agreement cannot be obtained at non-

* Lockwood used Burlaga's equation; Cline and McDonald used Parker's.

relativistic energies. Such energy sensitivity is possibly due to the fact that at relativistic energies, the gyroradii $rg \gtrsim L$, the correlation length, resulting in a quite different relationship between $K_\perp$ and $K_\parallel$ than pertains at lower energies. While it is clear that much remains to be done in the solution of the diffusion problem as a function of $\theta_0$ using more recent knowledge of $K_\parallel$ and $K_\perp$, Burlaga's treatment serves as a useful guide to the behaviour at relativistic energies.

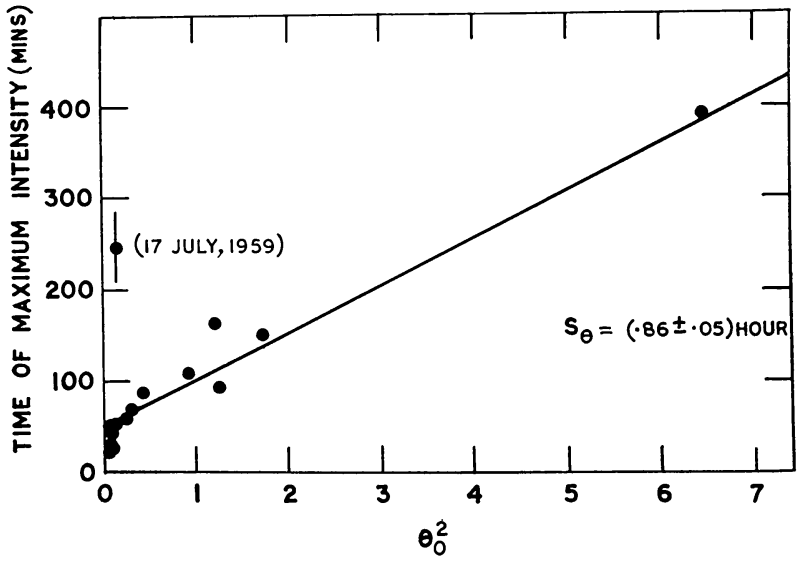


Fig. 11a. The time required for a prompt flare effect to attain maximum intensity, plotted against $\theta_0^2$, where $\theta_0$ is the angular separation between the nominal Archimedes spiral line of force at the Sun, and the parent flare. Based on Burlaga (1967).

Recently Švestka (1970) has pointed out that Burlaga's theory predicts a factor of two higher incidence of flare effects originating in parent flares on the invisible solar hemisphere than has been observed. Further study is necessary to determine whether the more modern knowledge of the interplanetary field permits reconciliation of the theory with the observations.

While Figure 11a shows a modest agreement with theory, it is also clear that the time scales of events with similar values of $\theta_0$ can vary quite widely. Thus the relativistic events of February 23, 1956 and May 4, 1960 show time scales differing by 4:1 (McCracken, 1962), while the values of $\theta_0$, and the pre-event interplanetary conditions (Forbush decreases) were quite similar. In each case, $\theta_0 \simeq 0.5$ radians, and either Equation (3.2) or (3.3) can be used to infer four-fold differences in the parallel diffusion coefficient $K_\parallel$. Such differences are entirely in accord with the variability of $K_\parallel$ noted in Table III, or in the day to day magnetic power spectra.

It has been suggested that there might be large solar cycle variations in the Sun-Earth propagation conditions (from PCA observations, Warwick and Wood-Haurwitz (1962); from satellite observations, Fichtel and McDonald (1967)). The observed data suggest average time scale variations of a factor of 2–4 over the solar cycle, indicating similar variations in $K_\parallel$. In view of the magnetic and cosmic ray evidence that exists

for 0(5) day to day variations in $K_{\|}$, the existence of solar cycle variations would appear both likely on theoretical grounds, and difficult to establish in terms of the small amount of data at hand.

### 3.5. The time profile of the prompt flare effect (2) Late Times

The study of the decay phase of the flare effect is of value in that it provides information on the manner in which the solar cosmic rays escape from the vicinity of the inner solar system. For parent flares occurring within about $\pm 45°$ of the center of the solar disk, the observed decay phase is greatly modified by the passage of a plasma disturbance past the point of observation some 1–2 days after the flare, and by an accompanying delayed particle event, and hence, while useful for studying the properties of the magnetic fields associated with such disturbances, such flare effects are not suitable for study of the escape of the cosmic rays from the interplanetary field averaged over the whole solar system. For such a study, flare effects due to parent flares situated more than 45° from the center of the solar disk that do not produce a plasma disturbance and Forbush decrease at the point of observation are the more desirable.

The study of the decay phase of the flare effect is dominated by convection-diffusion models, such as that originally advanced by Meyer *et al.* (1956). Assuming a homogeneous isotropic,, spherically symmetric and uniformly expanding diffusing region centred on the Sun, and ignoring energy change terms, the cosmic ray density $U(r, T, t)$ satisfies the differential equation

$$\frac{\partial U}{\partial t} + \frac{1}{r^2}\frac{\partial}{\partial r}\left(r^2 V_P U - r^2 K \frac{\partial U}{\partial r}\right) = 0, \tag{3.4}$$

where $T$ is kinetic energy, $V_P$ the plasma velocity, $K$ the diffusion coefficient and $r$ and $t$ have their usual meanings.

Since the solar wind is expanding, the cosmic rays will suffer deceleration, hence an energy change term must be added to the above equation (Parker, 1965). Thus the differential equation becomes (Fisk and Axford, 1968)

$$\frac{\partial U}{\partial t} + \frac{1}{r^2}\frac{\partial}{\partial r}\left[r^2 V_P U - r^2 K \frac{\partial U}{\partial r}\right] - \frac{1}{3r^2}\frac{\partial}{\partial r}(r^2 V_P)\cdot\frac{\partial}{\partial T}(\alpha T U) = 0 \tag{3.5}$$

where $\alpha = (2 m_0 c^2 + T)/(m_0 c^2 + T)$.

The majority of the studies to date have been based on Equation (3.4). If the boundary conditions are (a) impulsive injection near the origin, (b) a spherical symmetric boundary to the diffusing region, beyond which the cosmic rays excape freely, then the decay curve is a power law in time until such time as particles start to escape from the boundary. Once this occurs, the decay becomes an exponential function of time.

At relativistic energies the above behaviour is observed for parent flares on the western portion of the solar disk. However, Burlaga (1967) reports that parent flares

on the eastern portion of the disc exhibit exponential decay curves throughout the decreasing intensity phase. This may simply be a consequence of the slow rise time of such events, the Earth only sampling the radiation at late times when the radiation has already reached the 'boundary'.

At subrelativistic energies, the decay curves tend to be exponential in nature (e.g. McCracken *et al.*, 1967; Fan *et al.*, 1968). The distances to the 'boundary' required to satisfy these decay curves are variable (2–10 AU), and in view of the artificial nature of some of the assumptions upon which the theory is based, these distances must be regarded with scepticism. In this regard, the theory as developed from (3.4) should best be regarded as an indication of the behaviour to be expected with one unique model of the solar system.

At low energies (0 (10 MeV) and less), the cosmic radiation anisotropy at late times is principally convective (i.e. parallel to the radius vector) (McCracken *et al.*, 1968; Forman, 1970a, b). Hence the $\partial U/\partial r$ term in (3.5) can be neglected. For $\alpha=2$ and $V_P=$ $=$const., then from (3.5)

$$U(r, T, t)=\left(\frac{r_1}{r_2}\right)^2\left(\frac{r_2}{r_1}\right)^{4/3} U\left(r_1, T(r_2/r_1)^{4/3}, \quad t-(r_2-r_1)/V_P\right) \qquad (3.6)$$

that is, the cosmic rays are convected outwards with the solar wind, changing their energy as $T/(r)^{4/3}$. With the advent of satellite measurements at different radial distances from the Sun, confirmation of these deceleration effects are practicable (Gleeson and Palmer, 1970). Such effects will cause a flare effect to decay more rapidly than suggested by the more commonly used theory summarised by Equation (3.4).

Forman (1970b) has recently shown that the temporal decay of a flare effect will be exponential, with a time constant of $\tau=3r/2V_p(2+\alpha\gamma)$ for the interval of time for which convective effects dominate (i.e. for $T\gtrsim 1$ day). In the above formula $V_p$ is the solar wind velocity and $r$ is the exponent of the differential energy spectrum. At very late time ($T\gtrsim 4$ days), a sunward diffusion decreases the effective value of the convective velocity to about half the solar wind velocity, and hence the time constant due to convection is about twice that given above (McCracken *et al.*, 1970). The 'convective' time constant at all times $T\gtrsim 1$ day can be written in terms of the anisotropy amplitude $\delta$ and phase $\varphi$ as $\tau=3r/2V\delta\cos\varphi$, where $r$ is the distance from the Sun, and $V$ is the particle velocity.

The observed time decay may be quite different from that computed above. Thus, a dependence of cosmic ray density upon heliocentric longitude $\eta$ will result in a modification to the 'convective' time constant discussed above. If the variation in cosmic ray density $U$ with $\eta$ is characterized by $\mathrm{d}U/\mathrm{d}\eta=U/\eta_0$ at the point of interest where $\eta_0$ is measured in degrees, then it can be shown that the observed time constant, $T$, is related to $\tau$ by

$$1/T=0.54/\eta_0+1/\tau$$

where $T$ and $\tau$ are measured in hours. For $E\sim 10$ MeV the variation with $\eta$ can be mark-

ed, and examples with $\eta_0 \simeq 30°$ have been observed. Two examples of the dependence of cosmic ray flux on $\eta$ are given in Figure 11b. For $\tau \simeq 30$ h, $\eta_0 \simeq 30°$, the observed time constant will either be $\simeq 67$ h or $\simeq$ 19 h, depending on whether the observer is to the West, or the East of the cosmic ray population injected by the parent flare. There is good agreement between the observed values of $T$, $\eta_0$, $\delta$, and $\varphi$ (McCracken *et al.*, 1970).

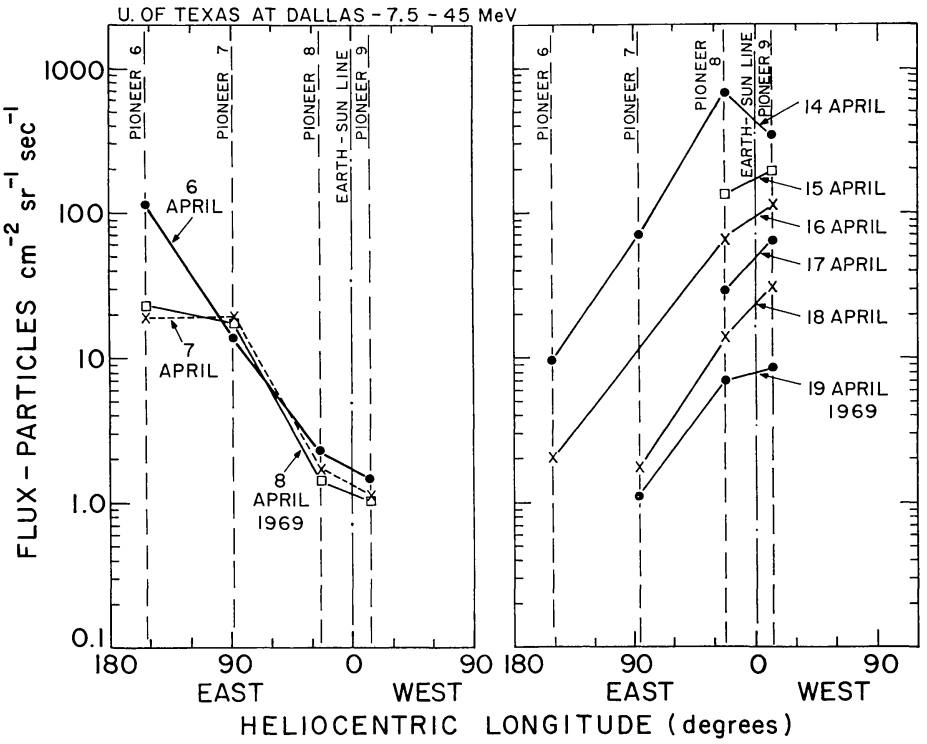


Fig. 11b. The cosmic ray flux as a function of heliocentric longitude at very late times in two flare effects. The data for the period 6–8 April, 1969 illustrate the situation when the observer is on the Western side of the population, so that the increase in flux due to the corotation of the cosmic ray population partially cancels the depletion of the population due to convection and diffusion. The period 14–19 April illustrates the opposite situation, when the observer is on the Eastern side of the population (after McCracken *et al.*, 1970).

### 3.6. Short term fluctuations in the prompt event time profile

Given sufficient statistical precision, the observer detects relatively small amplitude aperiodic fluctuations in the intensity of even 'well behaved' prompt events. Such fluctuations at early times (e.g. November 15, 1960. See McCracken, 1962) are to be expected in terms of particle bounce time phenomena, and in terms of the observer sampling different tubes of force while there are still marked spatial inhomogeneities, both perpendicular and parallel to the magnetic induction vector (e.g. Bartley *et al.*, 1966).

Such variations persist, however, long after the radiation has become essentially isotropic. Bryant *et al.* (1965a) observed quasi-periodic fluctuations at particle energies of $\simeq$6–90 MeV, with time scales of $\simeq$90 min. The fluctuations were phase synchronous throughout the above energy range, and were of rms amplitude $\simeq 7\%$ at 15 MeV.

Stone (unpublished) has studied the short term fluctuations in the prompt event of September 28, 1966, as observed at energies $\gtrsim 7.5$ MeV by the Pioneer VII spacecraft. Aperiodic fluctuations persisted throughout five days of the decay of this event, there being no systematic increase or diminution of the percentage amplitude of the fluctuations with the passage of time. Power spectra for frequencies less than the nyquist frequency (60 cycles per hr) provided no evidence for any favoured frequencies. Other events showed behaviour consistent with the above properties.

The synchronism of the fluctuations at different energies (i.e. lack of energy dispersion) indicates a local origin for the fluctuations (Bryant *et al.*, 1965a). The absence of a decrease in the fluctuation amplitude with time suggests that the fluctuations are not relics of the injection process, since spatial inhomogeneities would decrease over times $\gtrsim 0\,(10^5$ sec). By inference, it appears that they are local fluctuations in the cosmic ray density associated with the presence of small scale irregularities in the interplanetary magnetic field. To verify this hypothesis, correlative studies of the cosmic ray fluctuations and of the magnetic field itself are required.

### 3.7. The charge composition of solar cosmic rays

The presence of nuclei of $Z \geqslant 2$ in the solar cosmic radiation was reviewed in 1964 by Biswas and Fichtel (1965), and will not be treated in depth herein. We will merely mention some recent results, and briefly summarise those facets of the charge spectrum studies that are central to the understanding of the solar cosmic radiation event, as a whole.

The virtue of charge spectra measurements are twofold:

(1) Since $A/Z \simeq 2$ for all nuclei with $A \geqslant 4$, all $He^4$ or heavier nuclei moving with the same velocity will have essentially the same rigidity (and hence the same gyroradii), and will behave identically during propagation through a time independent magnetic field. That is, no dispersive effects can occur, even if $K_{\|} = K_{\|}(R)$. Consequently, the charge spectrum for $Z \geqslant 2$ will be a faithful reproduction of the chemical composition of the solar cosmic rays at the point of acceleration. This proposition gains strong support from the observed agreement between the relative abundances observed in 5 solar flare events, and at several epochs during three of these flares. Four of the events (3 September, 1960; 12 November, 1960; 15 November, 1960; and 18 July, 1961) were reviewed by Biswas and Fichtel (1965); suffice it to say that three separate observations during the fifth flare (2 September, 1966) were in complete agreement with the earlier results, and the interpretations based thereon (Durgaprasad *et al.*, 1968). The average relative abundances for $2 \leqslant Z \leqslant 28$ derived from the totality of data are in good agreement with recent spectroscopic measurements of the photospheric abundances (Table IV).

(2) Protons and $He^4$ nuclei of the same velocity have rigidities that differ by a factor of two. Consequently, any dependence of path length upon rigidity which is introduced by the particle diffusion process* will result in the time profiles of the two

* In a field in which $\sin^2\theta/B$ for a gyrating particle is rigorously constant, the Sun-observer path length is independent of rigidity, although the gyroradius varies as $R$.

TABLE IV

Comparing the chemical composition of solar cosmic rays, and those of the photosphere (or lower chromosphere) and the corona. The various data are normalised to unity (Durgaprasad *et al.*, 1968).

| Element | Solar cosmic rays | Sun photosphere | Sun corona |
|---|---|---|---|
| $2^{He}$ | $107 \pm 14$ | ? | 445 |
| $3^{Li}$ | – | $< 10^{-5}$ | – |
| $4^{Be}$–$5^{B}$ | $< 0.02$ | $< 10^{-5}$ | – |
| $6^{C}$ | $0.59 \pm 0.07$ | 0.6 | 1.3 |
| $7^{N}$ | $0.19 \pm 0.04$ | 0.1 | 0.1 |
| $8^{O}$ | 1.0 | 1.0 | 1.0 |
| $9^{F}$ | $< 0.03$ | 0.001 | – |
| $10^{Ne}$ | $0.13 \pm 0.02$ | ? | 0.11 |
| $11^{Na}$ | – | 0.002 | 0.01 |
| $12^{Mg}$ | $0.043 \pm 0.011$ | 0.027 | 0.20 |
| $13^{Al}$ | – | 0.002 | 0.01 |
| $14^{Si}$ | $0.033 \pm 0.011$ | 0.035 | 0.22 |
| $15^{P}$–$21^{Sc}$ | $0.057 \pm 0.017$ | 0.032 | – |
| $22^{Ti}$–28 | $\lesssim 0.02$ | 0.006 | $\sim 0.1$ |

nuclei being different. That is, the proton/helium abundance ratio for particles of the same velocity would be a function of time.

Biswas *et al.* (1963) and Durgaprasad *et al.* (1968) have demonstrated that the proton/helium ratio was time dependent during the flare events of 15 November, 1960 and 2 September, 1966. That is, the data infer that $K_{\parallel} \sim \beta R^n$, where $n \neq 0$. Durgaprasad *et al.* also show that $n \neq \frac{1}{2}$ and $n \neq 1$ for the latter event. By way of contrast, Biswas *et al.* (1962) deduced that $K_{\parallel} = \beta R^0$ for the 12 November, 1960 flare event (shown in Figure 9). This flare effect was superposed upon one of the largest and best studied Forbush decreases in the history of cosmic ray research, and the Biswas *et al.* results indicate that the Sun-Earth propagation conditions both inside and outside of this major shock front evidenced $K_{\parallel} = \beta R^0$. We note in particular that while the velocity compensation technique cannot be applied if there are spatial inhomogeneities in the solar cosmic radiation, this restriction is not applicable in the comparison of the proton/helium relative abundances, since these studies are made at the same particle velocity.

### 3.8. Anisotropy – ionic radiation

It has long been recognised that solar flare cosmic radiation exhibits pronounced anisotropies (Firor, 1954; McCracken, 1962). The observation that the anisotropy in the flare effect of May 4, 1960 made an angle of 50° to the west of the Earth-Sun line was, in fact, the first experimental confirmation of the validity of the Archimedes spiral model for the interplanetary magnetic field (Parker, 1958; McCracken, 1962c).

Even at the earliest times, however, the pitch angle distribution of the solar cosmic radiation is inconsistent with a perfectly smooth field between the Sun and the Earth.

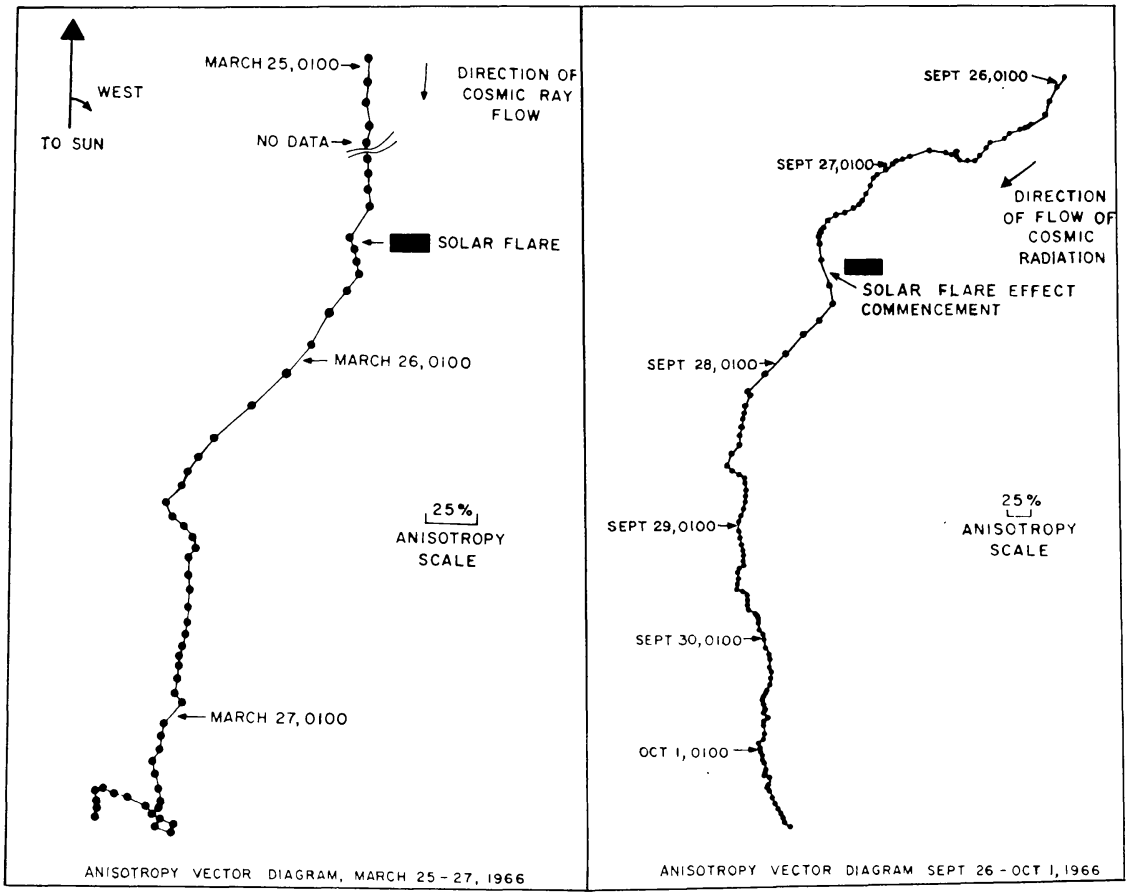


Fig. 12. The anisotropy vector addition diagrams for two prompt events, depicting the overall flow characteristics of the solar cosmic radiation. Hourly anisotropy vectors are plotted. Note that following the two flares the anisotropy is field aligned, and of large magnitude, and that this anisotropy decays into a small, constant ($\sim 7\%$ at 10 MeV) radially directed anisotropy at late times. After McCracken *et al.* (1967).

This is the result of cosmic ray scattering in the small scale irregularities in the interplanetary magnetic field that give rise to the magnetic spectral power at frequencies near $10^{-4}$ Hz.

With the passage of time, the anisotropic nature of the prompt flare event changes. At relativistic particle velocities, the radiation becomes isotropic (anisotropy amplitude $\lesssim 1\%$, McCracken, 1962b), while at non-relativistic velocities, the amplitude of the anisotropy declines asymptotically to a value that is a function of particle velocity (Rao *et al.*, 1967; Vernov *et al.*, 1969), while the streaming vector orients itself radially away from the Sun (see Figure 12). By comparing the anisotropy and the magnetic field data observed by the same spacecraft (Figure 13), it has been demonstrated (McCracken *et al.*, 1968) that the anisotropy vector is aligned with the magnetic field at early times while it's vector direction is independent of the magnetic field at late times ($1 \lesssim T \lesssim 4$ days). It is inferred that at such times, the anisotropy vector is parallel to the solar wind velocity.

This behaviour can be understood as follows (McCracken *et al.*, 1968; Rao *et al.*,

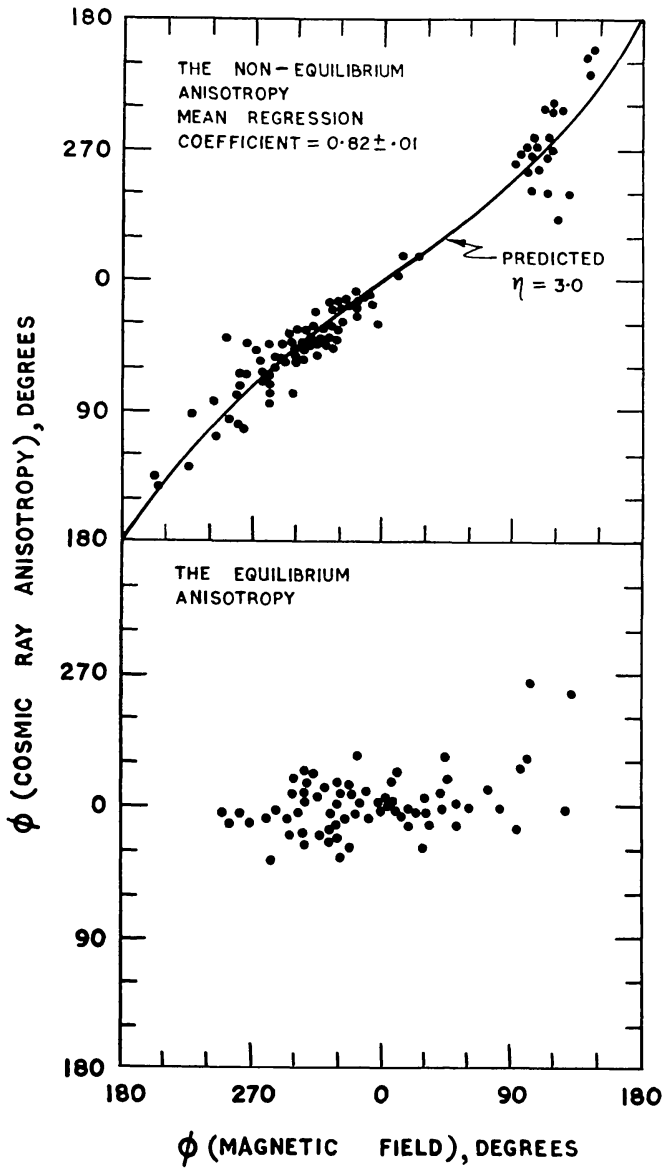


Fig. 13. Illustrating the dependence of the cosmic ray anisotropy direction and that of the interplanetary magnetic field vector. The top diagram corresponds to early times in a flare effect, and the bottom to late times. The solid curve in the top diagram indicates the relationship to be expected for a perfectly field aligned anisotropy superposed on a convective (equilibrium) anisotropy. The bottom diagram indicates that the anisotropy is independent of field direction at late times. After McCracken *et al.* (1968).

1968b). At early times, the collimating effect of the interplanetary magnetic field dominates over the scattering effects, and consequently the particle pitch angles near the orbit of Earth are small, and there are strong density gradients along the magnetic lines of force. Consequently, the particle anisotropy is field aligned. With time, scattering broadens the pitch angle distribution, until the radiation is approximately isotropic in the frame of reference of the moving solar wind (i.e. in the frame of reference of the scattering medium). The observer is moving relative to this frame of reference

and will therefore see an anisotropy given by Forman (1970) to be

$$A = (2 + \alpha\gamma)\frac{V_P}{V}, \tag{3.7}$$

where the differential energy spectrum is assumed to vary as $E^{-\gamma}$, and where $V_P$ and $V$ are the plasma and particle velocities respectively, and $\alpha = (2\,m_0c^2 + E)/(m_0c^2 + E)$. That is, the characteristics of this species of anisotropy are (a) direction is radially away from the Sun; (b) the percentage amplitude is invariant with respect to time. As $E \to \infty$, the above equation tends asymptotically to $A = (2+\gamma)\,V_P/V$, as given by Gleeson and Axford (1968).

Our experience at ion energies $E \approx 10$ MeV indicates that the equilibrium (convective) anisotropy becomes dominant shortly after the maximum of the flare effect has been attained. This is usually some 10–15 h (i.e. 10–15 times the nominal Archimedes spiral propagation time) after the onset of the flare effect. At $\approx 10$ MeV, the equilibrium anisotropy has never failed to appear in prompt events. Figure 14a summarises the available evidence regarding the energy dependence of the effect, and it can be seen that there is general agreement with the convective theory outlined above.

The equilibrium anisotropy provides a method of measuring the 'age' of a particle

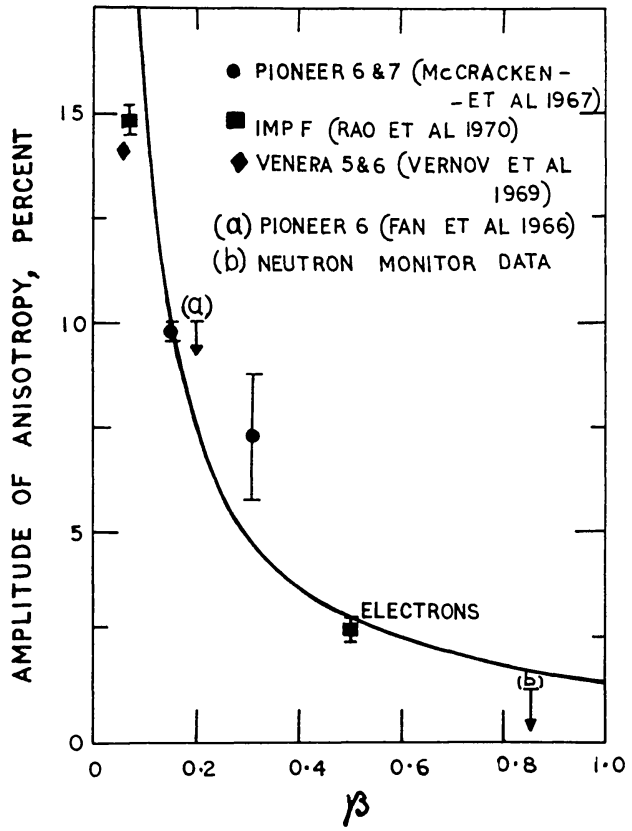


Fig. 14a. The observed amplitudes of the equilibrium (convective) anisotropy plotted against particle energy. No attempt has been made to allow for the fact that these data were obtained at widely different epochs in time. Nevertheless, a reasonable fit to the theoretical $\beta^{-1}$ dependence is noted.

population in the solar system. The experimental data, as well as the relevant scattering theory (Jokipii, 1968) indicate that a field aligned anisotropy will decay within 10–15 h. Consequently, the observation of a field aligned anisotropy indicates that either (a) portion of the population has been released in the vicinity of the Sun within the previous 10–15 h, or (b) that interplanetary effects have resulted in the redistribution of pitch angles to yield an anisotropy within the previous 10–15 h. This can be a useful diagnostic tool in the study of solar cosmic ray effects.

At very late times in a flare effect, ($T \gtrsim 4$ days) the equilibrium anisotropy swings to the East of the spacecraft-Sun line, and tends to adopt a direction $\simeq 45°$E (McCracken *et al.*, 1970). This is illustrated in Figure 14b. This behaviour invariably occurs at very

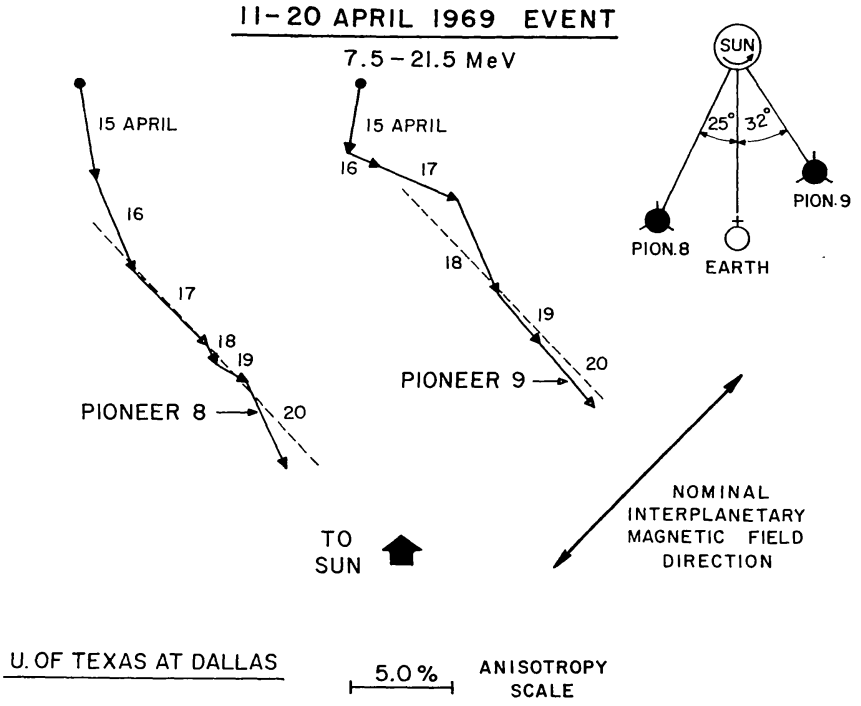


Fig. 14b. The cosmic ray anisotropy vector diagrams for Pioneers 8 and 9 for the decay phase of the flare effect of 11 April, 1969. The dashed line is drawn 45° to the East of the spacecraft-Sun direction (after McCracken *et al.*, 1970).

late times, and is believed to be due to the development of a positive gradient in the solar cosmic ray density.

The earliest stages of a solar flare effect permit study of the scattering process in some detail. The cosmic rays are first observed travelling from the Sun along the interplanetary magnetic field lines; after some time has passed enough particles have been scattered to yield a detectable flux from the opposite direction. Concurrent measurements of both fluxes permit an estimate (McCracken *et al.*, 1967) of the 'back scatter' mean free path $\lambda_b$, while the time profile subsequent to the first few hours yields a measure of the 'diffusion' mean free path $\lambda_d = 3\,K_{\|}/\beta c$ (as per Equation (3.2)). Jokipii has shown that the ratio $\lambda_b/\lambda_d$ of these empirical quantities is a strong function

of the shape of the magnetic power spectrum; e.g.

$$\lambda_b/\lambda_d = \begin{cases} 1 & \text{for} \quad P_{SS}(f) \sim f^{-1} \\ \gg 1 & \text{for} \quad P_{SS}(f) \sim f^{-1.5}. \end{cases} \tag{3.8}$$

This is due to the fact that the power spectral frequency producing maximum scattering for a given particle rigidity varies as $f_0/\mu$, where $\mu$ is the cosine of the pitch angle and $f_0$ is the 'resonant' scattering frequency for $\mu = 1$. (i.e. for which gyroradius $= 0$ (scale size)). The scattering probability is therefore a function of pitch angle. For example, 10 MeV protons 'resonate' at spectral frequencies of $\approx 4 \times 10^{-3}$ Hz when $\mu = 1$, and at $2 \times 10^{-2}$ Hz for pitch angles $\simeq 85°$. Jokipii shows that the scattering probability is independent of $\mu$ in the case of an $f^{-1}$ power spectrum: hence it will decrease with decreasing $\mu$ if the power spectral exponent $< -1$. The scattering will, in fact, slow down greatly when $\mu \simeq 0$, since the gyrating particle is moving very slowly in the $B_{\|}$ direction, and hence only sensitive to high frequency spectral power which is deficient if the spectral exponent is $< -1$.

The experimental data from several flare events in 1966 reveal $\lambda_b/\lambda_d = 0$ (10), which Jokipii considers to be consistent with the $f^{-1.5}$ power spectrum observed by Mariner IV (Figure 2). More detailed studies of this kind would seem to be warranted, especially if it appears that spectra such as observed by Mariner II (varying as $f^{-1}$) are observed sporadically.

It is an observed fact that at relativistic energies, the degree of anisotropy of the solar flare radiation is a function of the longitude of the parent flare (Table V) and that events on the eastern portion of the solar disc tend to be classed as isotropic. In many of these cases, the time to maximum intensity, $t$ is much greater than the 'isotropising' time $t_s$ due to interplanetary scattering (as estimated from events like May 4, 1960, and from the power spectral data). Consequently, the anisotropy automatically varies as $(t - t_f)^{-1}$, where $t_f$ is the instant of flare particle release, for $t - t_f > t_s$. (This is due to the dilution of any anisotropic component by the isotropised relics of radiation observed more than $t_s$ earlier). Since adequate statistical precision is seldom attained until mean near maximum intensity, the dilution effect can be strong indeed, and the majority of the properties of the anisotropy noted in Table IV are possibly the inevitable consequence of the long rise time times.

The situation at low energies is quite different as is illustrated in Figure 15. The particle transit times are short for some parent flares on the eastern hemisphere, and the 'rise time' for the fluxes from the sunward direction are small compared to the isotropising time (McCracken *et al.*, 1967; Fan *et al.*, 1968). Hence the dilution effect is small. The strong anisotropy indicates relatively scatter free propagation from near the Sun to the Earth, the fast rise time that little time was spent in diffusion from the point of production to the foot of the observer's field line.

Fan *et al.* (1968) have argued that near-Sun diffusion is too slow to explain the rapid onset, and have suggested that the meandering nature of the interplanetary lines of force may be the reason for this behaviour. In this view, the observer's field line may have originated far to the east of the theoretical Archimedes spiral position. Anderson

TABLE V

Table of relativistic cosmic ray events

| S.No. | Date | Relative rise time* (in hours) | Position of flare on the disk | Intensity enhancement | Anisotropy | Ratio = highest enhancement / lowest enhancement |
|---|---|---|---|---|---|---|
| 1 | February 28, 1942 | 13 | 4°W | 100% | Poorly defined | – |
| 2 | March 7, 1942 | 7 | 90°W | 1000% | Marked | – |
| 3 | July 25, 1946 | 17 | 15°E | 1200% | Not noticeable | – |
| 4 | November 19, 1949 | 6 | 70°W | 600% | Very marked | – |
| 5 | February 23, 1956 | 4 | 80°W | 2500% | Marked | 6 |
| 6 | August 31, 1956 | 1 | 15°E | 2% | – | – |
| 7 | July 17, 1959 | 36 | 30°W | 5% | None | – |
| 8 | May 4, 1960 | 1 | 90°W | 200% | Very marked | 15 |
| 9 | September 3, 1960 | 50 | 90°E | 3% | None | – |
| 10 | November 12, 1960 | 20 | 10°W | 100% | Poorly defined | 2.5 |
| 11 | November 15, 1960 | 6 | 45°W | 150% | Very marked | 50 for first 45 mts |
| 12 | November 20, 1960 | 1 | 90°W | 6% | – | – |
| 13 | July 18, 1961 | 1 | 50°W | 15% | Isotropic | – |
| 14 | July 20, 1961 | 1 | 90°W | 5% | Very marked | 10 |
| 15 | July 7, 1966 | 1 | 45°W | 2.5% | Not very marked | – |
| 16 | January 28, 1967 | 3 | 60° beyond Western limb | 18% | Isotropic | 1.1 |
| 17 | September 29, 1968 | 1 | 52°W | 1.5% | Isotropic | – |
| 18 | November 18, 1968 | 1 | 87°W | 12% | Not marked | 2 |
| 19 | February 25, 1969 | 1 | 37°W | 15% | Marked | 4 |

* Rise time is the time interval between the commencement of enhancement and the time for reaching the maximum intensity.

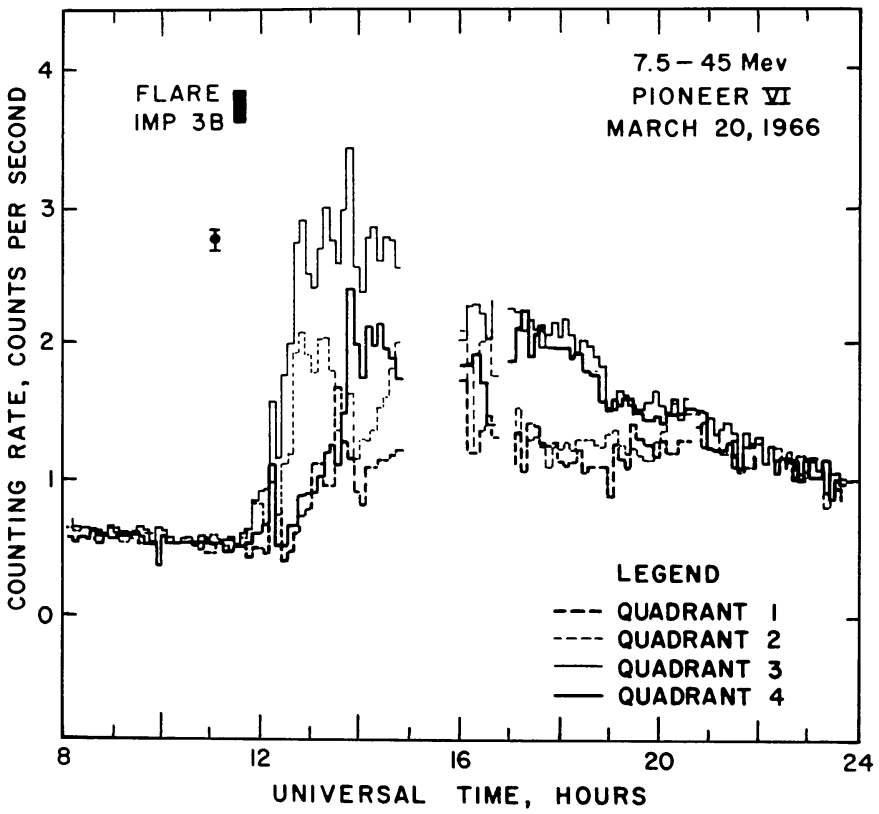


A SOLAR FLARE EFFECT AS SEEN BY ALL FOUR QUADRANTS OF PIONEER VI

Fig. 15. A prompt event that was observed following a solar flare that occurred at 16°E of CMP. Note the rapid transit times (cf. 56 min for direct Sun-Earth propagation) and the strong and persistent anisotropy. Quadrants 1 through 4 counting rates refer to fluxes arriving from the following directions (1) anti-Sun, (2) Earth orbit retrograde, (3) Sun, (4) Earth orbital velocity. After McCracken *et al.* (1967).

(1969) does not accept this view on the grounds that there is frequently more than one active center on the solar disc, and that he can 'see nothing that would allow one center to spread its lines above all the others'. We observe that if there is mixing of the lines of force from a active region with those from far outside the active region (as required by Fan *et al.*, 1968), and since the interplanetary transverse diffusion coefficient is small (Jokipii, 1968; Lin *et al.*, 1968), then the time profile or the prompt flare effect should show strong modulation as the motion of the solar wind causes the observer to sample tubes of force from inside, and outside the active region. This is not seen. In our opinion, the sum total of the evidence suggests that meandering does not result in major mixing effects between active centers, and in particular, that it cannot explain the rapid onset of flare effects when the parent flare is near 30°E of CMP.

An alternate suggestion is that although the flare showing time correlation with the particulate event is far removed from the observer's line of force, acceleration of particles to suprathermal energies has occurred on or near that line of force. One such example would be 'sympathetic' flares, however, such should be apparent in the solar

patrol. Recent studies at radio wavelengths, to be reviewed in Section 6, clearly establish that coronal shock waves frequently travel over $>90°$ of the solar disc, and then trigger non-flare phenomena that generate new shock waves, and type IV radio emission, indicative of the generation of a second population of near-relativistic electrons. It is very unlikely that the triggered events would be noted by the flare patrol. The propagation velocities of the shock waves observed to date are in the range 1000–2000 km $sec^{-1}$, hence the time delays inherent in a 'triggered release' 90° away from a flare would be 6–12 min. Such time delays are completely consistent with the observations at low energies ($\lesssim$10 MeV), where the data of concern have been obtained. In our opinion, sequences of solar phenomena such as occurred on February 25, 1968; May 4 and 6, 1968 (Wild *et al.*, 1968; Labrum and Smerd, 1968) leave no doubt that such 'remote' triggering does occur, and that such must contribute to the cosmic ray behaviour. It remains to determine whether all anomalous events can be explained in this manner.

While such a model should also admit the possibility that a fast rise time event might be observed at relativistic energies due to such a 'triggered release', we deem the absence of such an observation to be of little consequence at present, since (a) the sample of relativistic events is small; (b) the occurrence of an acceleration process effective enough to generate relativistic protons would almost certainly produce optical emissions due to particles impinging on the photosphere (as Elliot has advocated (1964, 1969)), which would be classified as a flare. The fast rise relativistic event would then tend to be associated with this latter 'flare' effect.

In the last analysis, the test of this secondary injection model will depend on comparison of cosmic ray, and radio measurements of high temporal and spatial resolution. See Section 6. This still remains to be done.

### 3.9. Anisotropy – electrons

In discussing the destruction of the initial anisotropy of the ionic radiation, we have quoted Jokipii's conclusion that the scattering probability decreases rapidly with decreasing scale size for power spectra steeper than $f^{-1}$. The power spectra themselves, and the large values of $\lambda_b/\lambda_d$ observed in practice (Equation (3.8)) indicate that the scattering probabilities do normally decrease strongly with decreasing scale size. That is, the magnetic field appears to become increasingly smooth for particles of progressively lower energy.

Since the gyroradius of a 70 keV electron is $0(10^{-2})$ that of an 0(1 MeV) ion, such electrons will suffer 'resonate' scattering for scale sizes some $10^{-2}$ smaller than those applicable to the lowest energy ionic radiation studied to date. They 'resonate' at power spectra frequencies of 0(0.5 sec). If then the power spectrum of the interplanetary magnetic field is steeper than $f^{-1}$ between $10^{-2}$ and 1 Hz (an unexplored region of the power spectrum), the scattering probability would be expected to be very small for electrons. Hence strongly collimated anisotropic beams of cosmic ray electrons would be anticipated.

The evidence, although somewhat conflicting, suggests that such is not the case.

Thus detailed anisotropy measurements of some sixteen prompt electron events using the Explorer 34 spacecraft indicate that the degree of anisotropy of the 70 keV electron flux is in general less pronounced (by a factor of 2 or 3) than that of the ionic radiation of O(1 MeV) observed by the same spacecraft (Rao *et al.*, 1969; Allum *et al.*, 1970). The electron radiation for one event (October 30, 1967) has shown a pronounced (50%) anisotropy at early times, but this then decayed to an anisotropy of $\lesssim 20\%$ within 60 min. This suggests that the destruction of the electron anisotropy proceeds much more rapidly than in the case of O(1 MeV) ionic radiation (of order several hours). The decay time of the anisotropy is in accord with the predictions of Fisk and Axford (1968).

Anderson and Lin (1966) and Lin (1968) obtain results at variance to those quoted above. They use data from two geiger counters, and also a lunar occultation technique to infer very strong anisotropies. Thus Lin infers from lunar occultation observations that $\gtrsim 90\%$ of the electrons in two prompt events were proceeding outwards along the interplanetary field lines. We suggest, however, that the argument that Van Allen and Ness (1969) used to explain the lunar shadowing in the magnetotail can equally well explain the solar electron occultations outside of the magnetosphere, even though the electron flux might be isotropic. Thus the small $k_\perp$ applicable to the interplanetary magnetic field means that there is little transverse diffusion, and hence the cavity between the Moon and the magnetosphere will be inaccessible to solar electrons. It will be rapidly 'drained' of the electrons therein (0 (5 sec)), and hence the deep electron shadows produced, even though the radiation in interplanetary space is isotropic.

Lin (1970b) has suggested that the tendency towards isotropy noted by Rao *et al.* (1969) and Allum *et al.* (1970) might be a local effect, due to an anisotropic flux of electrons being scattered and rendered isotropic by shock waves proceeding up stream from the magnetopause. That is, he envisages a local diffusing region on the sunward side of the Earth that would destroy any interplanetary electron anisotropies. Such a model would, however, suggest that the electron flux would always be isotropic. The fact that the event of October 30, 1967 was initially strongly anisotropic would therefore require that the near Earth diffusing region had dissipated prior to the flare, and then had been re-established $\sim 60$ min after the flare occurred. We might, on such a premise, also expect to see transient anisotropies appearing and disappearing during an electron event (i.e. not synchronous with the flare onset). Such events have not been seen during the 16 events studied to date. We consequently feel that the small anisotropy of the electron flux is unlikely to be the result of such a near-Earth scattering process.

We therefore conclude that the electron fluxes are remarkably isotropic, and that this is due to interplanetary scattering. The consequences insofar as the properties of the interplanetary magnetic field are concerned remain to be explored.

At late times, the electron flux shows a convective anisotropy consistent with the understanding of this phenomenon derived from the ionic events. Thus the electrons of energy $\gtrsim 70$ keV ($\beta \approx 0.5$) exhibit a 2.6% convective anisotropy (Allum *et al.*, 1970) which agrees with the $\beta^{-1}$ dependence predicted by Equation (3.4). Figure 14a shows

this agreement for both the electron and ionic radiation. As in the case of the ionic cosmic radiation, the electron anisotropy at very late times is also directed from 45 °E of the Sun (Allum *et al.*, 1970).

## 4. Delayed Events

A number of authors have recognised the existence of solar cosmic ray phenomena which are distinctly different from the prompt events discussed previously. A number of different phenomenological categories of such events have been advanced, however, following Anderson (1969), we adopt the view that much is to be gained by discussing the several categories together, since it appears likely that the various species of events may be generically related.

The basic properties of delayed events can be stated as follows:

(1) They are either observed late in the decay phase of a prompt event as a gross enhancement above the established decay curve, or in complete isolation from either a prompt event, or a solar flare.

(2) There is a strong tendency towards association with depressions in the intensity of the galactic cosmic radiation. The more prominent time changes in the delayed

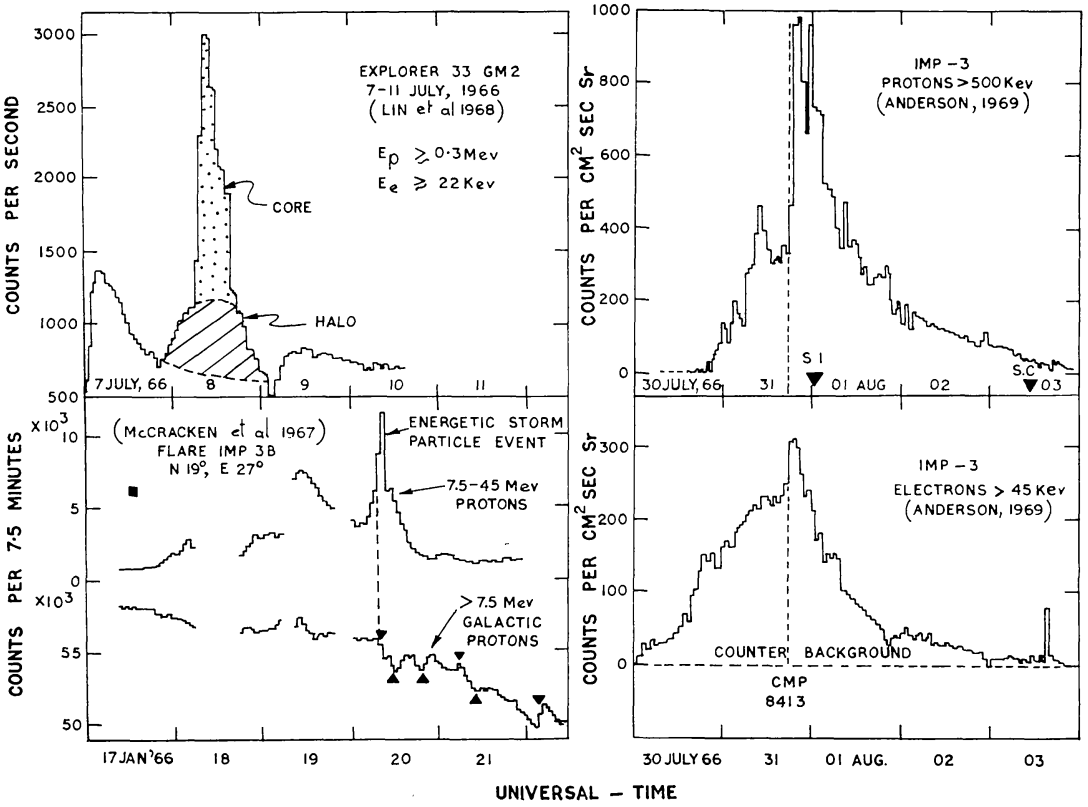


Fig. 16. The time profiles of three delayed events. The events of 8 July, 1966 and 19 January, 1966 are delayed events superposed on prompt events. The former is the original example of a 'core-halo event', the latter is a typical 'energetic storm particle event'. The event of 31 August, 1966 is observed in isolation from a recognisable parent flare. Note the manner in which the electron event develops prior to the proton event. This is an example of electron-proton splitting.

event often exhibit a loose time correlation with marked geomagnetic and solar wind variations, and with the onset phase of a Forbush decrease.

(3) The time profiles are markedly dissimilar from that of the 'classical' flare effect. Two subdivisions can be made: (3a) those delayed events in which the intensity varies relatively smoothly with time, e.g., the halo of Lin *et al.* (1968); the proton regions of Fan *et al.* (1968) and Rao *et al.* (1970), or the recurrent events of Bryant *et al.* (1965b). See Figures 16 and 17. (3b) those events in which the intensity varies rapidly and erratically with time, as exemplified by (I) the energetic storm particle event (Bryant *et al.*, 1962, 1965a; Rao *et al.*, 1967), (II) the spike-like enhancements at low energies ($\sim$1 MeV) associated with magnetic sudden storm commencements (Palmeira *et al.*, 1970), and (III) the core event (Lin *et al.*, 1968).

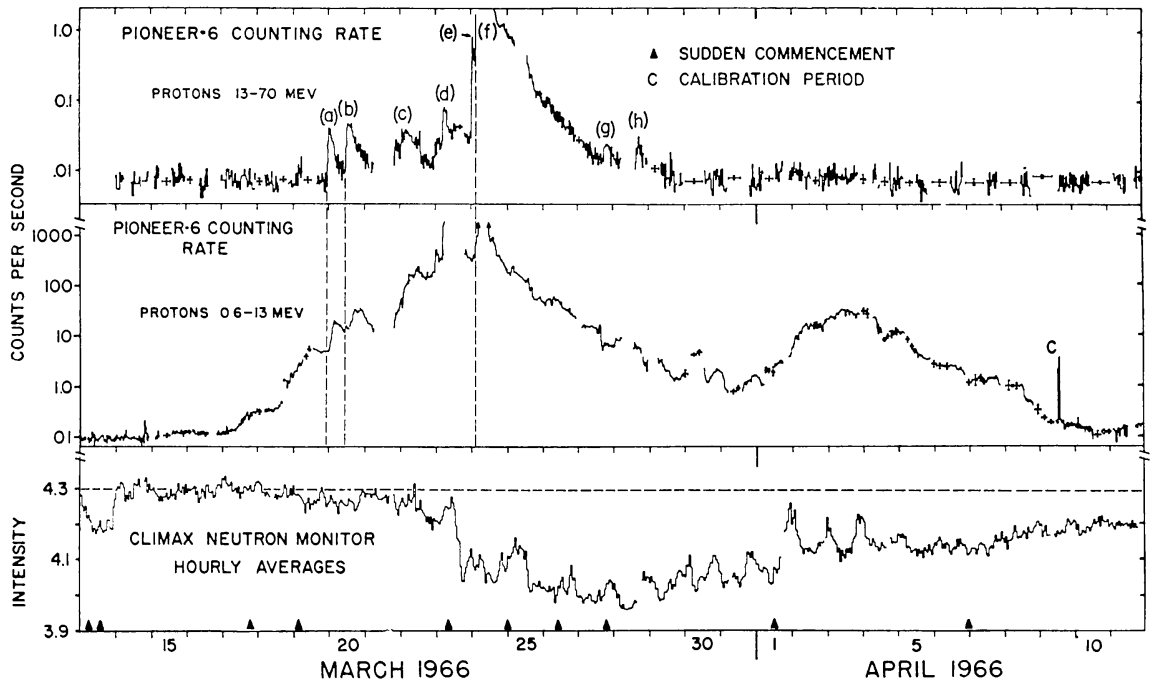


Fig. 17. Illustrating the cosmic ray behaviour at 0 (1 MeV); 0 (10 MeV); and 0 ($10^4$ MeV) during the transit of a well developed active centre across the solar disc. Note that while the behaviour at 10 MeV is impulsive, at 1 MeV the impulsive nature has almost completely disappeared. After Fan *et al.* (1968).

(4) The radiation exhibits strong, field aligned anisotropies over long ($\geqslant$1 day) periods of time in the (3b) class of delayed events.

(5) The energy spectrum of the radiation in the delayed event is considerably steeper than that of the prompt flare effect. The delayed event is rarely seen at energies $\gtrsim$ 20 MeV. while it is commonly the most prominent solar cosmic ray variation at $E \lesssim 5$ MeV, These and other features of the delayed event will now be discussed in more detail.

### 4.1. Energy spectrum

The delayed event is observed principally at low particle energies ($\lesssim$20 MeV for ions). When observed superposed upon a prompt event as in Figure 16, the prompt event

exhibits the normal 'classical' time profile at higher energies, while the delayed event dominates at low energies. That is, the spectrum of the delayed event radiation is steeper than that of the prompt event, as is shown in Figure 18. When observed in isolation from a prompt event, the delayed event will usually be seen exclusively at low ($\simeq 1$ MeV) ion energies, the higher energy portion of the spectrum ($\gtrsim 10$ MeV) being unaffected, or even exhibiting a decreased particle flux due to the accompanying Forbush decrease. See Figure 17.

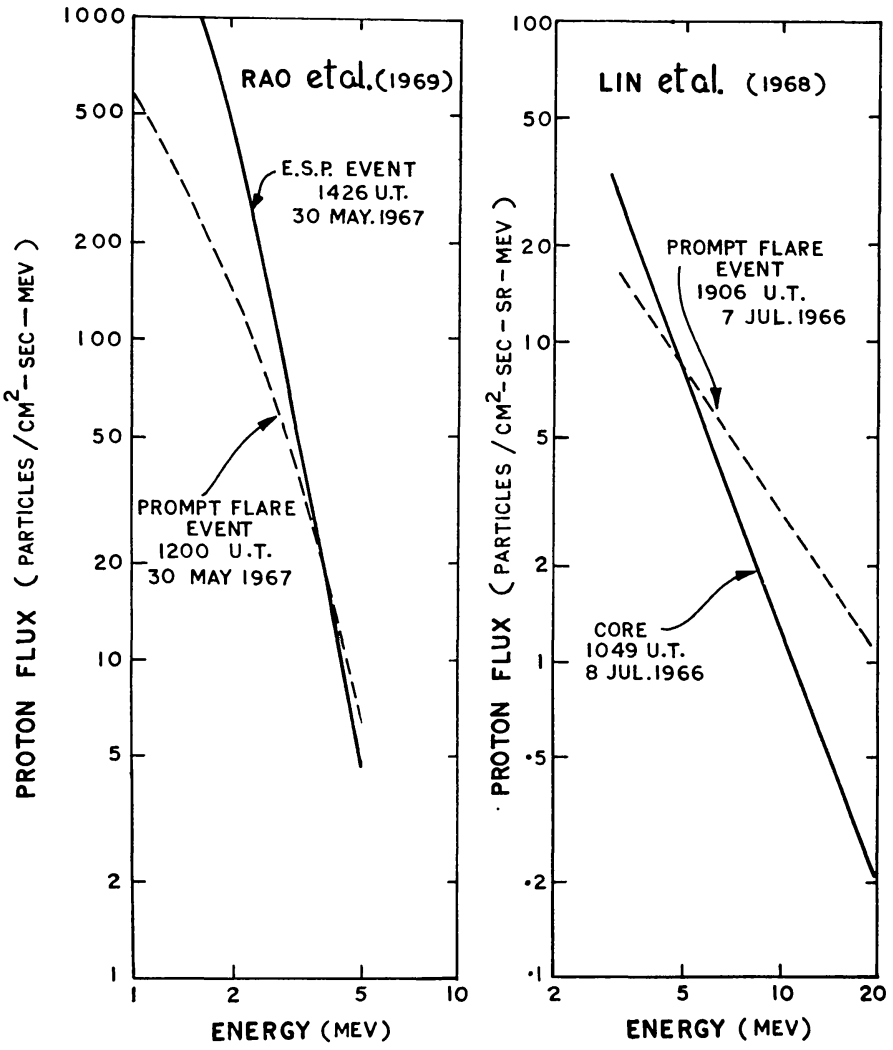


Fig. 18. The energy spectra of correlated prompt and delayed events as observed by Lin *et al.* (1968) and Rao *et al.* (1969). The spectra have been taken as close together in time as is possible to avoid spurious effects. It will be noted that in each case the delayed event exhibits the steeper spectrum.

The detailed nature of the delayed event is a strong function of energy. This is well illustrated by the comprehensive observations of Anderson (1969), as illustrated by the event in Figure 19. The differences are marked: the $>15$ MeV ionic radiation and the electron data exhibit single, non-synchronous (and not even overlapping) peaks; the $\sim 1$ MeV ionic data exhibit two peaks. The energy spectrum of the ionic compo-

nent clearly changes abruptly at about the time of the geomagnetic sudden storm commencement. Furthermore, Anderson (1969) reports that while the delayed event is normally seen in both the ionic and the electron components of the cosmic radiation, there are occasions on which one will be observed to the exclusion of the other. These several observations illustrate the inadvisability of basing models on one species of data alone: clearly there are features of the physical process occurring on December 12–14, 1966 (Figure 19) that are not even hinted at by any one of the data species, alone.

### 4.2. The profile of the delayed event

Both slow and fast temporal variations are observed during delayed events, both

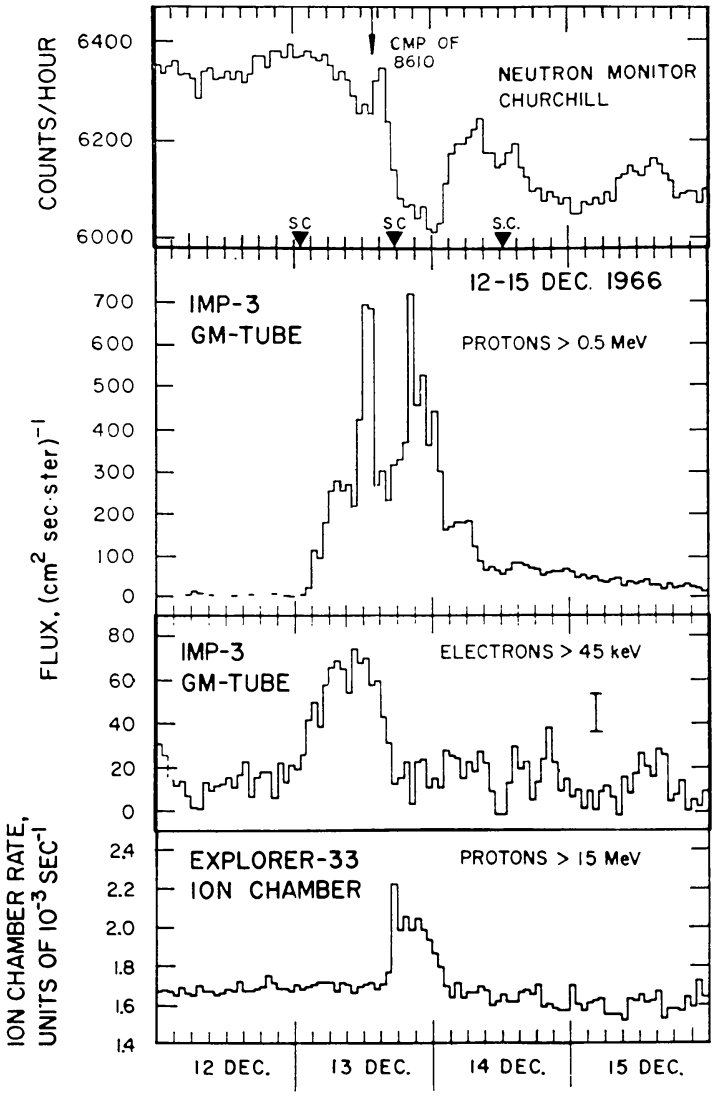


Fig. 19. Illustrating the marked dependence upon energy and particle species event in delayed events. Note particularly the marked differences between the time histories of the electron and $> 15$ MeV proton data. This event is an example of the 'proton-electron' splitting phenomenon. These data are from Anderson (1968).

modes being distinctly different from the classical 'prompt event' profile. The events of 17 January, 1966, 8 July, 1966, and 31 July, 1966 displayed in Figure 16, and that of 18–30 March, 1966 in Figure 17 are typical.

Lin *et al.* (1968) have proposed that the temporal fluctuations during the 8 July, 1966 event (Figure 16) can be usefully considered as two superposed phenomena, the halo variation (slowly time varying) and the core (rapidly, erratically varying). A

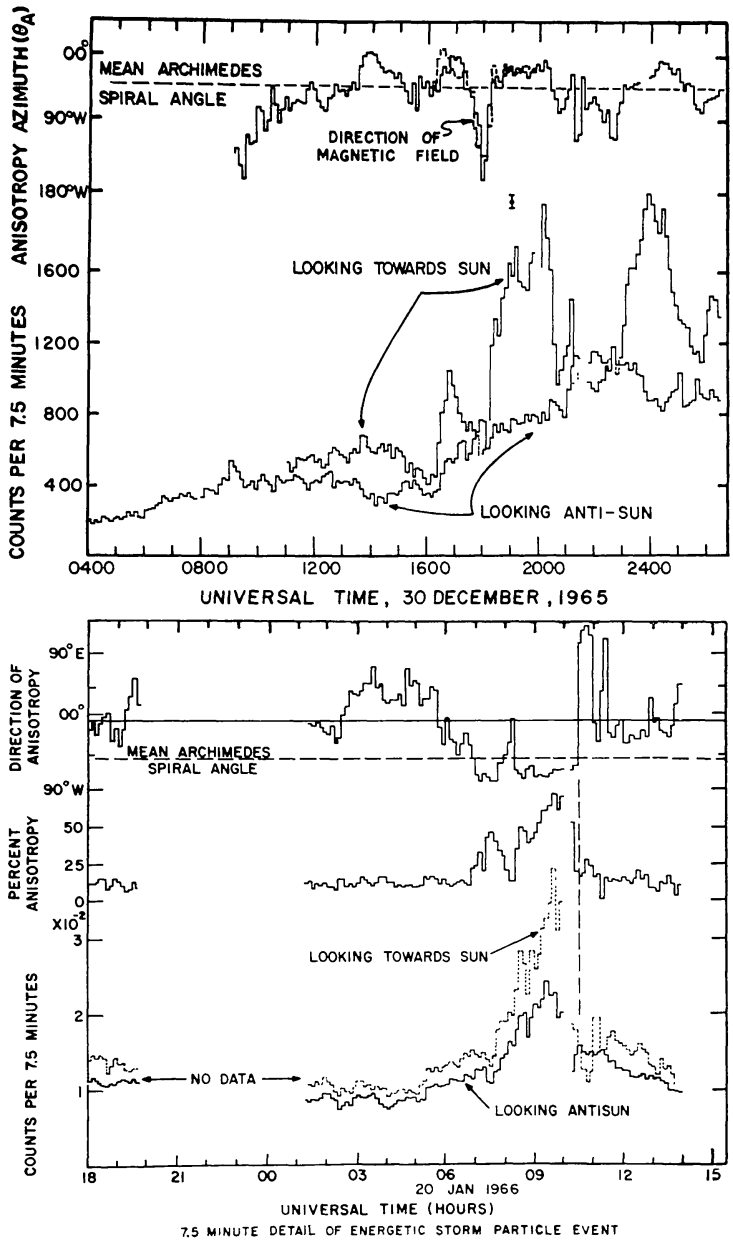


Fig. 20. Illustrating the anisotropic character of the delayed event. The counting rates from both the Sun and anti-Sun direction are plotted to roughly indicate the magnitude of the anisotropy. The anisotropy direction computed from all the cosmic ray data are presented, along with a small portion of the concurrent magnetic data. Note the large amplitude of the anisotropy, its variable direction, and its alignment with the magnetic field. These data are from Bartley *et al.* (1966) and Rao *et al.* (1967).

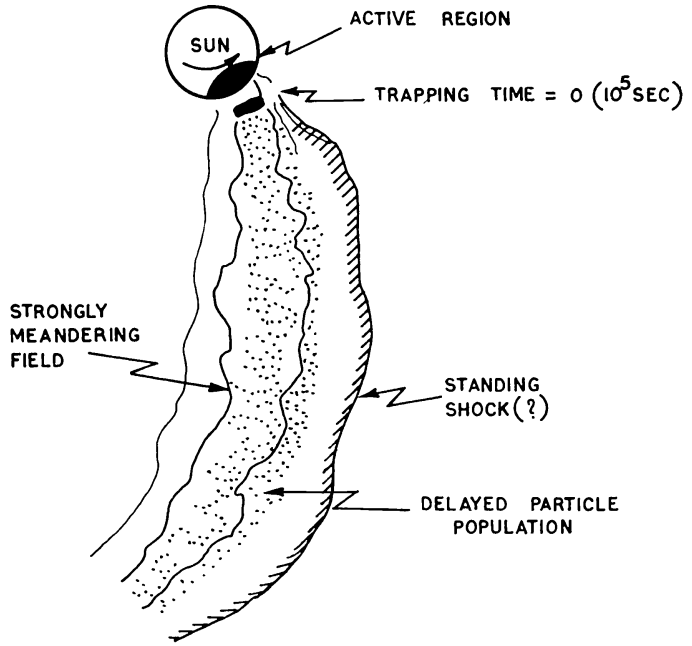


Fig. 21. A sketch of the working hypothesis for the delayed particle event in the absence of a large solar flare. This field regime is due to the enhanced and variable plasma flow from an active centre. The trapping times indicated are for ion energies of order 1 MeV.

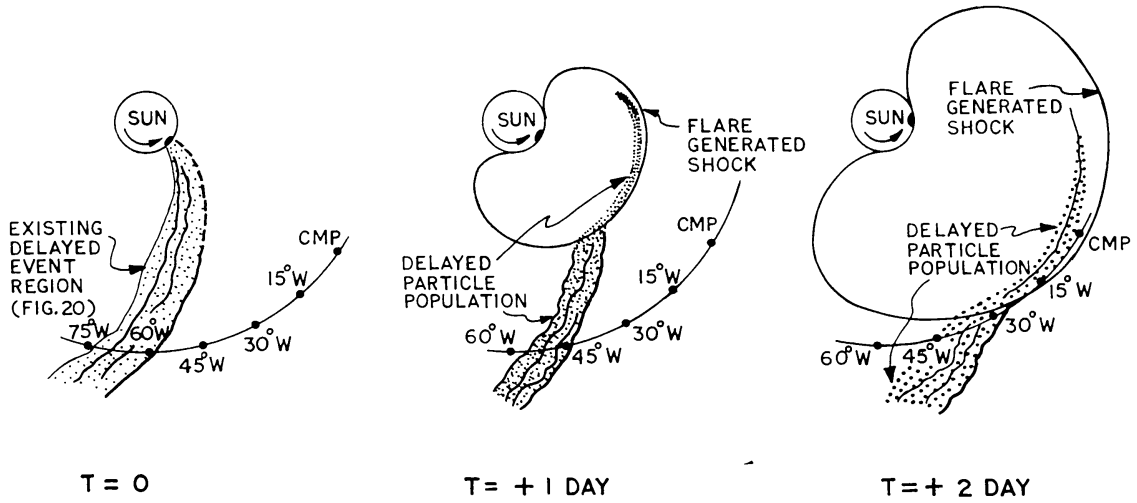


Fig. 22. A sketch of the working hypothesis for the delayed particle event zero, one and two days after a major flare. The positions of the Earth relative to the delayed particle population are shown on the assumptions that the parent flare was seen from Earth to be at CMP, 15°W, 30°W, 45°W, 60°W, and 75° West of CMP. After Kahler (1969).

temporal fluctuation similar to the halo is frequently seen in other events as a smoothly varying lower envelope upon which rapid time variations are superposed (e.g. all 3 events in Figure 16, and the event of 30 December, 1965, Figures 20 and 26). We will henceforth adopt the halo-core nomenclature as a useful phenomenological subdivision of the observations.

The temporal fluctuations of the 'core' component are observed to be strongly

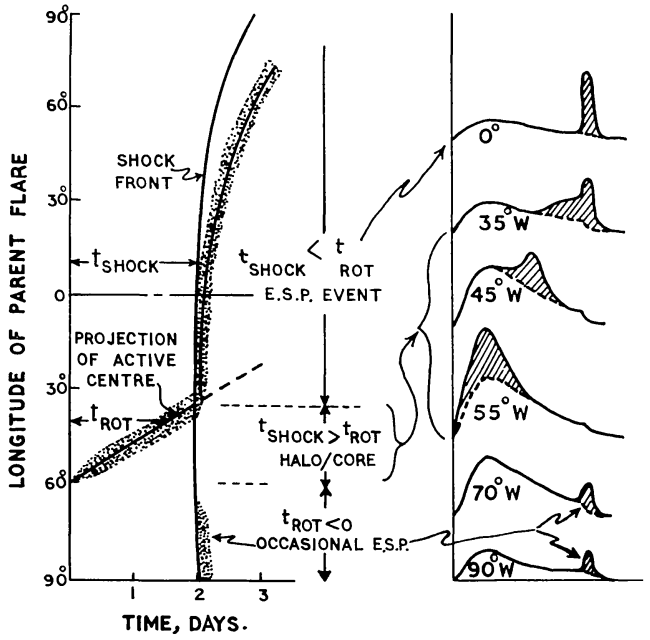


Fig. 23. The predicted times of arrival of the shock front, and the delayed particle population, relative to the time of occurrence of the flare, as a function of the position of the parent flare on the solar disc. From this diagram, the idealised time profiles on the right were prepared. The profiles are essentially cross-sections of the diagram at the left, taken at the longitude of the parent flare.

correlated with the local environment of the observer. Thus, the mean (omnidirectional) intensity, as well as the directional intensities, and the amplitude and direction of the cosmic ray anisotropy, are all strongly correlated with the properties of the interplanetary magnetic field. Figure 20, portion of the data in the upper diagram of Figure 13, and Figure 21 demonstrate these correlations. Furthermore, the 'core' type fluctuations observed by two spacecraft separated by distances $\sim 0$ ($10^6$ km) are not synchronous; they are separated by the corotation time

$$\tau_c = t_2 - t_1 = (\varphi_2 - \varphi_1)/\Omega + (r_2 - r_1)/v_P \tag{4.1}$$

appropriate to the separation of the spacecraft in heliocentric longitude $\varphi$ and radial distance $r$ from the Sun (Fan *et al.*, 1966; Lin *et al.*, 1968). Identifiable features of a core event have been observed to persist for 16 h (McCracken *et al.*, 1970) and much longer life times can be inferred in those cases of a core event following a prompt event if the assumption is made that the core came into existence immediately after the cosmic rays were injected into the solar system by a solar flare. These, and other observations indicate that the 'core' type fluctuations are due to long lived, sharply spatially limited populations of cosmic rays propagating along selected interplanetary tubes of magnetic force. By virtue of the close association between the halo and core type phenomena, Lin *et al.* (1968) infer that the halo is also a persistent, spatially limited population of particles, which 'co-rotates' with the Sun.

Fan *et al.* (1968) have studied the low energy (0.6–13 MeV) particle fluxes associated with active regions, and note that they can extend over $\sim 100$–$180°$ in solar

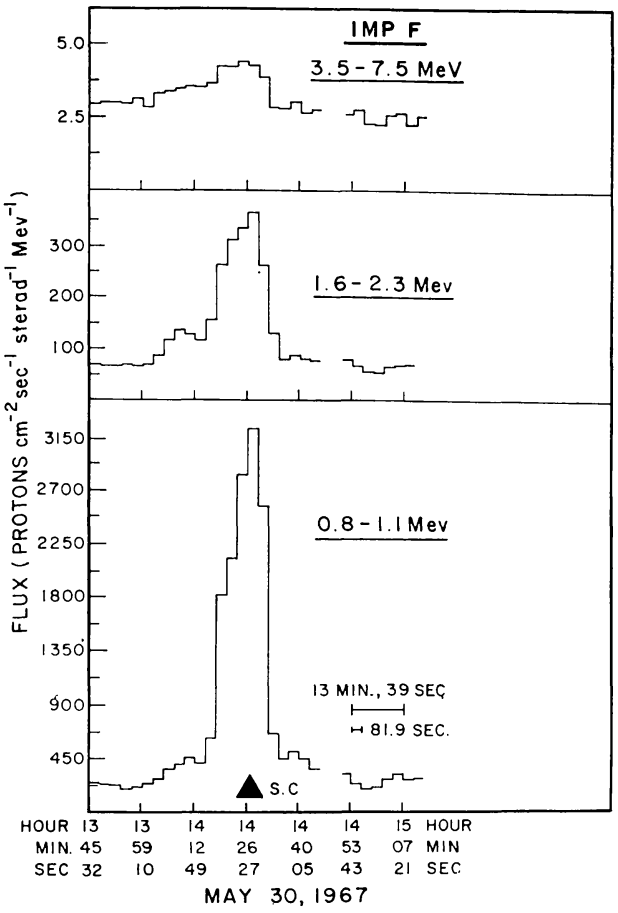


Fig. 24a.

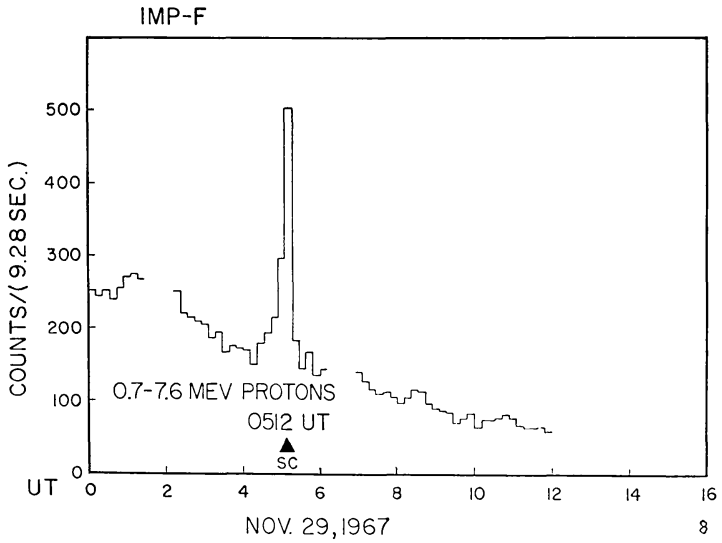


Fig. 24b.

Figs. 24a–b. Examples of the spike-like enhancements of low energy (~ 1 MeV) protons associated with magnetic sudden storm commencements. Figure 24a illustrates the strong dependence on energy. After Palmeira *et al.* (1970).

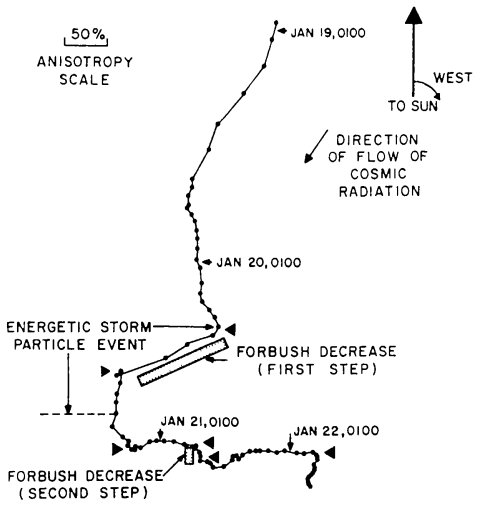


Fig. 25. Illustrating the major changes in the anisotropy amplitude and direction (for 7.5–45 MeV protons) associated with magnetic storm and Forbush decrease commencements. These major effects are all associated with an energetic storm particle event (i.e. a species of delayed event), as shown in Figure 20. The wedge symbols indicate times at which major changes in the time rate of change of cosmic ray intensity have occurred. After Rao *et al.* (1967).

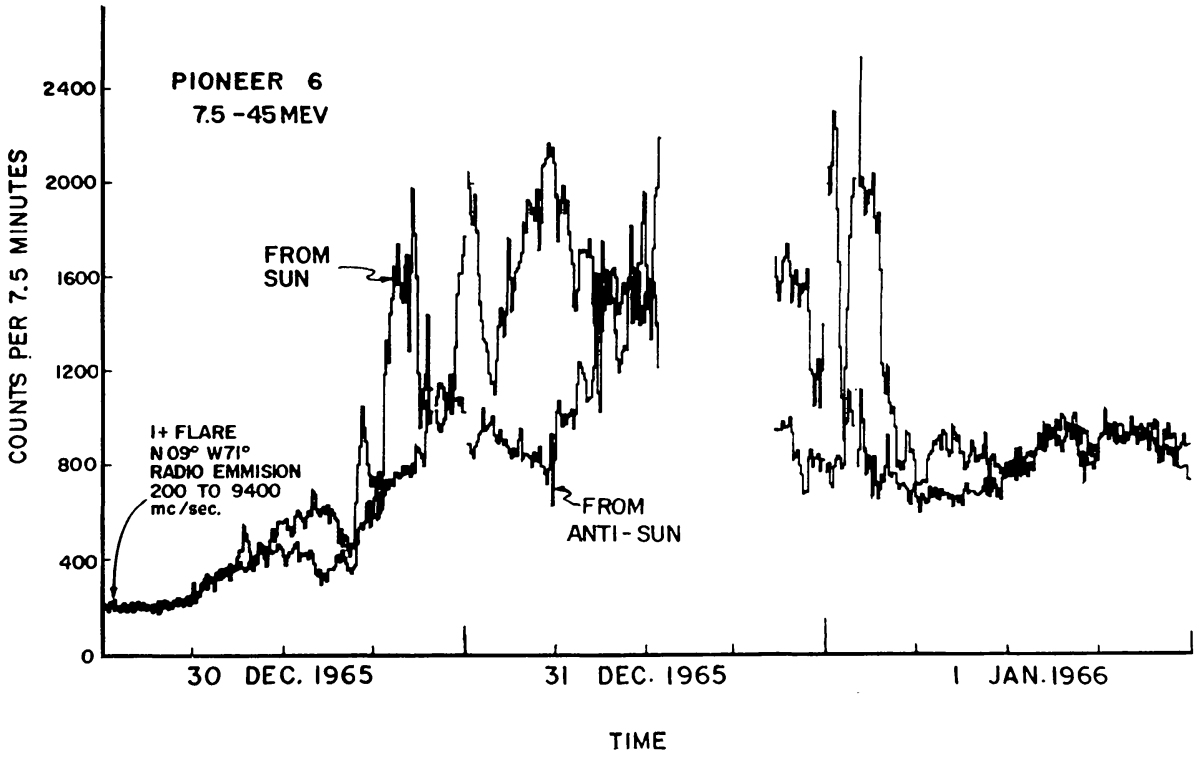


Fig. 26. Illustrating the longevity of the anisotropy in delayed particle events. During this period of time there were many marked changes in anisotropy direction (as shown in Figure 27). After Bartley *et al.* (1966).

longitude (e.g. Figure 17). While the particle populations which they have studied have varied smoothly with longitude as do the 'halo' populations, some examples have been noted in which the solar cosmic ray flux shows an abrupt onset or cessation. Some of these phenomena coincide with marked variations in the galactic cosmic radiation, indicating that the interplanetary magnetic field is acting as an impediment to the azimuthal diffusion of both the solar, and the galactic cosmic radiation. Fan *et al.* (1968) report that these onsets and cessations show a loose correlation with sector boundaries in the interplanetary magnetic field.

## 4.3. Association with other phenomena

### 4.3.1. *Solar Phenomena*

Detailed studies by Fan *et al.* (1968) and Anderson (1969) have established that there is an intimate relationship between delayed proton events, and active solar regions. Fan *et al.* (1968) conclude that the active regions showing the greatest flare activity correlate in a one to one manner with the delayed particle populations in the solar system. These, and other studies point conclusively to a model in which the delayed event is the consequence of a particle population associated with the lines of force that connect with the solar corona near the active centre (e.g. Figure 21). These populations are observed to have life-times of order 27 days, or greater, and since they are to be identified with lines of force that connect to a fixed point on the Sun, they themselves 'co-rotate'.

It is widely agreed (Bryant *et al.*, 1965b; Lin *et al.*, 1968; Fan *et al.*, 1968; Kahler, 1969; Anderson, 1969) that flare activity replenishes the delayed event particle population. The actual details of this process will be discussed after the correlations with Forbush decreases and geomagnetic Sudden storm commencements have been discussed, and in Chapter 6.

## 4.4. Association with Forbush decreases and sudden storm commencements

With few exceptions, the delayed event is broadly associated with a Forbush decrease, or a depression in the galactic cosmic ray intensity (e.g. Figures 16, 17, and 19). Thus 27 day recurrent events (Bryant *et al.*, 1965b); Energetic Storm Particle Events (Bryant *et al.*, 1962; Rao *et al.*, 1967, 1968a); the proton regions of Fan *et al.* (1968), and the EDP category of Anderson (1969) correlate with the observation of decreased galactic cosmic ray fluxes at energies up to, and in excess of 30 GeV. Likewise, there is a broad association with the observation of sudden storm commencements. The detailed relationship between the phenomena is not simple, however.

The evidence available to date indicates that the relationship depends systematically on whether the delayed event is superposed upon a prompt event (i.e. whether it is a 'new' particle population); and if so, on the longitude of the parent flare. Lin *et al.* (1968) and Kahler (1969) have gained a very perceptive insight into these differences, and we now present their model as a 'working hypothesis' in terms of which the delayed event can be discussed in detail.

## 4.5. THE WORKING HYPOTHESIS FOR THE DELAYED EVENT

### 4.5.1. *Delayed Event not Associated with a Major Flare*

Many delayed events are not associated with a flare of any note (Anderson, 1969). They are, however, associated with an active region, which produces flare activity, geomagnetic disturbances, and depression of the cosmic ray intensity. The prolonged existence of these active regions means that a region embodying these various properties will corotate with the Sun, and persist from one solar rotation to the next.

The working hypothesis for the 'delayed' event in this case is presented in Figure 21. This model is similar to those described verbally by Bryant *et al.* (1965b); Fan *et al.* (1968) and Anderson (1969). An enhanced flow of plasma from the active region establishes a corotating field regime. The occurrence of flares in the active region will impart wide fluctuations to the plasma flow velocity, resulting in exaggerated meandering of the field lines. The mean velocity of the plasma from the active region will exceed the plasma velocity from surrounding regions of the corona, and hence a 'standing shock' may develop on the leading edge of the enhanced plasma flow. This, the plasma itself, and the generally enhanced magnetic field entrained in the plasma, result in the geomagnetic effects, and a Forbush decrease.

Low energy ions and electrons generated in flares in the active region are injected into the field regime described above, resulting in a delayed particle population that adheres to the field that connects to the active centre. A delayed event is therefore seen in rough time coincidence with enhanced geomagnetic activity, and a reduction in the galactic cosmic ray intensity. The nature of the delayed particle population near the Sun will be discussed in Section 6; suffice it to say here that there is good evidence to suggest relatively good 'storage' of low energy ($\sim$1 MeV ions) near the Sun for a time of order $10^4 - 10^5$ sec.

### 4.5.2. *Delayed Event Subsequent to a Major Flare*

An active region on the verge of producing a major flare would almost certainly have a prior history of flare activity. Consequently, it would have associated with it a plasma/field/delayed particle population regime as outlined above, and as sketched in Figure 21.

Let now a major flare occur. Figure 22, which is patterned after Figure 4 of Kahler (1969), summarises the situation 0, 1 and 2 days after the flare. Initially the flare would strongly augment the delayed particle population in the field attached to the active centre. On the basis of the observations of the July 9, 1966 delayed event (Lin *et al.*, 1968), we show this population as having a FWHM of $\sim 10°$.

Consider the situation corresponding to a parent flare occurring 45°W of the central solar meridian (Figure 22). The delayed particle population would not have access to the observer initially, and therefore a prompt event would be seen in isolation. With the passage of time, the delayed population would be convected (or stated alternatively, it would 'corotate') to a position such that it would start to be observed (See Figure 22, $T = +1$ day). Its centroid would pass the observer about 1.2 days

after the occurrence of the flare, and it would pass out of view of the observer shortly before the arrival of the shock. In this case, then, the delayed event would be seen as an upward deviation from a prompt event, but would, in all other respects, correspond to the 'no major flare' model (Figure 21). The time profile of this event is sketched in Figure 22. Note that while this delayed event would coincide with the geomagnetic/Forbush events associated with the enhanced plasma flow from the active region, there would be no correlation with those phenomena associated with the shock generated by the flare. Since these latter phenomena would be considerably more pronounced than those associated with the enhanced plasma flow, the initial impression would be of a lack of correlation.

Figure 22 makes it clear that the situation outlined above is unique to a flare near 45 °W. For example, in the case of a flare at CMP, the shock would arrive at the observer prior to the delayed particle population. In this case, then, the time profile of the delayed event would be quite different, and its temporal associations with other phenomena would also differ from the case outlined above.

Figure 23 demonstrates the dependence of the properties of the delayed event upon longitude in a different manner. The times of arrival at the observer of the shock, and of the lines of force that are the magnetic projections of the active centre are shown. Writing the Sun-Earth propagation time of the shock as $t_{\mathrm{SHOCK}}$, and the arrival time of the nominal Archimedes spiral field line that connects to the parent active region as

$$t_{\mathrm{corot}} = \frac{1}{\Omega}\{\varphi_{\mathrm{FIELD}} - \varphi_{\mathrm{FLARE}}\}, \tag{4.2}$$

where $\varphi_{\mathrm{FIELD}}$ is the solar longitude at the Sun of the nominal Archimedes spiral field line that passes through the observer and time is measured from the instant at which the flare occurred, then three clear cut cases emerge:

(1) $t_{\mathrm{SHOCK}} < t_{\mathrm{corot}}$. The shock will reach the observer first (e.g. flare at CMP, Figure 22). Hence the delayed particle population is embedded in the shock region (Figures 22 and 23), and is compressed radially by a factor of $|\mathbf{B}|_{\mathrm{shock}}/|\mathbf{B}|_{\mathrm{preshock}} \approx 4$. A prompt event is therefore seen up to the time of the arrival of the shock, at which time the delayed particles are seen as a shortlived enhancement in time association with a SSC and the start of a Forbush decrease. This situation corresponds to the Energetic Storm Particle events of Bryant *et al.* (1962) and Rao *et al.* (1967, 1968a). The model predicts that these events will be seen for parent flares at longitudes to the east of about 30 °W. This is in accord with observation.

(2) $t_{\mathrm{SHOCK}} > t_{\mathrm{corot}} > 0$. Corotation brings the particle population to the observer before the shock reaches him. The type of variations then can be observed are summarised in Figure 23, thus:

(2a) if $t_{\mathrm{SHOCK}} \approx t_{\mathrm{corot}}$, e.g. for a flare at 35 °W (Figure 22 or 23) the first portion of the delayed population is seen ahead of the shock as a monotonically rising deviation from the prompt event profile, while the remainder of the delayed population is seen embedded in the shock as a short-lived enhancement with energetic storm particle properties. In this case the delayed event will commence before the SSC (in time

correlation with the geomagnetic effects associated with the enhanced plasma flow from the active region).

(2b) if $t_{corot} \approx \frac{1}{2} t_{SHOCK}$; e.g. a flare at 45 °W (Figures 22 or 23), or the event of July 9, 1966 which is shown in Figure 15 (Lin *et al.*, 1968). In this case, the delayed particle population is swept past the observer during the interval prior to the arrival of the shock front. Hence the delayed event tends to be symmetrical about the time the nominal Archimedes spiral from the active centre connects with the observer. In this case, there will be no fixed time correlation between the delayed event, and the Forbush decrease and SSC associated with the shock. There is, however, correlation with those same phenomena associated with the active region itself. This situation closely approximates the 'no major flare' model, only in this case the delayed event is superposed on a prompt event.

(2c) if $t_{corot} \approx 0$ (Figures 22 or 23, 55 °W), the observer is favourably placed so that he sees both the prompt and delayed populations immediately after injection into the magnetic field. In this case, corotation sweeps the delayed population away from the observer during the decay phase of the flare event, so that the flare effect time profile is superficially similar to a normal prompt event. Neither a halo/core nor an ESP event will be recognised in the data. Geomagnetic disturbance, and a Forbush decrease due to the active region itself will be in progress at the time at which the flare occurs.

(3) if $t_{corot} < 0$. That is, the delayed population at the time of injection is already to the west of the observer. Corotation will not cause the delayed population to be seen: the only possibility is that portion of the population may be embedded in the trailing edge of the shock as discussed by Kahler (1969). This would probably be an unusual occurrence.

The 'large flare' model (Figure 22) would convert to the earlier (no flare) version of the model (Figure 21) at times long compared to the Sun-Earth shock transit time; i.e. for times greater than 3 or 4 days.

The above model predicts a variety of delayed events, showing general agreement with those observed in practice. The predictions of the correlation with geomagnetic and cosmic ray phenomena are also in good accord with observation (Kahler, 1969). The model has the great advantage that it accommodates within itself all the types of delayed particle event that have bedeviled the literature. It will be clear that, according to this model, the nature of the event is partially determined by solar activity, partially by history, and partially by the position of the observer relative to the parent active centre.

We emphasize that great care must be exercised in the study of correlations between the various phenomena. According to the 'large flare' model, at least two recognisable, and distinctly different episodes of geomagnetic/galactic cosmic ray disturbance will occur. The flare induced shock will be the more pronounced, and may tend to obscure (or cause subjective rejection of) the phenomena associated with the active region itself. Nevertheless, the latter may be the crucial correlative phenomena, insofar as the delayed events are concerned.

The Energetic Storm Particle events exhibit (a) a duration of order 6 h, i.e. $\simeq 0.25\times$ duration of the 'no flare' delayed event; (b) a loose time correlation ($\pm$ few hours) with the magnetic sudden storm commencement. In addition, a phenomenon is observed at low energies showing exact time correlation with the SSC. Two such events are shown in Figure 24, and are reported in detail elsewhere (Palmeira *et al.*, 1970). They are seen in the ionic radiation; are short-lived ($\sim 1$ h total duration); are strongly dependent on energy as evident from Figure 24a; and on each occasion on which they have been observed they have been quite accurately centred on the SSC. From an analysis of a number of energetic storm particle events observed with instrumentation on board the Vela 4 satellite, Singer (1970) has shown that the low energy particle spikes are associated only with shock waves and not with solar wind discontinuities. Singer has explained these spike-like enhancements are due to acceleration of particles in the shock front itself, a suggestion first put-forward by Parker (1965) and Rao *et al.* (1967).

### 4.6. The degree of anisotropy of the radiation in delayed events

The ionic cosmic radiation is markedly anisotropic during Energetic Storm Particle events, as is illustrated by the event of 20 January, 1966 (Figure 20), and by the 'vector diagrams' of Figure 25. The anisotropy has increased greatly, has been unidirectional, and has been closely field aligned throughout all the energetic storm particle events studied to date (Rao *et al.*, 1967). In terms of the Kahler model (Figures 22 and 23), this implies that the delayed particle population is streaming in an anisotropic manner in the region behind the advancing shock front. The persistence of the anisotropy of the Energetic Storm Particle population implies that the particles are not trapped in the shock front for any appreciable periods of time ($\lesssim 1.5$ h) (Rao *et al.*, 1967).

In the region behind the shock front, and behind the ESP population, the remnants of the solar radiation exhibit a bidirectional anisotropy; that is, the fluxes are maximal from the directions parallel, and antiparallel to the interplanetary magnetic field vector (Rao *et al.*, 1967). This bidirectionality is also seen in the galactic radiation at $E \gtrsim 10$ GeV as a 12 h periodicity in the Forbush decrease (e.g. Rose and Lapointe, 1961). It has been proposed (Rao *et al.*, 1967) that both bidirectionalities are due to the fact that in both cases the cosmic ray density is greater outside, than inside the shock front. In this situation, cosmic ray leakage into the region behind the shock will produce an enhanced flux from the antisun direction (and parallel to **B**), and this will mirror at the Sun to yield the bidirectionality. Injection at the Sun is unable to explain the observations in an adequate manner.

Detailed studies have been made of the solar cosmic ray spectra prior to, and during ESP events of 20 January, 1966, and 23 September, 1966. It is noted that in addition to the well known softening of the spectrum during the ESP event, the spectra prior to the events were functions of direction of viewing, the softest spectrum being observed from the direction towards the shock front. This result, and in addition, the calculated particle outflows in the periods of time prior to the ESP, are not explicable in terms of leakage, or simple reflection effects at the moving shock front. These results are taken

as tentative suggestions that there is some incremental acceleration in the shock front, thereby causing the cosmic ray spectrum to shift to higher-energies (Rao *et al.*, 1967).

Figure 26 displays a delayed event exhibiting very great, and persistent (>2 days) anisotropies. An active region centred at 71 °W at the time was the parent region for a number of solar flares that resulted in prompt events. There was no marked geomagnetic activity until January 1 (and even then it was minor), however enhanced diurnal variations of the galactic cosmic radiation commenced about 01 UT on December 31, so we interpret this as an example of the 'no large flare' model, Figure 21. That is Figure 20a indicates the anisotropic behaviour of the radiation in the delayed particle population of Figure 21, or the delayed event in the $t_{corot} < t_{SHOCK}$ case of Figures 22 or 23.

The most striking feature of Figure 26 is undoubtedly the great longevity of the anisotropy. It is to be noted that the ionic flux from the antisolar direction varies relatively smoothly with time, while the flux from the Sun exhibits very marked temporal variations. Furthermore, we note that the lower envelope of the flux from the Sun is in rough agreement with the antisun flux. This leads us to propose that the halo radiation at $E \approx 10$ MeV is to a first approximation isotropic, and that the 'core' of Lin *et al.* is due to strongly anisotropic, field aligned streams of radiation. The correlation coefficients of 0.88 noted by McCracken and Ness (1966) between the anisotropy and magnetic field directions during the period of violent intensity fluctuations in Figure 26 are strong evidence of the field aligned nature of the 'core' radiation. The above inference that the halo radiation would be approximately isotropic needs some slight modification: since the delayed particle population is being convected away from the Sun by the solar wind, it would, of necessity, exhibit an equilibrium (or convective) anisotropy. (Figure 14a).

The situation appears to be considerably different for $E \sim 1$ MeV. Fan *et al.* (1968) report anisotropy measurements for the energy range 0.6–13 MeV, and find that the smoothly varying proton flux associated with one active center was field aligned at all times. Clearly more observations are needed at both 0 (1 MeV) and 0 (10 MeV), however, the present data suggest that the long persistent, low energy proton populations retain field aligned anisotropies even in the 'halo', while at higher energies, the 'halo' exhibits convective removal properties. In Section 6, we will argue for a strongly energy dependent trapping of charged particles near the Sun, which would strongly differentiate between 0 (1 MeV) and 0 (10 MeV) ions. This could possibly explain the observations.

To divorce the conclusion from the nomenclature: we propose that the delayed particle event in Figure 21 comprises (1) a component exhibiting a convective anisotropy, and a smooth spatial dependence; and (2) a component which exhibits a strong, field aligned anisotropy, and a strong spatial dependence. The variable azimuth of the cosmic ray anisotropy and magnetic field (Figure 27) are interpreted as a consequence of the exaggerated meandering nature of the interplanetary magnetic field associated with the disturbed plasma region of Figure 21.

The great longevity ($\gtrsim 2$ days) of the anisotropy on the delayed event of 30 December, 1965 (Figure 26) is to be compared with the relatively short time ($\sim 12$ h) required for a prompt event to decay to the convective anisotropy condition. The implication is either (a) that the parallel diffusion coefficients, $K_{\parallel}$ are much greater than normal; or (b) that there is continued injection at the Sun. This matter will be discussed in Section 6.

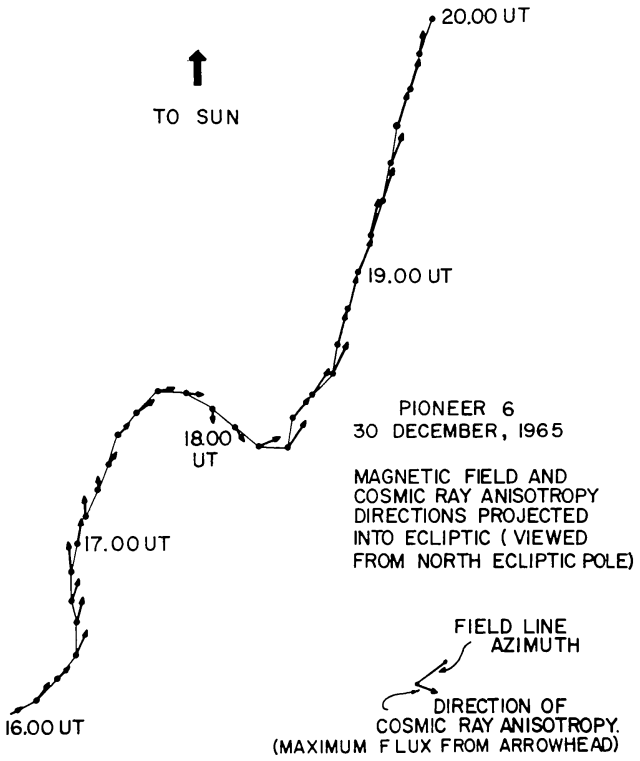


Fig. 27. Illustrating the field aligned nature of the cosmic ray anisotropy (7.5–45 MeV data). Note the close tracking of the changes in the cosmic ray and magnetic vector azimuths. After McCracken and Ness (1966).

## 4.7. Electron-proton splitting

Figures 16 and 18 demonstrate the electron-proton splitting reported by Anderson (1969) for delayed events that do not correlate with a large flare (i.e. the model in Figure 21). In each of the events studied, the electron event precedes the ionic by a few hours ($\simeq 1$–$2°$ in corotation).

Jokipii (1970) has considered the gradient and curvature drifts of $\sim 1$ MeV protons and $\sim 40$ keV electrons in the interplanetary magnetic field. He concludes that a temporal separation

$$\tau_{\mathrm{del}} \simeq \frac{\langle V_d \rangle r}{K_{\parallel} \Omega} \tag{4.3}$$

will apply between the proton and electron components, where $r$ is the distance from the Sun, $K_{\parallel}$ is the parallel diffusion coefficient, $\Omega$ is the solar angular velocity, and $V_d$ is the sum of the curvature and gradient drift velocities. The drift in the electron

population is negligible on account of the small gyroradii: all the separation is due to proton drift. For $K_{\|} = \frac{1}{3}c\beta L$ (Equation (2.1)), Jokipii derives $T_{del} \approx 0$ (hours). That is, the mechanism provides the right magnitude of separation.

Figure 28 demonstrates the drifts that proton populations would experience in terms of Jokipii's model. In each case, the protons drift in such a sense as to ultimately trail the electron population, as is observed. This diagram also suggests the reason for some of the 'pure' electron or proton events: namely, that the protons have drifted into the opposite solar hemisphere than the electrons, so that a single observer will only see one, or other of the two populations.

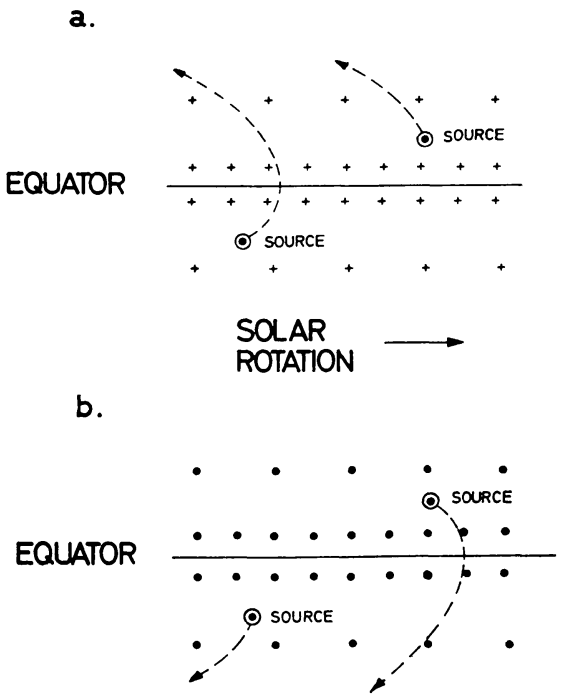


Fig. 28. A theoretical model illustrating the curvature and gradient drifts of low energy protons in the interplanetary magnetic field. There is negligible drift of ~40 keV electrons. A drift of the protons to the left of the source will result in an electron-proton splitting in which the electrons are observed prior to the protons, as is observed. After Jokipii (1970).

## 5. Optical and Other Electromagnetic Information

A minor generalisation of the available evidence indicates that a prompt solar flare effect invariably occurs in association with a solar flare as observed at optical, and other electromagnetic wavelengths.* Such observations add considerably to our ability to discuss propagation and production processes, and also provide a predictive capability with practical applications. We therefore review here the pertinent information, insofar as it pertains to cosmic ray processes.

* Note that we do not wish to imply that an optical/EM flare will be seen from Earth corresponding to each prompt event. Some of the flares correlated with the observed prompt events occur on the invisible solar hemisphere. We do assert however that a one to one correspondence would be obtained if there were a continuous survey of the 'whole Sun' (i.e. visible and invisible hemispheres).

A notable milestone in the study of the acceleration of cosmic rays in solar flares was made by the IAU-IQSY 'Proton Flare Project, 1966'. Of particular note was the great breadth of optical, radio, X-ray and particulate data obtained during two periods of major solar activity. Detailed case histories and reviews are available (Annals of the IQSY Number 3 (1968); Simon and Švestka (1968); Švestka and Simon (1969); Švestka (1969) and should be consulted for any serious study of this subject.

To summarise the situation:

(a) Cosmic radiation is injected into the solar system within about $\pm 1$ min of the 'Flash' phase of a flare. This corresponds to the period of maximum X-ray emission at high photon energies ($\sim 50$ keV) and at microwave ($\sim 3$ cm) wavelengths.

(b) Active regions of a high degree of magnetic complexity ($\beta\gamma$ or $\delta$) and showing enhanced 9400 MHz radio emission relative to 4000 MHz (approaching equal flux densities) are likely candidates to produce flares with significant particle production. The propensity for a specific region of the Sun to produce flares embodying effective particle production is often very long lived. Thus there was preferred flare particle production at Carrington longitudes of 80°–140° and 320°–340° for solar cycle 19 (1954–1963).

(c) The characteristics of the flares that have produced very copious cosmic ray fluxes are (1) great brightness, (2) a twin filament characteristic, the filaments enchroaching on the sunspot umbrae, (3) occurrence in regions of strong magnetic fields and strong spatial gradients, (4) strong microwave ($\sim$ centimetric) and X-ray ($\sim 50$ keV) emission coincident with the flash phase of the flare.

We will now discuss the circumstances before, during, and after the occurence of a particle producing flare in some detail.

### 5.1. The sunspot group

Particle acceleration processes are usually associated with large, evolving sunspot groups. Thus Jonah (1966) finds that 92% of all polar cap absorption events are associated with flares in sunspot groups of area $\gtrsim 500$ millionths of the solar disk.

Cosmic ray producing flares normally occur in Spot Groups exhibiting complex magnetic configurations ($\beta\gamma$ or $\delta$). Flares in spot groups with $\beta\gamma$ magnetic classification (bipolar; no clear cut boundary between N and S polarities) show impulsive microwave emission indicative of appreciable particle acceleration, and delayed particle fluxes are frequently observed at the orbit of Earth (Fan *et al.*, 1968; Švestka and Simon, 1969) centred about 1–3 days after the CMP of the group. Prompt events will also be produced by some flares in the group. Further evolution to the $\delta$ category (complex field structure; sunspots of opposite polarity within the same penumbra) increases the probability that any given flare will produce a significant quantity of cosmic radiation.

It has been suggested that a particular configuration of spots, called, the 'A' configuration (Figure 29) is particularly favourable for the occurrence of a particle producing solar flare. (Avignon *et al.*, 1963; Simon and Švestka, 1969). Close proximity of spots of opposite polarity (Avignon *et al.*, 1965), and strong gradients in the

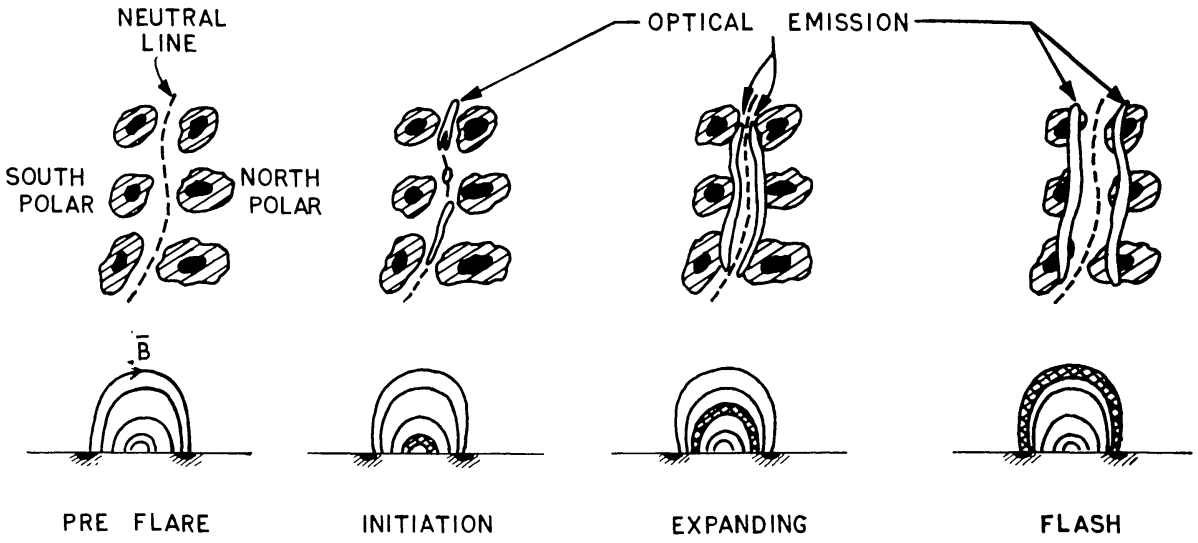


Fig. 29. An idealised sketch of the development of an optical flare. The upper sketch is the plan view, the lower a cross-section in the plane normal to the neutral line. The cross-hatched tube of force in the lower diagram indicates the tube terminating in the enhanced optical emission. The evolution sketched above occupies some 10 min of the duration of the flare.

line of sight component of the magnetic field $B_{\|}$, (Severny, 1963) are other phenomenological characteristics that have been reported to be indicative. A rapid increase (time scale $\sim$ days) in the gradients of $B_{\|}$ in the vicinity of the neutral line (i.e. $B_{\|}=0$ separating North and South polarities) to values of $0(1\text{G km}^{-1})$ has been observed in the periods immediately prior to the occurrence of major cosmic ray producing flares (Howard and Severny, 1963; Severny, 1968).

The flux density of the slowly varying microwave radiation (1–20 GHz) from sunspot groups normally peaks in the vicinity of $\sim$3 GHz (10 cm). Tanaka and Kakinuma (1964) indicate that as a spot group becomes complex, and a potential cosmic ray flare producer, so does the spectral peak shift to higher frequencies ($\sim$8 GHz). In particular, they suggest that the ratio $F_{9.4\text{ GHz}}/F_{4\text{ GHz}}$ is a useful index of the likelihood of cosmic ray production, a ratio of unity indicating a high event probability. The shift of the spectral peak to higher frequency tends to coincide with the attainment of the $\delta$ magnetic classification. We note, however, that some major cosmic ray flares have occurred while the spectral peak was still near 3 GHz (e.g. 28 August, 1966; Kruger, 1968).

### 5.2. The solar flare

Certain optical features appear to be systematically associated with cosmic ray production. Firstly the flares that result in relativistic events tend to be observed in white light (McCracken, 1959; Švestka, 1966). The optical emission of flares associated with type IV radio bursts (itself a good indicator of particle acceleration) usually encroaches on the umbra of a large sunspot (Dodson and Hedeman, 1960). Martres and Pick (1962) have concluded that the covering of the umbra or penumbra is the determining factor in the association of a flare with centimetric type IV. They have

also demonstrated a tendency for the centimetric (microwave) type IV to start as the optical flare expands to cover the penumbra. Ellison *et al.* (1961a) have attributed significance to the occurrence of two bright strands of emission within each of the optical flares that were associated with a number of relativistic flare effects, the strands obscuring the umbrae of highest field strength. Avignon *et al.* (1963) have obtained a similar result from a study of the flares responsible for 15 PCA events as has Bruzek (1968). The absolute brightness of the flare emission in H$\alpha$ is also a useful indicator (Bruzek, 1964). A useful review of pertinence to this whole subject is given by Kundu (Chapter 11, 1965).

The twin filament structure noted above is not unique to cosmic ray producing flares at the threshold levels that currently pertain. Švestka states (private communication) that many of the twin filament flares that do not result in cosmic ray production do not have intimate contact with a sunspot (and presumably large gradients of $B_{\|}$) but that some do show all the correct geometrical relationships, and yet do not produce detectable quantities of cosmic rays.

While it may not be a unique indicator of cosmic radiation production, the twin filament character gives a valuable clue to the physical structure of a solar flare. Figure 29 depicts a sunspot group in the 'A' configuration, with a neutral line ($B_{\|}=0$, and sometimes called the magnetic axis) roughly bisecting the magnetic dipole of the group. The initial optical emission is from two parallel ribbons on either side of the neutral line. The ribbons then separate rapidly; the separation velocity decreasing as the ribbons approach and start to cover the sunspot umbrae. That is, the ribbons are (roughly) magnetic conjugates of one another, and this suggests that the suprathermal processes responsible for the flare emissions are occurring in the tubes of force connecting the two ribbons. According to this view, the flare process initially occurs at a low altitude above the chromosphere, and moves to tubes of force whose aphelia are higher as the flare proceeds. The mean free path for ions and electrons associated with the flare therefore increases as the flare progresses to the 'flash' phase, and this therefore allows the possibility of appreciable acceleration.

Various suggestions have been made as to other optical indicators of particle acceleration: e.g. (1) that the filaments show a characteristic *Y* shape, the two filaments being connected at one end (Krivsky, 1963); (2) that in 95% of the observed cases, the filaments formed a characteristic loop at late times in the life of a particle producing flare (Bruzek, 1964); (3) that a dark halo, or 'nimbus' surrounding the portion of the optical flare is a direct, optical indicator (through mechanisms unknown) of the presence of relativistic electrons near the flare (Ellison *et al.*, 1961b). There is neither the experimental confirmation nor the theoretical justification to permit any of these techniques to be regarded as reliable indicators of particle acceleration at the present time.

Type IV radio noise, attributed to synchrotron radiation from relativistic electrons accelerated in the flare, is the most certain indicator of particle acceleration (Dodson *et al.*, 1953; Hakura and Goh, 1959; Warwick and Haurwitz, 1962). The intensity of the centimetric Type IV has been reported to be broadly related to the particle flux

observed at Earth (Warwick, 1962; Covington, 1959), and hence of potential use in propagation studies. We note, however, that with the great increase in particle detection sensitivity in late years (by a factor of $10^4$, see Figure 7), the strong correlation between cosmic ray events and type IV that was once evident (Fokker, 1963) has disappeared, probably due to a threshold effect in the type IV measurements.

It has been suggested by Castelli *et al.* (1967) that the radio frequency spectrum of type IV emission may show a pronounced dip at decimetric frequencies if due to a 'proton' flare. The correlation is not perfect, the type IV failing to exhibit a U-shaped spectrum for some PCA events. In view of the close affinity between the currently accepted theories for the type IV and prompt events, however, further critical studies of their inter-relationship appear to be warranted.

### 5.3. X-RAY AND MICROWAVE BURSTS

Solar X-ray bursts at low photon energies ($h\nu \simeq 4$ keV) are extremely common, normally outnumbering the optical flares observed over the same period of time. At higher photon energies ($h\nu \gtrsim 50$ keV) the X-ray event is more selective, and is associated with the larger solar flares. Thus from an examination of over 75 energetic X-ray events during 1964–1967, Arnoldy *et al.* (1968) have found a 100% correlation between optical flares of importance 2 N or larger and hard X-ray bursts in the energy range 10–50 keV. Similarly they established that every radio event with a flux greater than 80 units (i.e. $> 80 \times 10^{-22}$ W m$^{-2}$ Hz$^{-1}$ at both 3 and 10 cm) showed a hundred percent association with energetic X-ray bursts (see Table VI). The poor correlation for the weaker radio bursts is possibly due to the X-ray emission being less than the detector threshold.

Since electrons of 100 keV are needed to produce 50 keV photons, it is clear that high energy X-rays are a direct indicator of the presence of high energy electrons in a flare. It has also been noted that there is a strong similarity between the temporal variations in hard X-rays and microwave radiation and that this similarity persists until the peak intensities have been passed (Peterson and Winckler, 1959; Kundu,

TABLE VI

X-ray events observed by OGO satellite (Arnoldy *et al.*, 1968) and their association with radio bursts

| Peak radio flux ($10^{-22}$ W m$^{-2}$ Hz$^{-1}$) | 10 cm | | | 3 cm | | |
|---|---|---|---|---|---|---|
| | Total No. of known radio bursts* | Correlated X-ray bursts** | Percent correlation | Total No. of known radio bursts* | Correlated X-ray bursts** | Percent correlation |
| 3–6 | 44 | 2 | 5 | 15 | 0 | 0 |
| 6–20 | 41 | 8 | 20 | 22 | 3 | 14 |
| 20–80 | 8 | 6 | 75 | 11 | 9 | 82 |
| > 80 | 11 | 11 | 100 | 12 | 12 | 100 |
| Unknown | – | 3 | – | – | 6 | – |

* All known radio bursts during September 5, 1964–July 30, 1966.

** X-ray burst ($10 < E < 50$ keV) of intensity $> 3 \times 10^{-7}$ erg cm$^{-2}$ sec$^{-1}$.

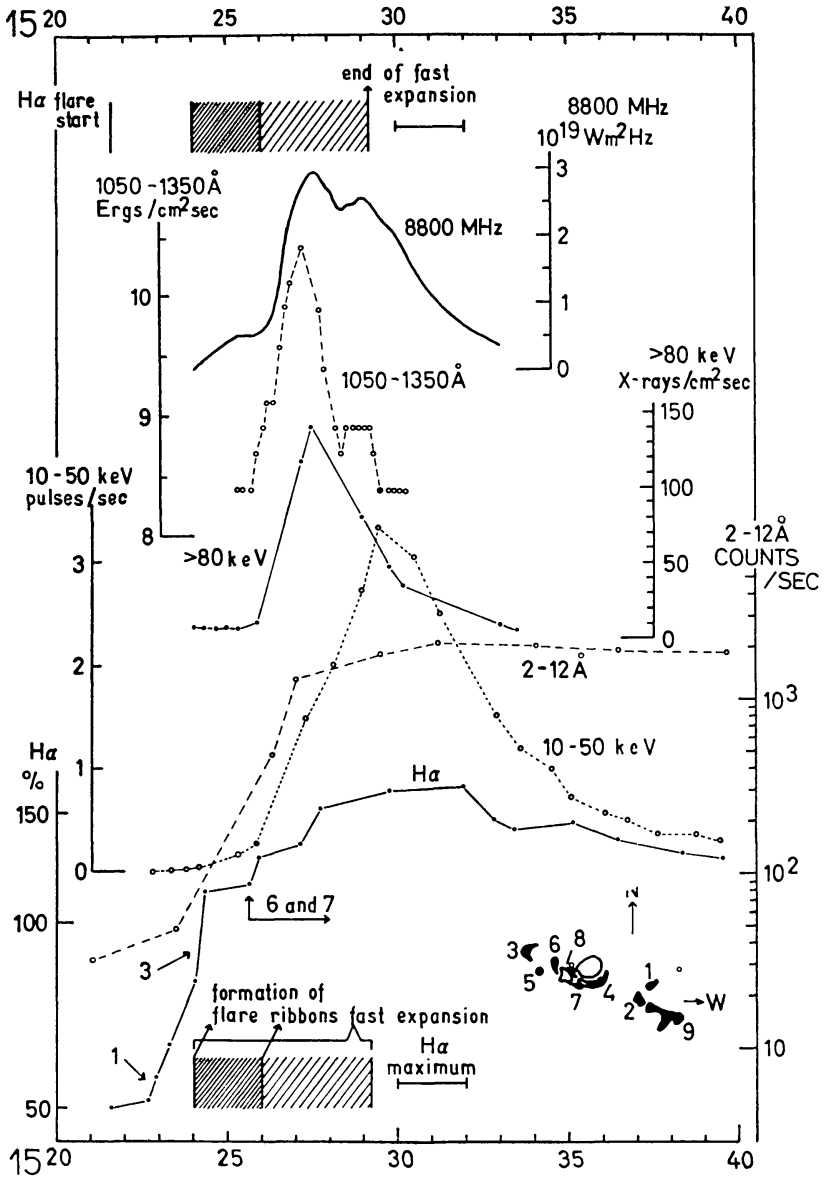


Fig. 30. A synopsis of the development of the several electro-magnetic radiations from the particle producing flare of August 28. Note the strong similarity between the microwave (8.8 GHz) and hard X-ray (> 80 keV) emissions, and the coincidence with the latter part of the fast expansion phase of the optical flare. After Švestka and Simon (1969).

1961; Takakura, 1969). This time correlation, and the relationship to other phenomena is illustrated in Figure 30.

Figure 31 displays the excellent correlation observed between the peak microwave radio flux and hard X-ray flux observed by Kane and Winckler (1969). These authors also demonstrate a striking similarity between the decay characteristics of the X-ray flux and the microwave (3–9 GHz) radiation from large flares. These several results provide the basis for using the easily observed microwave data as indicators of charged particle acceleration processes instead of the more directly related, but less easily observed hard X-ray bursts.

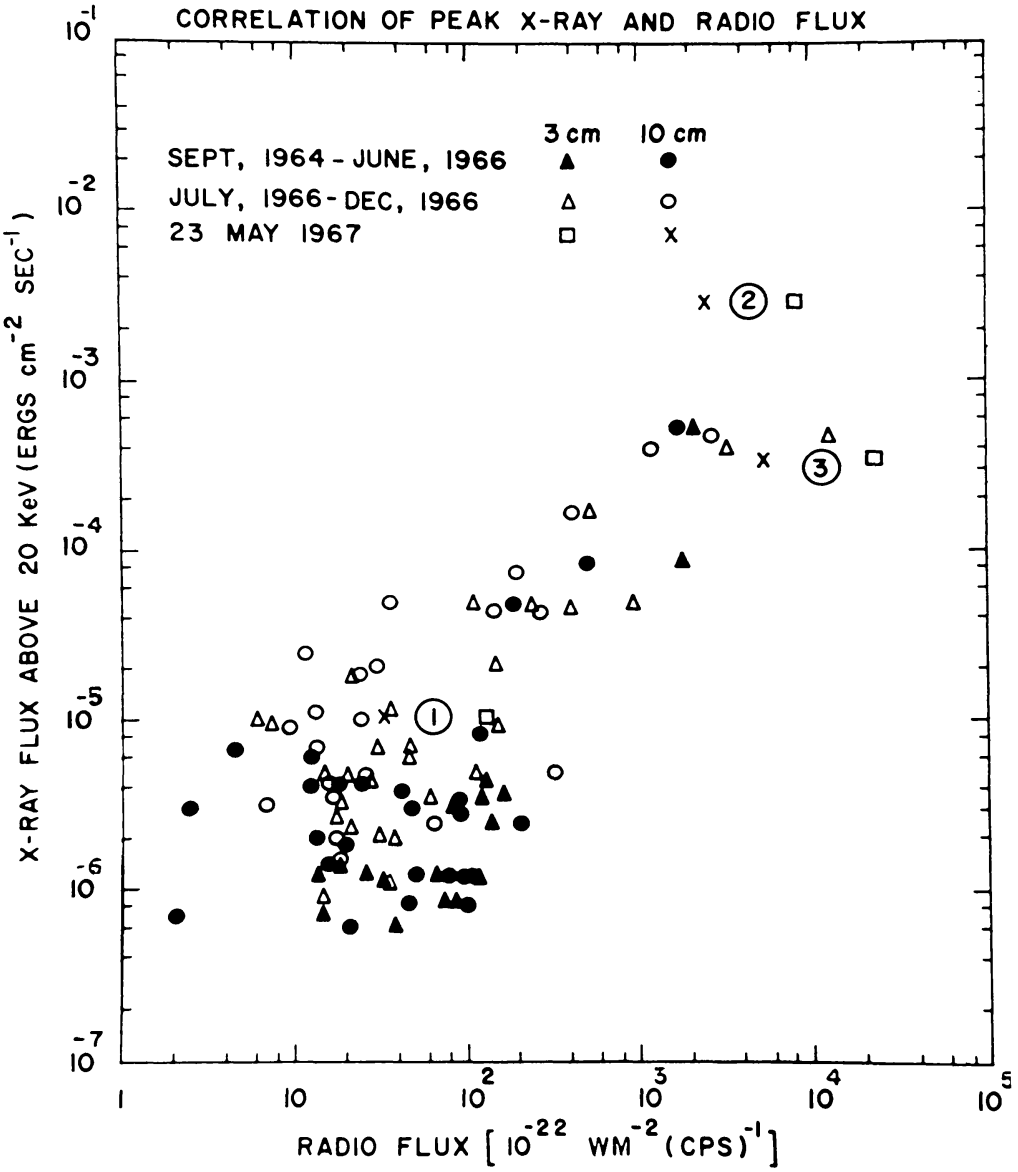


Fig. 31. Demonstrating the correlation between the peak values of the hard X-ray and microwave radiations from solar flare events. After Kane and Winckler (1969).

Various explanations have been advanced to explain the correlated microwave and hard X-ray radiations. Takakura (1969) has recently reviewed the subject, and advances the following model to explain the correlations, and also the differences evident between soft and hard X-rays, and microwaves. His model invokes (a) a hot coronal condensation, generated in the flash phase, of temperature $10^7$–$10^8$ K, that radiates the soft X-rays, and the gradual microwave burst; (b) two suprathermal electron populations of spectrum $dN = \text{const. } E^{-\gamma} dE$, where $\gamma = 2$–3. One of these populations is entrained in the condensation, and generates high energy X-rays through Coulomb bremsstrahlung, while the other population generates the microwave burst through gyro-synchrotron radiation in $\sim 10^3$ G sunspot fields. The escape of portion of these electron populations would give rise to the cosmic ray event at the

orbit of Earth. It is assumed that ions would be accelerated concurrently with the electrons.

The proposition that the energetic particles are accelerated and released from the environs of the flare at the time of the hard X-ray/microwave burst receives good experimental support. Thus Webber (1963) concludes that the relativistic ion events are consistent with this view ($\pm 1$ min), and Cline and McDonald (1968) show that the relativistic electron events of July 7, 1966 and 27 February, 1967 provide good diffusion fits when the time of the X-ray burst is taken as the origin of time (accuracy $\pm$ few min). It does appear, however, that the low energy electrons may be released somewhat earlier ($\sim 3$ min; Lin, 1970). This may simply be an effect of the finite rise time of the hard X-ray event, and of the hardening of the electron spectrum (from $\gamma = 3$–2) as the flare grows (Takakura, 1969), so that substantial quantities of low energy electrons are present some minutes prior to the maximum of X-ray output. The observed tendency for the X-ray spectrum to harden rapidly during the rising portion of the X-ray burst supports this hypothesis (Kane and Winckler, 1969; Cline *et al.*, 1968).

Zirin and Lackner (1969) have discussed the relationships of the hard and soft X-ray bursts to the optical effects of the flare of 28 August, 1966 (see Figure 30). They note that the hard X-ray burst coincides with the rapid motion of the two emission filaments away from one another, which is coincident with the 'flash' phase of the flare.

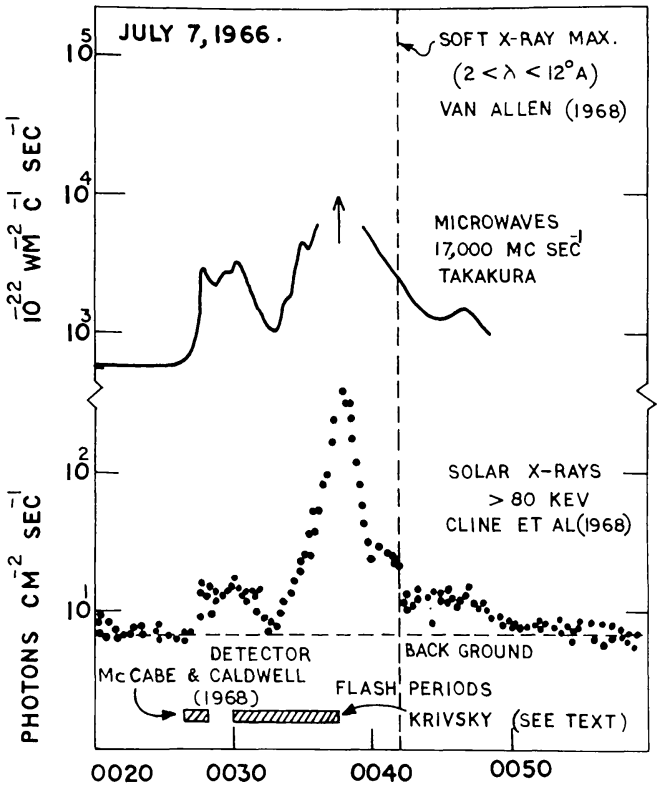


Fig. 32. A further illustration of the strong resemblance between microwave and hard X-ray flare events, and their approximation in time to the flash periods of the optical flare. Note that the maximum of the soft X-ray event occurs later in time. Based on Cline *et al.* (1968).

The presence of the hard X-ray indicates that this is the period of time (of duration $\sim 3$ min) in which acceleration to the highest energies is effective. The soft X-rays, by contrast, correlate with the total emission in H$\alpha$, presumably being correlated with the electron content, and temperature of the coronal condensation. A similar behaviour to the above has been reported for the event of July 7, 1966 (Figure 32); thus McCabe and Caldwell (1969) report a rapid expansion, and a 'flash' phase between 0026 and 0027, coinciding with the first hard X-ray burst. Krivsky (as reported on page 479, by Simon and Švestka, 1969) reports a separation of the two flare ribbons starting at 0030 and ending at 0037, coincident with the maximum of the second, and largest hard X-ray burst. On the basis of the agreement between these exceptionally well observed events, we feel that the identification of the period of ribbon separation as the period of particle acceleration is quite persuasive,

### 5.4. Post flare observations

A marked decrease in the total area of the parent sunspot following the occurrence of major cosmic ray flares was reported by Howard (1963). Subsequently, however, this relationship has been thrown into great doubt: Sivaraman (1969) showing that the effect became inconclusive after errors in Howard's original analysis were removed. During the well studied event of 7 July, 1966, the group area increased for two days after the flare, although the spot area immediately under the brightest part of the flare did decrease (McIntosh and Sawyer, 1968). Other large events observed during the IQSY Proton Flare Project likewise failed to provide any real support for this proposal (e.g. Švestka and Simon, 1969).

By way of contrast, the few detailed measurements that exist suggest that drastic changes do occur in the adjacent sunspot magnetic fields during major solar flares. Howard and Severny (1963) deduced a factor of 3 decrease in $B_{\|}$ in the day straddling the occurrence of the large (relativistic) cosmic ray flare of 16 July, 1959, the total magnetic energy density of the whole sunspot region decreasing by $\sim 50\%$ ($\sim 10^{33}$ erg). The major cosmic ray flare of 7 July, 1966 likewise exhibited major field changes in a period of one day straddling the flare. Thus the gradient in $B_{\|}$ across the neutral line decreased from 1 G km$^{-1}$–$\sim$0.2 G km$^{-1}$, while the energy content of the total vector field $B$, having increased to $\sim 10^{33}$ erg in the days prior to the flare, decreased to $\sim 10^{32}$ erg in the day straddling the flare. The changes are more pronounced at lower chromospheric levels. To date, observations of the fields have not been obtained immediately before and after a large flare, and hence it cannot be said with certainty that these changes in energy have occurred at the time of the flare. In view of the similarity between the observed energy change, and the known energy release in a large flare, the relationship would appear to be a direct one, however.

Severny (1968) has reported that the brightest emission of the flare of 7 July, 1966 coincided with the maximum vertical electrical currents (calculation based on curl of **B**). Previously, Moreton and Severny (1966, 1968) had shown that 80% of flare 'knots' (bright emission) coincide with maximal vertical currents, a result suggestive of the Alfvén and Carlquist (1967) conductive instability model for the solar flare.

### 5.5. The persistence of centres of activity

Guss (1964), Warwick (1965) and Švestka (1968) have investigated the distribution of cosmic ray flares in solar (Carrington) longitude. All three authors find a striking longitude dependence. Figure 33 (Warwick, 1965) displays the distribution of PCA producing groups (as distinct from PCA flares, since this can be unduly biased by a short lived active period) and the strength of this persistence is clearly evident. From a study of 174 solar flares associated with type IV radio bursts, Švestka (1968) concluded that new active regions form preferentially near old decaying regions, and hence the persistence is established.

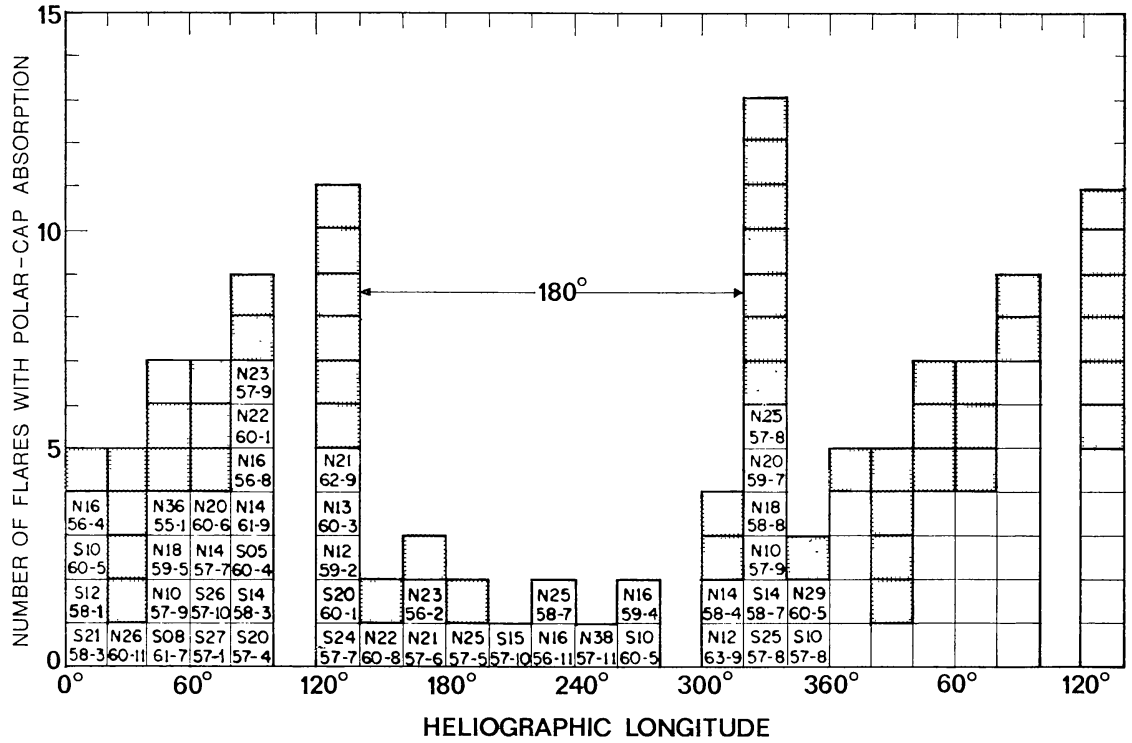


Fig. 33. Demonstrating the strong tendency evident during 1954–1963 for particle producing flares to occur at preferred heliographic (Carrington) longitudes. The latitude and date of independent events are indicated in the left half of the figure. The shaded squares represent flares from recurrent active regions, the first event of the series being included in the unshaded boxes. After Warwick (1965).

Bumba and O'Bridko (1969) have investigated the relationship between the flare active longitudes, and the position of the interplanetary magnetic field sector structure (Ness and Wilcox, 1967). For the period 1962–1966, they note that 11 out of 14 flare active regions occur within 15° of the sector boundary. In view of the uncertainties, this is an impressive result. Clearly, a common cause would seem to control the long lived persistence of sunspots, active regions, flaring regions, and sector boundaries.

## 6. Near Sun Effects

The facts that are known with considerable precision are:

(1) For many big flares, particle injection occurs near the flare, at the time of the X-ray/microwave burst.

(2) There is little true transverse diffusion in interplanetary space for low ionic energies ($\lesssim 1$ GeV) apart from that introduced by the meandering of the field lines. There is effective longitudinal diffusion.

(3) Delayed particle populations are long lived, and exhibit long lived field aligned anisotropies, while prompt events rapidly loose their field aligned anisotropies.

(4) Delayed events are characterised by marked spatial gradients in the cosmic ray density. By contrast, the prompt events are less strongly dependent on longitude, and do not show the strong small scale density changes observed for the delayed events.

(5) Prompt events show energy dispersion indicative of individual particle (as distinct from cooperative particle) travel from Sun to Earth. Delayed events show no energy dispersion.

It has been proposed that the origin of some of these properties is to be found in phenomena near the Sun. Clearly, the presence of strong magnetic fields and magneto-hydrodynamic waves near the Sun will inevitably have a considerable effect on cosmic rays of solar origin, and it is conceivable that near Sun effects could be of major importance. Some of the current proposals regarding near Sun effects will therefore be discussed.

### 6.1. Cosmic ray storage near the Sun

Storage of cosmic rays in the general vicinity of the Sun has been invoked to explain the persistence of the prompt cosmic ray flare effect (Anderson *et al.*, 1959); the persistence of delayed events (e.g. Bryant *et al.*, 1965a; Anderson, 1969); and the persistence of strong field aligned anisotropies for times long compared to the 'isotropising' time noted for prompt events (Bartley *et al.*, 1966).

Undoubtedly the most cogent evidence for some temporary storage is the long life time of the type IV emitting region near the parent flare. Thus the electron cyclotron

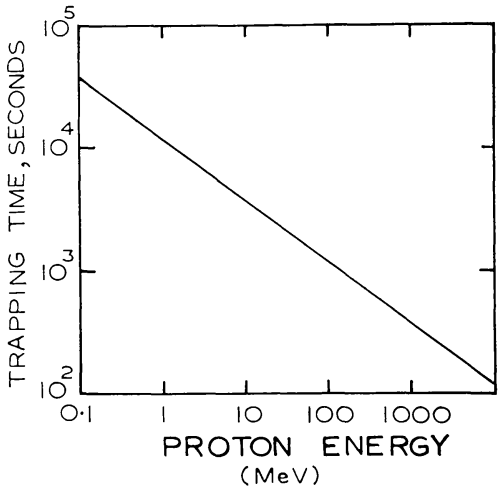


Fig. 34. A crude estimate of the energy dependence of the trapping time for protons in the vicinity of the Type IV C emission region.

period is 0 ($10^{-7}$ sec); the electron travel time across the dimensions of the type IV region is 0 (1 sec); while the life time of the type IV C emission is 0 ($10^4$ sec). If the fields were diverging the electrons would receede from the Sun immediately, hence they must be forcibly impounded. The observed fact that the type IV B emission region has a noticeable radial velocity shortly after the flare, and moves as a well defined entity speaks further for the concept of a trapped spatially limited population of suprathermal charged particles.

Type IV radiation is due to near relativistic electrons, and hence 40 keV electrons, and $E \lesssim 0.5$ MeV ions will experience trapping similar to that observed for the type IV population. The assumption of a trapping 'time constant' of 0 ($10^4$–$10^5$ sec) for relativistic electrons (appropriate to type IV C), and further, the assumption of a trapping effectiveness varying as (rigidity)$^{-1}$, yields the relationship in Figure 34. Note that this suggests that ionic trapping is relatively unimportant for energies greater than 0 (10 MeV). This is in general agreement with the observed fact that delayed events in the absence of a parent flare are never seen at energies $\gtrsim 10$ MeV (Fan *et al.*, 1968).

The type IV emitting region in the more important flares recedes radially from the Sun and then assumes a stationary position for the remainder of the type IV event (Kundu, 1965). Weiss and Sheridan (1963) have studied the angular dimensions of the radio emission at this phase (called the type IV C phase by some authors, and type IV m (for metric) by others) at 40–60 MHz, and show that it is primarily concentrated in a region of dimension $\approx 4'$ between half power points, superposed on a wider distribution of width 40′ (see Figure 35).* The emission of angular width 4′–10′ dies away slowly with a time constant of order $10^4$–$10^5$ sec. The emission at 40–60 MHz originates at $\simeq 2R_\odot$; hence the concentrated region of type IV emission

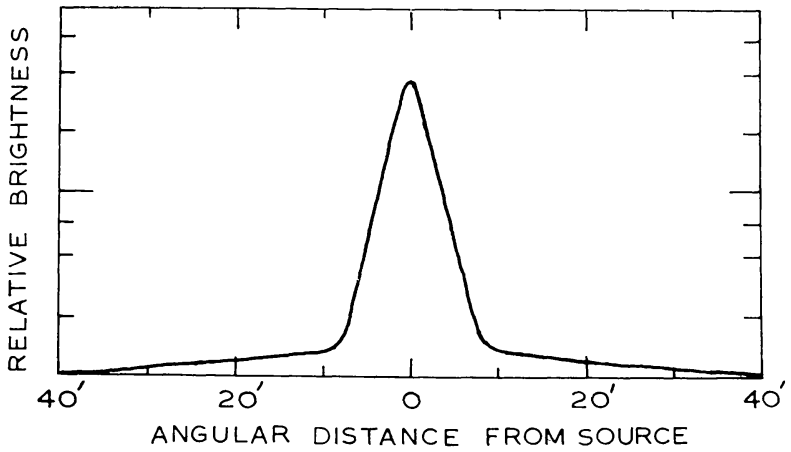


Fig. 35. The angular dependence of the radio emission from the Type IV C burst from the particle producing flare of 15 November, 1960. Note the well defined 'core' of emission which has angular dimensions comparable to the angle that the 'core' of delayed particle event subtends at the Sun. After Weiss and Sheridan (1962).

* Weiss and Sheridan have called these the 'core' and 'halo' of the radio emission. By good fortune, Lin *et al.* (1968) independently chose their nomenclature such that the radio 'core' corresponds to the cosmic ray 'core', and the haloes likewise.

subtends an angle of $\simeq 8°$ at the centre of the Sun. This corresponds to $\simeq 0.6$ days of solar rotation, which is similar to the observed time scale of the 'core' type delayed event, for which the pronounced long lived anisotropy also indicates continuous leakage from a storage region near the Sun.

Lin *et al*, (1968) have discussed storage near the Sun, and point out that the absence of a flattening of the spectrum at low ion energies indicates that there has been no serious ionization loss on the part of the particles of energy $\approx 3$ MeV. This clearly sets an upper limit to the storage time. Lin *et al.* estimate $\sim 3$ h, however, this appears to be an underestimate. Thus if the region of cosmic ray storage coincides with the type IV C radio emission, the cosmic rays are stored at $\gtrsim 1\ R_\odot$ above the photosphere. The relevant density ($\lesssim 8 \times 10^{-18}$ g cm$^{-3}$) yields an upper limit to the average storage time of $\approx 10^5$ sec ($\sim 1$ day) before ionisation loss effects would be apparent at ion energies $\approx 3$ MeV. Hence the absence of any indication of ionisation loss is consistent with storage times of $\lesssim 1$ day, which is itself consistent with the observed life times of type IV C radio emission.

From the foregoing, we conclude that there is considerable evidence that the type IV C event indicates the position, dimensions, and life time of the storage processes which are active for ions $\lesssim 10$ MeV and all electron energies $\lesssim 100$ MeV. As Anderson (1969) and others have suggested, we propose that the particle leakage from this type IV storage region gives rise to the 'core component' of the delayed cosmic ray population in the solar system. Since the observed duration of the cosmic ray 'core' event is similar to that predicted by the azimuthal extent of the magnetic projection of the type IV C population to the orbit of Earth, and since the core usually exhibits strong spatial gradients on its boundary (as does the type IV radio emission), we conclude that the particles leak out of the storage region without any appreciable lateral diffusion. That is, we infer that if there are near-Sun diffusion processes, they occur at heliocentric distances $\lesssim 2\ R_\odot$. This is consistent with the low values of $K_\perp$ deduced by Lin *et al.* (1968) for the halo/core event of July 8, 1966.

### 6.2. Near sun diffusion

Diffusion close to the Sun has been advocated quite frequently (e.g. Sekido and Murakami, 1955; Reid, 1964; Axford, 1965b). The recent applications of near Sun diffusion have been directed to explaining the observation of prompt flare effects far from the Archimedes field line of injection at low energies where the transverse interplanetary diffusion is known to be negligible (see Chapter 2). Thus models have been invoked in which there is a relatively thin diffusing region close to the Sun, so that the cosmic rays produced in the flare are distributed widely in solar longitude. It is further assumed that when the cosmic rays escape from the immediate vicinity of the Sun, they are collimated ($\sin^2\theta/B = \text{const}$) in the interplanetary magnetic field. In this manner, the longitude effects, the initial anisotropy, and the diffusion-like dispersion effects have found partial explanation. Difficulties do arise however. For example, Fan *et al.* (1968) show that the times calculated for the near Sun diffusion for prompt events in March 1966 are much shorter than those predicted by the Reid (1964)

diffusion model. Since Reid's choice of mean free path was somewhat arbitrary, this may be merely an indication of a rather different diffusion coefficient.

The meandering nature of the interplanetary field (Michel, 1967; Jokipii and Parker, 1968) produces a degree of variability into the model that will also explain the discrepancies noted by Fan *et al.* Thus some parent flares near CMP and even on the eastern portion of the solar disc do produce prompt flare effects near Earth with very fast rise times, little dispersion, and strong anisotropies. It is these events that suggest rapid propagation along meandering field lines. Other prompt events show slower rise times, but still considerable anisotropies suggesting diffusion near the Sun, followed by relatively scatter free propagation from Sun to near Earth.

The strong azimuthal gradients associated with delayed events (0 (100) per 30° of heliographic longitude) are considerably greater than those associated with prompt events (0 (10) per 30°). It is difficult to use exactly the same model of localised injection, near Sun diffusion and Sun-Earth propagation along meandering field lines to fit both sets of observations (e.g. Lin *et al.*, 1968). For example, it is difficult to explain the tendency for parent flares at $\approx 60°$W to produce classical prompt events, which show relatively weak azimuthal gradients, while the delayed particle populations of the same flare may show much greater, and long lived, gradients. What appears to be needed is a model in which the diffusion process is selectively experienced by the prompt event particles, alone.

Figure 36 is our conception of such a model. We first note the various suggestions that the solar corona is heated by the dissipation of hydromagnetic waves originating lower in the solar atmosphere. (Billings, 1966). Estimates vary as to the thickness of this region of dissipation, although they tend to suggest low altitudes, that is, they indicate marked hydromagnetic wave propagation is confined to low altitudes. ($\lesssim 0.5\ R_\odot$ above the photosphere).

We suggest that near Sun diffusion occurs in the region traversed by the hydromagnetic waves, the waves providing the magnetic irregularities necessary to permit

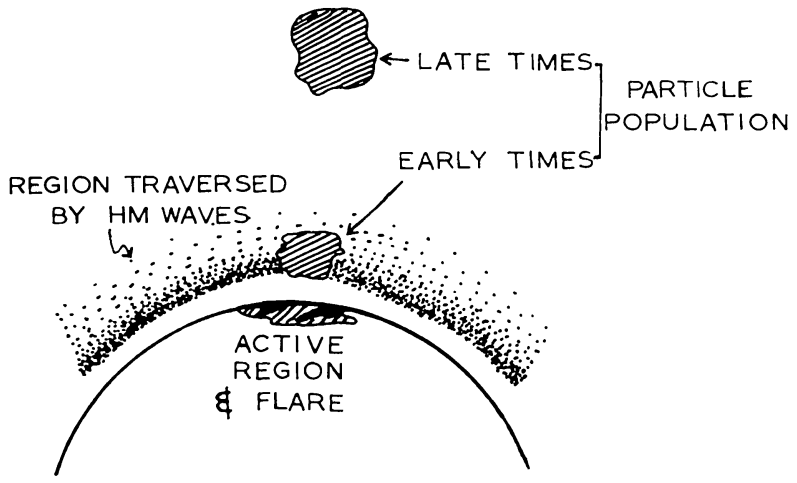


Fig. 36. A suggested model wherein diffusion in solar azimuth can occur near the Sun. Diffusion is therefore effective at early times, but not at late times when the principal population of cosmic ray particles is stored $\gtrsim 1\ R_\odot$ above the chromosphere.

the diffusion. Above the dissipation region, the magnetic fields would be more ordered, and transverse diffusion not important.

For such a model, the following predictions can be made. Let a flare occur in the active region, then:

(1) at early times ($\lesssim$20 min), the flare cosmic ray population is low in the corona, in close contact with the diffusing region (see Figure 36). Diffusion therefore proceeds rapidly. Consequently, the solar cosmic radiation would be widely distributed in longitude, and there would be smoothly varying cosmic ray densities in the diffusing region, and consequently the prompt event would vary smoothly with azimuth near the orbit of Earth;

(2) with the passage of time, the cosmic ray population moves radially away from the Sun (the type IVB phase) till the type IV C phase is reached ($R \gtrsim 2\ R_\odot$). At this time, the particle population is no longer in good contact with the diffusing region, and transverse diffusion is therefore not important. Hence the spatial distributions in the type IV C distribution are preserved. These distributions would therefore dictate the azimuthal distribution in interplanetary space of the 'core' radiation in the delayed event. A strong spatial variation in the storage region would result in a strong spatial variation of cosmic ray density near the orbit of Earth.

### 6.3. Continuous production

Bryant *et al.* (1965b) have suggested the existence of a continuous cosmic ray acceleration mechanism associated with active solar regions. They envisage this process to be in addition to the intermittent production associated with solar flares. As evidence, they cite sunspot minima observations (epoch 1963) of solar protons detected on seven successive solar rotations with little concurrent flare activity. They conclude that the observations are not explicable in terms of flare production, and subsequent trapping. While other authors have made tentative suggestions along the same lines, the Bryant *et al.* proposition is the only substantive argument for a continuous production mechanism known to the authors of this review.

Fan *et al.* (1968) and Anderson (1969) have discussed the large, delayed events observed at 0 (1 MeV) cosmic ray energies. Fan *et al.* note that the active regions which are correlated with the delayed event exhibit a high degree of flaring, with many microwave radio noise bursts accompanying the flares. For example, the proton data in Figure 17 correspond to an active centre which produced 143 optical flares, and 125 radio bursts at 10 cm during its passage across the disc. While only 8 discrete prompt events could be discerned during this time, the connection between microwave radio emission and charged particle acceleration (Section 5) suggests that there may have been subliminal prompt events. With a radio burst rate of $\sim 9\ \text{day}^{-1}$, and an inferred storage time from type IV measurements of from 3–24 h, the implication is that the stored population ($E_p \lesssim 10$ MeV, $E_e \lesssim 100$ MeV) would, at any given time, be the sum of the populations from a number of flares. That is, the population would not be greatly sensitive to any one given flare, but would vary with time and space in a smooth manner, partially determined by the flare rate. Fan *et al.* (1968) conclude that

the recurrent proton streams observed by them in 1966 are explicable in terms of impulsive flare acceleration, alone.

Anderson (1969) has discussed delayed events correlated with active centres, but of a less extreme nature than in the case of Fan *et al.* (e.g. one event he has considered is displayed in Figure 19). He nevertheless reaches the same conclusion.

In view of the frequent occurrence of flares in active centres, and of the 0 ($10^4$–$10^5$ sec) particle storage time, it is going to be very difficult to prove or disprove the existence of a continuous production component based on cosmic ray data alone, except at sunspot minimum (e.g. Bryant *et al.*, 1965b). Even then an absolute proof will be very difficult, since flare events still do occur. For the present, the reviewers conclude that the evidence indicates that the majority of the observed effects are due to particles accelerated in flares, there being no radio or cosmic ray evidence to suggest otherwise except, possibly, at sunspot minimum. Clearly, it does not appear to be an effect of any major consequence.

### 6.4. Dispersed acceleration effects

Most considerations of flare effects have been based on the assumption of a single, localised region of injection for the cosmic rays. A considerable amount of evidence exist that suggests that this is a gross over-simplification.

Anderson (1969) has reported two 'prompt' flare effects which exhibited extremely atypical profiles (Anderson, 1969, his Figure 14). Whereas electron prompt events normally show a prompt rise time, little fast temporal structure, and a smooth decay phase, the two events in question showed great temporal structure, were short lived and ceased abruptly. The decay time constants were an order of magnitude shorter than those applicable to prompt events, in general.

Anderson suggests that these events are the result of electron acceleration on the observers field line, at a point near the Sun. He suggests that flare waves (Athay and Moreton, 1961) are a possible source of such acceleration processes. He reports that similar phenomena occur superposed on other prompt events. Since the diffusion process is believed to control the decay rate of prompt events, the prompt event profile being essentially the transient response function of the solar system to a delta function particle injection at the Sun, such an explanation would require that the diffusion coefficients on the observers line of force should be very large, of order $10^{23}$ cm$^2$ sec$^{-1}$. Such values have not been observed.

An alternate explanation of the observations might be that the two events quoted by Anderson are examples of prompt events showing strong spatial gradients. Some support is given to this hypothesis in that the more remarkable of the two events occurred at the minimum of a pronounced Forbush decrease.

The fact remains that flare initiated shock waves are known to exert a powerful influence on remote parts of the Sun. The occurrence of sympathetic flares is one such example, although the fact that the triggered flare will be observed by the flare patrol means that little mystery will be introduced into the cosmic ray interpretation by this phenomenon.

Of much greater import is the species of phenomena recently noted by Wild and his coworkers using the Culgoora radio heliograph, as already mentioned in Section 3. It had been shown earlier (Athay and Moreton, 1961) that a flare can produce a shock wave that disturbs filaments at great distances from the parent flare. With the advent of 'photography' at 3.75 metre wavelengths, Wild and his coworkers (e.g. Wild, 1969; Wild *et al.*, 1968; Labrum and Smerd, 1968) have shown that the shock wave can trigger catastrophic changes in prominences, that then initiate shock waves, and type IV radio emission of their own. That is, there is clear radio evidence of direct particle injection into the solar system at points far removed from the flare proper. The triggering delay due to the shock wave propagation time ($\lesssim$12 min) is certainly consistent with some cosmic ray observations, as discussed in Section 3.

Wild (1969) and Kai (1969) note another phenomenon of major interest. This is the almost simultaneous observation of radio emission from points on the Sun which are separated by distances of order one solar radius. Wild interprets these as evidence for near relativistic electrons propagating between the two points along magnetic lines of force. This could therefore result in cosmic ray injection into the solar system on lines of force far removed from those in the vicinity of the parent flare.

These radio observations therefore indicate that the azimuthal distribution of solar cosmic radiation in the solar system may be due to a number of distinct mechanisms. In particular, we note that there may be more than one primary injection point into the solar system from which diffusion would then proceed at points near to the Sun. We note also that since the relative roles of these various mechanisms would vary greatly from time to time, there will be a wide variability in the details of the azimuthal dependence of cosmic ray density from event to event. Ad hoc descriptions on an event to event basis using a variable mixture of such mechanisms is clearly most unsatisfactory and unrewarding.

It is our opinion that the only satisfactory way to reduce the ad hoc nature of a multiple injection point model is to employ radio data to identify the presence, and position of the injection points at the Sun. This necessitates angular resolution of 0.1 solar diameters, or better, on a time scale of $\lesssim$10 sec. The Culgoora radio heliograph is the only instrument with this capability at the present time. It is only with such data, however, that definitive studies of the azimuthal distribution of cosmic rays in the solar system will be possible, in future, now that the work of Wild and his coworkers has so clearly indicated the importance of multiple injection processes.

## 7. PCA Events

The Earth's ionosphere was first recognised as an effective detector of low energy 0 (10 MeV) cosmic ray ions in 1956 (Bailey, 1957), and existing synoptic data permitted the study of low energy events from as early as 1947. Until the advent of essentially continuous studies using satellites in about 1963–65, ionospheric techniques were an important primary source of solar flare cosmic ray data (e.g. Figure 8).

The polar cap ionization density is not simply related to the solar cosmic ray flux

outside the geomagnetic cavity. Variable electron-ion recombination rates produce seasonal and diurnal variations into the sensitivity of an instrument, while time dependent geomagnetic cut-off rigidities also introduce a diurnal variation, as well as changes during the progress of magnetic storms. The directional properties of an ionospheric measurement are also complex, time variable, and model dependent. On account of all the other uncertainties, the extraction of energy spectra from ionospheric data is impossible.

For these reasons, ionospheric measurements can no longer be regarded as quantitative, primary measurements of the solar cosmic ray flux. They remain of interest as (a) a quick access technique for detecting solar cosmic rays, as will be needed to initiate a special experiment (e.g. a rocket flight); (b) as a method of studying the details of the Earth's magnetosphere and tail. That is, knowing the spectral and directional properties of a prompt solar flare event from measurements made with a satellite detector, the ionospheric measurements can be used to deduce the times and areas of impact of that radiation on the ionosphere, and hence as a test of models of the magnetosphere. It is in those two roles, then, that PCA events are included in this review.

The motion of charged particles in the Earth's magnetic field has been investigated by a number of workers (Hofmann and Sauer, 1968 and all references therein). Realistic models of the geomagnetic field of internal origin involving higher order harmonics have also been used by Sauer (1963), Shea *et al.* (1965), McCracken *et al.* (1965) and Gall *et al.* (1968) for calculating the cut-off rigidities at different locations on the Earth. Direct measurements of solar protons in the 1–10 MeV range with satellite detectors, however, have conclusively shown that the theoretical prediction of trajectory calculations (Shea and Smart, 1967) are much higher than the experimentally observed cut-offs (Paulikas *et al.*, 1968; Sawyer *et al.*, 1968) particularly above 50° latitude. A Sun oriented asymmetry is also evident. The inadequacy of the internal field theories to predict accurate cut-offs and thus the effects of low energy solar protons than can easily impinge at the high latitude stations is ascribed to the neglect of effects due to the presence of the magnetosphere and the geomagnetic 'tail', that is, to 'external' terms in the field expansion.

Direct interplanetary measurements with satellites and space probes conducted during the last few years have established the gross features of the interaction of the solar wind with the geomagnetic field and the shape of the Earth's magnetosphere. It is now accepted that the Earth's magnetic field is deformed into a comet like shape with the tail pointing away from the Sun (Ness *et al.*, 1964, 1969). Such a field configuration will affect the cosmic ray precipitation into the polar regions. Many theoretical models have been put forward, which although similar in gross configuration, do differ significantly in details. We will not attempt to describe the various magnetospheric models in detail in this review, since these have already been reviewed elsewhere (Roederer, 1969; Dungey, 1968) and it does not come under the purview of this review. The crucial difference between various theoretical models proposed lies in the extension of the geomagnetic tail and the manner in which the interplanetary

medium merges with the geomagnetic field. The model proposed by Dungey (1963) and further elaborated by Levy *et al.* (1964) and Axford *et al.* (1965) envisages appreciable merging between the geomagnetic and interplanetary magnetic fields resulting in a direct connection of the field lines from the polar cap with the interplanetary magnetic field within a distance of 1000 $R_E$. In contrast, Dessler and Juday (1965) proposed an open tail model, where the geomagnetic tail extends to 20–50 AU with practically no significant merging with the interplanetary field. Both the models predict access of low energy particles ($\simeq$1–100 MeV) into the polar cap regions, Axford and Dungey's model through direct access via polar field line connection with the interplanetary field and Dessler's model through diffusion from the magnetospheric boundary. The predictions regarding the temporal and spatial distribution of the particles will however differ, the latter model predicting the existence of large inhomogeneities lasting for several hours, i.e. intense proton bombardment taking place over a part of the polar cap and negligible bombardment over other parts. Dessler (1968) has re-examined his theory and considering the low plasma density in the tail concludes that the magnetic merging can take place in the tail region between 10 and 30 $R_E$. The magnetic merging would be more effectively accomplished when the plasma density is very low. Under these assumptions, there would be little difference in the prediction of the spatial and temporal distribution of sub-relativistic protons at high latitudes by the two theories.

The experimental observations show a well defined geomagnetic tail to a radial distance of 80 $R_E$ with evidence indicating a distorted, filamentary tail to 500 $R_E$ and 1000 $R_E$ (Mariani and Ness, 1969; Ness *et al.*, 1967). Thus the actual total extent of the tail still remains an open question.

The $\lesssim$100 MeV solar cosmic rays can only reach the upper atmosphere at high latitudes. They produce enhanced ionisation in the mesosphere as a result of inelastic collisions with ambient neutral gas molecules and thereby result in absorption of radio waves at $f \lesssim 50$ MHz. Thus one would expect to observe polar cap absorption events (PCA) at high latitudes in association with solar flares and the accompanying microwave X-ray and particle emission from the Sun.

The general nature and properties of PCA events have been extensively studied by a large number of workers (Hakura, 1964; Obayashi, 1964; Akasofu *et al.*, 1963) and have been well reviewed by Bailey (1964). Hakura (1967) who has made an extensive study of the onset phase of PCA events at various latitudes has found that the polar cap absorption usually starts at high latitudes within 2–3 h after the onset of the solar flare and then spread out to lower latitudes below 60° in a few hours. The development and spread of PCA to lower latitudes is not gradual but seems to occur in three distinct characteristic stages. The first increase in absorption takes place above 80° geomagnetic latitude. The ionisation is confined to a small region and is not spread uniformly in magnetic longitude. Hakura (1967) proposes that this portion of the PCA event is due to solar electrons ($0.1 < E < 40$ MeV). In the second stage, the ionisation becomes more intense and spreads to latitudes of $\gtrsim 65°$. The distribution is still asymmetric. Finally the enhanced ionisation appears in the lower auroral zone

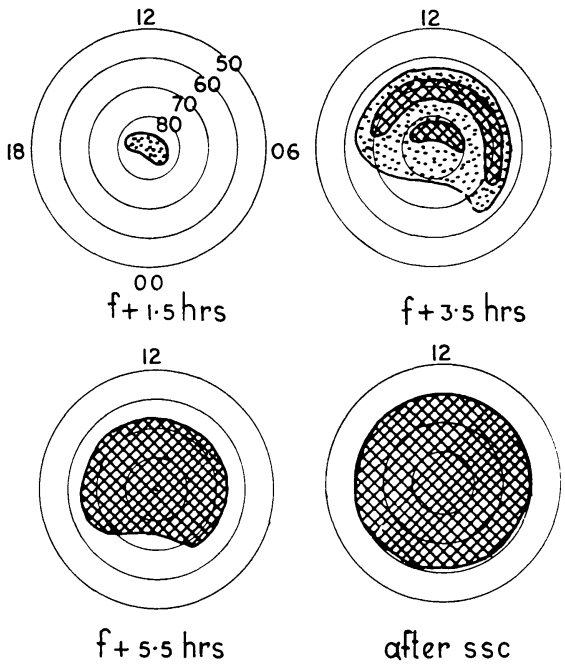


Fig. 37. Illustrating the temporal development of the PCA event. This event occurred on 7 July, 1958. The plot is polar, the coordinates being invariant latitude and local time. Dotted regions indicate weak to medium absorption, while cross-hatched regions indicate strong absorption. The diagrams correspond to observations 1.5, 3.5, and 5.5 h after the flare. After Hakura (1967).

($\approx 60°$ geomagnetic latitude) with the ionisation being distributed uniformly to achieve a complete polar black out. Figure 37 shows these stages in the development of the PCA onset. Hakura (1967) proposes that the second and third stages in the development of the PCA are due to the differential arrival of protons and $\alpha$ particles at the Earth. Table VII displays the time scales observed for the onset of the three stages during the PCA events which occurred on 7 July, 1958 as observed by Hakura. Since the observed time scales for different stages are larger than the rectilinear transit times for different particles, Hakura has suggested that this discrepancy indicates the importance of particle diffusion process in the geomagnetosphere. In view of the long time scales involved in interplanetary diffusion, such a conclusion must be regarded

TABLE VII

Time scales observed for the onset of three characteristic stages of PCA events on July 7, 1958 (after Hakura, 1967)

| Stage | Time after flare (in hours) | Latitude of PCA | Ionizing agents |
|---|---|---|---|
| 1st Stage | 1.5 | $\gtrsim 80°$ | Prompt electrons or protons |
| 2nd Stage | 3.5–7.5 | $\gtrsim 65°$ | Protons |
| 3rd Stage | 9.5 | $\gtrsim 60°$ (54–65°) | $\alpha$ Particles and protons |

as very tentative until confirmed by concurrent measurements of PCA events and satellite observations both inside and outside the geomagnetosphere.

Reid and Sauer (1967) have shown that large differences exist between the PCA effects observed at Antarctic stations between 68° and 82° invariant latitude. The PCA observations are consistent with the direct measurements of solar proton flux made by Paulikas *et al.* (1966) during the same event. The differences have been attributed by Reid and Sauer (1967) to the existence of a marked anisotropy in the low energy solar protons (Bartley *et al.*, 1966). Depending on the tube of force in the interplanetary field to which a particular location is connected, the sampling of solar protons will differ. Strong North-South asymmetries have also been reported by them. For example in the case of the PCA event on February 5, 1965, there was no evidence of PCA in the northern polar cap, observed corresponding to the PCA event in the southern polar cap.

A well known time variation often observed in PCA events in the so-called 'Midday recovery' which is a significant decrease in the absorption near local noon. Figure 38

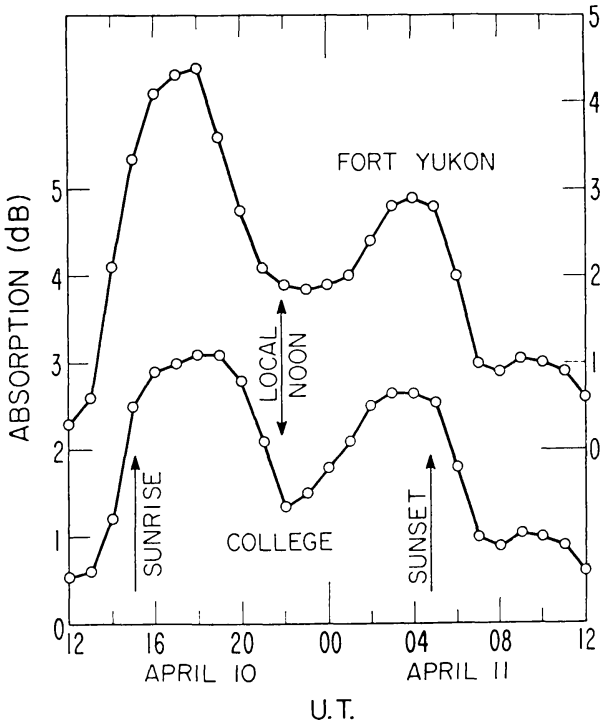


Fig. 38. Demonstrating the diurnal variation in the absorption observed by 27.6 MHz riometers. Insofar as riometer data are to be used as quantitative measurements of the solar cosmic ray flux, these diagrams are indicative of the diurnal variations in the instrument sensitivity. The diagram is from Leinbach, as reported by Hoffman and Sauer (1968).

shows a typical example of the midday recovery during a PCA event (Leinbach, as reported by Hoffman and Sauer, 1968). Besides this characteristic decrease in absorption, decreases are also observed at midnight which have been attributed to the electron attachment at night forming negative ions (Bailey, 1964). A midday recovery is observed to be almost symmetrical about its peak and it persists for some 6–10 h

(Leinbach, 1967). Most of the midday recoveries reach their peak at about 10–12 h local time. The magnitude of the recovery which is as high as 70% at high latitude is almost non existent at low latitudes. There is some inconclusive evidence showing that the peak of the midday recovery shifts progressively to earlier hours on successive days following the onset of the PCA event (Leinbach, 1967). The midday recovery is the result of an increase in the cut-off rigidity on the sunward side of the polar cap, due to the presence of the magnetosphere (Reid and Sauer, 1967; Gall *et al.*, 1968). Theoretical calculations show that for a station like Kiruna, the cut-off energy can change from 4 MeV at midnight to 47 MeV at noon.

Measurements of low energy cosmic ray protons by Paulikas *et al.* (1968) in an polar orbiting satellite have confirmed the diurnal variation in cut-off, the magnitude of the variation in the cut-off decreasing at higher energies. Taylor (1967) has calculated the detailed pitch angle distributions of low energy (1–2 MeV) protons in a model magnetosphere (Taylor and Hones, 1965) and concludes that on the day side at $\sim$2000 km altitude, only particles with large pitch angles can reach magnetic latitudes above 65° producing a loss cone for low energy protons on the day side of the polar cap.

Since the indirect balloon observation by Winckler *et al.* (1961), satellite experiments have directly measured the cut-off reduction associated with the geomagnetic storms. The enhancement in the low energy solar cosmic ray flux reaching the Earth during magnetic storms will cause a further enhancement of PCA. The increase in low energy cosmic radiation (Winckler *et al.*, 1961) as well as the enhancement in PCA (Leinbach *et al.*, 1965) during severe magnetic storms have both been observed experimentally. For stations near the boundary of the auroral zone, the enhanced absorption observed early in the main phase of the storm seems to recover immediately which might be due to softening of solar particle spectrum.

## Acknowledgements

The authors wish to express their thanks to Dr. Z. Švestka, Dr. K. V. Sheridan and Dr. R. P. Lin for their helpful comments and suggestions and to Dr. W. R. Webber and Dr. A. J. Masley for providing unpublished information on PCA events. One of us (KGMcC) is grateful to the Director, Physical Research Laboratory, Ahmedabad, India, for hospitality provided during his stay at Ahmedabad when most of the work presented here was completed. Part of the work was performed at the University of Adelaide, Australia, and was supported by funds from AFCRL contract AF 19-(628)-5039. The research in India was supported by funds from the Department of Atomic Energy, Government of India, and funds from the grant NAS-1492 from the National Academy of Sciences, U.S.A. Part of the work was done at the University of Texas under the NASA Contract NGL-44-004-001.

## References

Akasofu, S. I., Lin, W. C., and Van Allen, J. A.: 1969, *J. Geophys. Res.* **68**, 5327.
Alfvén, H. and Carlquist, D.: 1967, *Solar Phys.* **1**, 220.

Allum, F. R., Rao, U. R., McCracken, K. G., and Palmeira, R. A. R.: 1970, to be published in *Solar Phys.*
Anderson, K. A.: 1969, *Solar Phys.* **6**, 111.
Anderson, K. A. and Lin, R. P.: 1966, *Phys. Rev. Letters* **16**, 1121.
Anderson, K. A., Arnoldy, R., Hoffman, R., Peterson, L., and Winckler, J. R.: 1959, *J. Geophys. Res.* **64**, 1133.
Arnoldy, R. L., Kane, S. R., and Winckler, J. R.: 1968, *Astrophys. J.* **151**, 711.
Athay, R. G. and Moreton, G. E.: 1961, *Astrophys. J.* **133**, 935.
Avignon, Y., Martres-trope, M. J., and Pick, M.: 1963, *Compt. Rend.* **256**, 2112.
Avignon, Y., Caroubabes, C., Martres, M. J., and Pick, M.: 1965, *IAU Symp.* **22**, 373.
Axford, W. I.: 1965a, *Planetary Space Sci.* **13**, 115.
Axford, W. I.: 1965b, *Planetary Space Sci.* **13**, 1301.
Axford, W. I., Petschek, H. E., and Siscoe, G. L.: 1965, *J. Geophys. Res.* **70**, 1231.
Bailey, D. K.: 1957, *J. Geophys. Res.* **62**, 431.
Bailey, D. K.: 1964, *Planetary Space Sci.* **12**, 495.
Bartley, W. C., Bukata, R. P., McCracken, K. G., and Rao, U. R.: 1966, *J. Geophys. Res.* **71**, 3297.
Billings, D. E.: 1966, *A Guide to the Solar Corona*, Academic Press, New York.
Biswas, S. and Fichtel, C. E.: 1965, *Space Sci. Rev.* **4**, 709.
Biswas, S., Fichtel, C. E., and Guss, D. E.: 1962, *Phys. Rev. Letters* **128**, 2756.
Biswas, S., Fichtel, C. E., Guss, D. E., and Waddington, C. J.: 1963, *J. Geophys. Res.* **68**, 3109.
Bruzek, A.: 1964, *J. Geophys. Res.* **69**, 2386.
Bruzek, A.: 1968, *Ann. IQSY* **3**, 85.
Bryant, D. A., Cline, T. L., Desai, U. D., and McDonald, F. B.: 1962, *J. Geophys. Res.* **67**, 4983.
Bryant, D. A., Cline, T. L., Desai, U. D., and McDonald, F. B.: 1965a, *Astrophys. J.* **141**, 478.
Bryant, D. A., Cline, T. L., Desai, U. D., and McDonald, F. B.: 1965b, *Phys. Rev. Letters* **14**, 481.
Bumba, V. and O'Bridko, V. N.: 1969, *Solar Phys.* **6**, 104.
Burlaga, L. F.: 1967, *J. Geophys. Res.* **72**, 4449.
Burlaga, L. F.: 1968, *Solar Phys.* **4**, 67.
Boorman, J. A., McLean, D. J., Sheridan, K. V., and Wild, J. P.: 1961, *Monthly Notices Roy. Astron. Soc.* **123**, 87.
Carmichael, H.: 1962, *Space Sci. Rev.* **1**, 28.
Castelli, J. P., Aarons, J., and Michael, G. A.: 1967, *J. Geophys. Res.* **72**, 5491.
Cline, T. L. and McDonald, F. B.: 1968, *Solar Phys.* **5**, 507.
Cline, T. L., Holt, S. S., Hones, Jr., E. W.: 1968, *J. Geophys. Res.* **73**, 434.
Coleman, P. J.: 1966, *J. Geophys. Res.* **71**, 5509.
Covington, A. E.: 1959, *Paris Symposium on Radio Astron.* (ed. by R. N. Bracewell), p. 159.
Dessler, A. J.: 1968, *J. Geophys. Res.* **73**, 209.
Dessler, A. J. and Juday, R. D.: 1965, *Planetary Space Sci.* **13**, 63.
Dodson, H. W. and Hedeman, E. R.: 1960, *Astron. J.* **65**, 51.
Dodson, H. W., Hedeman, H. W., and Owren, L.: 1953, *Astrophys. J.* **118**, 169.
Dolginov, A. Z. and Toptygin, I. N.: 1966, *Book of Abstracts*, Symposium on Solar-terrestrial Physics (Belgrade).
Dungey, J. W.: 1963, *Planetary Space Sci.* **10**, 223.
Dungey, J. W.: 1965, *J. Geophys. Res.* **70**, 1753.
Dungey, J. W.: 1968, *Solar Terrestrial Physics* (ed. by J. W. King and W. S. Newman), Academic Press, New York, p. 91.
Durgaprasad, N., Fichtel, C. E., Guss, D. E., and Reames, D. V.: 1968, *Astrophys. J.* **154**, 307.
Elliot, H.: 1964, *Planetary Space Sci.* **12**, 657.
Elliot, H.: 1969, in *Solar Flares and Space Research*, North-Holland Publ. Co., Amsterdam, p. 356.
Ellison, M. A., McKenna, S. M. P., and Reid, J. H.: 1961a, *Dunsink Observ. Publ.* **1**, 53.
Ellison, M. A., McKenna, S. M. P., and Reid, J. H.: 1961b, *Monthly Notices Roy. Astron. Soc.* **122**, 491.
Fan, C. Y., Lamport, J. E., Simpson, J. A., Smith, D. R.: 1966, *J. Geophys. Res.* **71**, 3289.
Fan, C. Y., Pick, M., Pyle, R., Simpson, J. A., and Smith, D. R.: 1968, *J. Geophys. Res.* **73**, 1555.
Fichtel, C. E. and McDonald, F. B.: 1967, *Ann. Rev. Astron. Astrophys.* **5**, 351.
Firror, J.: 1954, *Phys. Rev.* **94**, 1017.
Fisk, L. A. and Axford, W. I.: 1968, *J. Geophys. Res.* **73**, 4396.

Fisk, L. A. and Axford, W. I.: 1969, *J. Geophys. Res.* **74**, 4973.
Fokker, A. D.: 1963, *Space Sci. Rev.* **2**, 70.
Forman, M. A.: 1970a, *Planetary Space Sci.* **18**, 25.
Forman, M. A.: 1970b, *J. Geophys. Res.* **75**, 3147.
Gall, R., Jimenez, J., and Camacho, L.: 1968, *J. Geophys. Res.* **73**, 1593.
Gleeson, L. J. and Axford, W. I.: 1968, *Astrophys. Space Sci.* **2**, 431.
Gleeson, L. J. and Palmer, I.: 1970 (in press).
Guss, D. E.: 1964, *Phys. Rev. Letters* **13**, 363.
Hakura, Y.: 1964, *J. Radio Res. Lab.* **11**, 273.
Hakura, Y.: 1967, *J. Geophys. Res.* **72**, 1461.
Hakura, Y. and Goh, T.: 1959, *J. Radio Res. Lab. Japan* **6**, 635.
Hoffman, D. J. and Sauer, H. H.: 1968, *Space Sci. Rev.* **8**, 750.
Holzer, R. E., McLeod, M. G., and Smith, E. J.: 1966, *J. Geophys. Res.* **71**, 1481.
Howard, R.: 1963, *Astrophys. J.* **138**, 1312.
Howard, R. and Severny, A.: 1963, *Astrophys. J.* **137**, 1242.
Jokipii, J. R.: 1966, *Astrophys. J.* **146**, 480.
Jokipii, J. R.: 1967, *Astrophys. J.* **147**, 405.
Jokipii, J. R.: 1968, *J. Geophys. Res.* **73**, 6864.
Jokipii, J. R.: 1969, *Proc. 11th Intern. Conf. Cosmic Rays*, Budapest.
Jokipii, J. R.: 1970 (in press).
Jokipii, J. R. and Parker, E. N.: 1968, *Phys. Rev. Letters* **21**, 44.
Jokipii, J. R. and Coleman, Jr., P. J.: 1968, *J. Geophys. Res.* **73**, 5495.
Jonah, F. C.: 1966, Report of Ling Temco Vought. Inc.
Kai, K.: 1969, *Proc. Astron. Soc. Australia* **1**, 186.
Kahler, S. W.: 1969, *Solar Phys.* **8**, 166.
Kane, S. R. and Winckler, J. R.: 1969, *Solar Phys.* **6**, 304.
Krimigis, S. M.: 1965, *J. Geophys. Res.* **70**, 2943.
Krivsky, L.: 1963, *Nuovo Cimento* **27**, 1017.
Kruger, A.: 1968, *Ann. IQSY* **3**, 70.
Kundu, M. R.: 1961, *J. Geophys. Res.* **66**, 4308.
Kundu, M. R.: 1965, *Solar Radio Astronomy*. Interscience, John Wiley and Sons, New York.
Labrum, N. R. and Smerd, S. F.: 1968, *Proc. Astron. Soc. Australia* **1**, 140.
Leinbach, H.: 1967, *J. Geophys. Res.* **72**, 5473.
Leinbach, H., Venkatesan, D., and Parthasarthy, R.: 1965, *Planetary Space Sci.* **13**, 1075.
Levy, R. H., Petschek, H. E., and Siscoe, G. L.: 1964, *Am. Inst. Aeron. Astronaut. J.*, 2065.
Lin, R. P.: 1968, *J. Geophys. Res.* **73**, 3066.
Lin, R. P.: 1970a, *Solar Phys.* **12**, 209.
Lin, R. P.: 1970b, *J. Geophys. Res.* **75**, 2583.
Lin, R. P. and Anderson, K. A.: 1967, *Solar Phys.* **1**, 446.
Lin, R. P., Kahler, S. W., and Roelof, E. C.: 1968, *Solar Phys.* **4**, 338.
Lockwood, J. A.: 1968, *J. Geophys. Res.* **73**, 4247.
Malinge, A. M.: 1963, *Ann. Astrophys.* **26**, 97.
Mariani, F. and Ness, N. F.: 1969, *J. Geophys. Res.* **74**, 5633.
Martres, M. J. and Pick, M.: 1962, *Ann. Astrophys.* **25**, 293.
McCabe, M. K. and Caldwell, P. A.: 1968, *Ann. IQSY* **3**, 175.
McCracken, K. G.: 1959, *Nuovo Cimento* **13**, 1081.
McCracken, K. G.: 1962a, *J. Geophys. Res.* **67**, 423.
McCracken, K. G.: 1962b, *J. Geophys. Res.* **67**, 435.
McCracken, K. G.: 1962c, *J. Geophys. Res.* **67**, 447.
McCracken, K. G.: 1969, in *Solar Flares and Space Research*, North-Holland Publ. Co., Amsterdam, p. 202.
McCracken, K. G. and Ness, N. F.: 1966, *J. Geophys. Res.* **71**, 3315.
McCracken, K. G. and Palmeira, R. A. R.: 1960, *J. Geophys. Res.* **65**, 2673.
McCracken, K. G., Rao, U. R., Fowler, B. C., Shea, M. A., and Smart, D. F.: 1965, IQSY Instruction Manual No. 10.
McCracken, K. G., Rao, U. R., and Bukata, R. P.: 1967, *J. Geophys. Res.* **73**, 4159.
McCracken, K. G., Rao, U. R., and Ness, N. F.: 1968, *J. Geophys. Res.***73**, 4159.

McCracken, K. G., Palmeira, R. A. R., Bukata, R. P., Rao, U. R., Allum, F. R., and Keath, E. P.: 1969, Presented at the 11th International Conference on Cosmic Rays, Budapest.
McCracken, K. G., Rao, U. R., Bukata, R. P., and Keath, E. P.: 1970, to be published in *Solar Phys.*
McIntosh, P. S. and Sawyer, C.: 1968, *Ann. IQSY* **3**, 169.
Meyer, P., Parker, E. N., and Simpson, J. A.: 1956, *Phys. Rev.* **104**, 768.
Michel, F. C.: 1967, *J. Geophys. Res.* **72**, 1917.
Moreton, G. and Severny, A.: 1966, *Astron. Zh.* **71**, 172.
Moreton, G. and Severny, A.: 1968, *Solar Phys.* **3**, 282.
Nathan, K.V.S.K. and Van Allen, J. A.: 1968, *J. Geophys. Res.* **73**, 163.
Ness, N. F.: 1969, *Rev. Geophys.* **7**, 97.
Ness, N. F. and Wilcox, J. M. 1966, *Astrophys. J.* **143**, 13.
Ness, N. F. and Wilcox, J. M.: 1967, Space Sci. Lab. – University of California, Berkeley, Series No. 8, Issue No. 40.
Ness, N. F., Scearce, C. S., and Seek, J. B.: 1964, *J. Geophys. Res.* **69**, 3531.
Ness, N. F., Scearce, C. S., and Cantarano, S. C.: 1967, *J. Geophys. Res.* **72**, 3769.
Obayashi, T.: 1964, *Space Sci. Rev.* **3**, 79.
Palmeira, R. A. R., Rao, U. R., Allum, F. R.: 1970, to be published in *Solar Phys.*
Parker, E. N.: 1958, *Astrophys. J.* **128**, 664.
Parker, E. N.: 1964, *J. Geophys. Res.* **69**, 1755.
Parker, E. N.: 1965, *Planetary Space Sci.* **13**, 9.
Paulikas, G. A., Freden, S. C., and Blake, J. B.: 1966, *J. Geophys. Res.* **71**, 1795.
Paulikas, G. A., Blake, J. B., and Freden, S. C.: 1968, *J. Geophys. Res.* **73**, 87.
Peterson, L. E. and Winckler, J. R.: 1959, *J. Geophys. Res.* **64**, 697.
Rao, U. R., McCracken, K. G., and Bukata, R. P.: 1967, *J. Geophys. Res.* **72**, 4325.
Rao, U. R., McCracken, K. G., and Bukata, R. P.: 1968a, *Can. J. Phys.* **46**, 5844.
Rao, U. R., McCracken, K. G., and Bukata, R. P.: 1968b, *Ann. IQSY* **3**, 329.
Rao, U. R., Allum, F. R., Bartley, W. C., Palmeira, R. A. R., Harries, J. A., and McCracken, K. G.: 1969, in *Solar Flares and Space Research*, North-Holland Publ. Co., Amsterdam, p. 267.
Rao, U. R., McCracken, K. G., Allum, F. R., Palmeira, R. A. R., and Bartley, W. C.: 1970, to be published in *Solar Phys.*
Reid, G. C.: 1964, *J. Geophys. Res.* **69**, 2659.
Reid, G. C. and Sauer, H. H.: 1967, *J. Geophys. Res.* **72**, 197.
Roederer, J. G.: 1969, *Rev. Geophys.* **7**, 77.
Roeloff, E. C.: 1965, Ph.D. Thesis, University of California, Berkeley.
Roeloff, E. C.: 1966, *Trans. Am. Geophys. Union* **47**, 80 (Abstract).
Rose, D. C. and Lapointe, S. M.: 1961, *Can. J. Phys.* **39**, 239.
Sari, J. W. and Ness, N. F.: 1969, *Solar Phys.* **8**, 155.
Sauer, H. H.: 1963, *J. Geophys. Res.* **68**, 957.
Sawyer, D. M., Ormes, J. F., Webber, W. R., and Bingam, R. G.: 1968, Proc. Int. Conf. on Cosmic Rays, Calgary, Mod., p. 105.
Sekido, Y. and Murakami, K.: 1955, Proc. Int. Conf. on Cosmic Rays, Guanajuato, Mexico.
Severny, A. F.: 1963, in *NASA-AAS Symposium on Physics of Solar Flares*, p. 95.
Severny, A.: 1968, *Ann. IQSY* **3**, 11.
Shea, M. A., Smart, D. F., and McCracken, K. G.: 1965, *J. Geophys. Res.* **70**, 4117.
Shea, M. A. and Smart, D. F.: 1967, *J. Geophys. Res.* **72**, 2021.
Singer, S.: 1970, Preprint from Los Alamos Scientific Laboratory, New Mexico.
Simon, P. and Švestka, Z.: 1968, *Ann. IQSY* **3**, 469.
Siscoe, G. L., Davis, Jr. L., Coleman, Jr. P. J., Smith, E. J., and Tones, D. E.: 1968, *J. Geophys. Res.* **73**, 61.
Sivaraman, K. R.: 1969, *Solar Phys.* **6**, 152.
Smart, D. F. and Shea, M. A.: 1970, *Space Res.*, in press.
Steljes, J. F., Carmichael, H., and McCracken, K. G.: *J. Geophys. Res.* **66**, 1363.
Švestka, Z.: 1966, *Space Sci. Rev.* **5**, 388.
Švestka, Z.: 1968, *Solar Phys.* **4**, 18.
Švestka, Z.: 1970, *Solar Phys.*, in press.
Švestka, Z. and Simon, P.: 1969, *Solar Phys.* **10**, 3.
Takakura, T.: 1969, *Solar Phys.* **6**, 133.

Takakura, T. and Ono, M.: 1962, *J. Phys. Soc. Japan* **17**, Suppl. A-II, 207.
Tanaka, H. and Kakinuma, T.: 1964, *Rep. Ion. Res. Japan* **18**, 32.
Taylor, H. E.: 1967, *J. Geophys. Res.* **72**, 4467.
Taylor, H. E. and Hones, E. W. Jr.: 1965, *J. Geophys. Res.* **70**, 3605.
Van Allen, J. A. and Krimigis, S. M.: 1965, *J. Geophys. Res.* **70**, 5737.
Van Allen, J. A. and Ness, N. F.: 1969, *J. Geophys. Res.* **74**, 71.
Vernov, S. N., Chudakov, A. E., Vakulov, P. V., Gorchakov, E. V., Kontor, N. N., Logecharev, Yu. I., Lubimov, G. P., Pereslegina, N. V., and Timofeev, G. A.: 1969, in *Proc. of Cosmic Ray Symposium*, Leningrad, p. 29.
Warwick, C. S.: 1962, *J. Geophys. Res.* **67**, 1333.
Warwick, C. S.: 1965, *Astrophys. J.* **141**, 500.
Warwick, C. S. and Haurwitz, M. W.: 1962, *J. Geophys. Res.* **67**, 1317.
Webber, W. R.: 1963, *NASA-AAS Symposium on Physics of Solar Flares*, p. 215.
Weiss, A. A. and Sheridan, K. V.: 1962, *J. Phys. Soc. Japan* **17**, Suppl. II, 223.
Wilcox, J. M. and Ness, N. F.: 1965, *J. Geophys. Res.* **70**, 5793.
Wild, J. P.: 1969, *Proc. Astron. Soc. Australia* **1**, 181.
Wild, J. P., Sheridan, K. V., and Kai, K.: 1968, *Nature* **218**, 536.
Winckler, J. R., Bhavsar, P. D., and Peterson, L.: 1961, *J. Geophys. Res.* **66**, 995.
Zirin, H. and Lackner, D. R.: 1969, *Solar Phys.* **6**, 86.